UC San Diego

UC San Diego Electronic Theses and Dissertations

Title

Stabilization of Coinage Metals With an Oxidation State of Zero /

Permalink

https://escholarship.org/uc/item/3t8574gc

Author

Weinberger, David S.

Publication Date

2014

Peer reviewed|Thesis/dissertation

eScholarship.org Powered by the California Digital Library
University of California

UNIVERSITY OF CALIFORNIA, SAN DIEGO

Stabilization of Coinage Metals With an Oxidation State of Zero

A dissertation submitted in partial satisfaction of the requirements for the degree of Doctor of Philosophy

in

Chemistry

by

David S. Weinberger

Committee in charge:

Professor Guy Bertrand, Chair
Professor Joshua Figueroa
Professor Carlos Guerrero
Professor Clifford Kubiak
Professor Thomas Murphy

2014

Copyright
David S. Weinberger, 2014
All rights reserved.

The Dissertation of David S. Weinberger is approved, and it is acceptable in quality and form for publication on microfilm and electronically:

Chair

University of California, San Diego
2014

TABLE OF CONTENTS

LIST OF FIGURES

LIST OF SCHEMES

LIST OF TABLES

ACKNOWLEDGEMENTS

In 2007, Arnie Rheingold, a family friend and now a collaborator, strongly suggested that I work for Prof. Guy Bertrand at UCR. Working for Guy is easily the best decision I could have made. Even when my chemistry wasn't working, which was often, he was always interested in what was new. His pursuit of new and exciting chemistry has significantly influenced the way I look at chemistry and makes me think constantly about new compounds yet to be made. I can't thank Guy enough for the past six years. It really has been a pleasure to work with him and in his lab, and on the golf course.

During my time in Guy's lab I've seen many great chemists come through. I owe part of my education to all of them. I've learned so much and had a great time with them both in Riverside and in San Diego. It would be remiss for me not to acknowledge them here: Allan, Matt, Adam, Glen, Eugenia, Emrah, Aholibama, Nicolas, Amos, Olivier, Daniel, Rei, Gregorio, Daniela, Maria, Caleb, Fabian and Gael.

During my tenure with Guy I also had the absolute pleasure to work with Michele. Whenever I needed anything in the lab, Michele was there to provide it. She made the run lab smoothly, and has been an invaluable resource.

During the middle of my PhD I was struggling to find a project that would work, and finally found one after some great discussions with Mo. This project turned out to be just what I needed. Mo has been a great collaborator and a friend; even though he would try his hardest to distract me and try to convince me to play golf every weekend.

In addition to everyone that I saw pass through the lab, there are those that are still there. While I hope that I have been as good to them as the others have been to me, I

have also learned a lot from them and appreciate all that they have done for me. Thank you: Martin, David R., David M., Cory, Janell, Daniel, Liqun.

I have to thank Prof. Arnie Rheingold and Dr. Curtis Moore for their encouragement of students to do their own crystallography. However, I really appreciate their help with the many crystal structures that I couldn't solve.

I also have to acknowledge the unwavering support of my family, who supported my decision to go to grad school on the other side of the country and have been there for me every day since. Finally, I can honestly say that I would not have been able to survive all the ups and downs of these past six years without the support of my fantastic wife, Sharon. We met at the beginning of my PhD, and she made this journey better every day.

Chapter 1 has been adapted from materials published in D. S. Weinberger, M. Melaimi, C. E. Moore, A. L. Rheingold, G. Frenking, P. Jerabek, G. Bertrand, *Angew. Chem. Int. Ed.* **2013**, 52, 8964-8967. The dissertation author was the primary investigator of this paper and the reactivity discussed above.

Chapter 2 has been adapted from materials published in D. S. Weinberger, M. Melaimi, C. E. Moore, A. L. Rheingold, G. Frenking, P. Jerabek, G. Bertrand, *Angew. Chem. Int. Ed.* **2013**, 52, 8964-8967. The dissertation author was the primary investigator of this paper and the reactivity discussed. The reactivity will be published in a future paper with the same set of authors.

Chapter 3 has been adapted from material published in: L. Jin, D. S. Weinberger, M. Melaimi, C. E. Moore, A. L. Rheingold, G. Bertrand *Angew. Chem. Int. Ed.* **2014**, *accepted*. The dissertation author initiated the project and participated in the chemistry.

Chapter 4 has been adapted from materials published in D. S. Weinberger, N. A. SK, K. C. Mondal, M. Melaimi, G. Bertrand, A. C. Stuckl, H. W. Roesky, B. Dittrich, S. Demeshko, B. Schwederski, W. Kaim, P. Jerabek, G. Frenking *J. Am. Chem. Soc.* **2014**, *136*, 6235. The dissertation author was the primary investigator of this paper.

Chapter 5 has been composed from results that have not been published. These results will be published in the future as D. S. Weinberger, M. Melaimi, C. E. Moore, A. L. Rheingold, G. Frenking, P. Jerabek, G. Bertrand. "Reactivity of Dinuclear Gold And Copper Complexes With a Variety of Substrates and Metals." The dissertation author was the primary investigator.

VITA

Academic History

2012-2014 **University of California, San Diego**: Ph.D., Chemistry; Advisor: Prof. Guy Bertrand

2008-2012 **University of California, Riverside**: Inorganic Chemistry; Advisor: Prof. Guy Bertrand

2006-2008 **Villanova University**: Research towards a Masters of Science, Inorganic Chemistry. Advisor: Dr. Scott Kassel

2002-2006 **Millersville University of Pennsylvania**: Bachelor of Science, Chemistry

Research Experience

2008-2014 **University of California, San Diego (San Diego, CA), Department of Chemistry & Biochemistry.**
University of California, Riverside (Riverside, CA), Department of Chemistry.
Advisor: Professor Guy Bertrand
Isolation and characterization of the first ligated Au, Cu and Ag complexes in the zero oxidation state. Utilizing cyclic alkyl amino carbenes, the first Au_2 and Cu_2 dimers were synthesized and used for reactivity with electron poor alkynes, alkenes and a series of small molecules.

2012-2014 **University of California, Riverside (Riverside, CA), Department of Chemistry.**
Part time appointment as Visiting Scholar with Professor Vince Lavallo
Characterization of the first carborane-fused triazole radical anion by cyclic voltammetry, electron paramagnetic resonance and x-ray diffraction.

2006-2008 **Villanova University (Villanova, PA), Chemistry Department.**
Advisor: Professor Scott Kassel
Synthesis and characterization of chiral diimine nickel, copper, and zinc complexes for catalytic investigation and examination of intrinsic crystal properties.

2005-2006 **Carnegie Institute of Washington (Washington D.C.), Geophysical Laboratory.**
Advisor: Dr. George Cody
Synthesis of hydrocarbon chains via naturally occurring transition metal catalysts at hydrothermal vent (high pressure, high temperature) conditions.

2004-2005 **Millersville University (Millersville, PA). Independent Undergraduate Research.**
Advisor: Professor Patricia Hill
Analysis of ancient chemical dyes in paintings and textiles using NMR and FT-IR.

Relevant Work Experience

2012-Current **University of California, San Diego**: Graduate Student Researcher.

2008-2012 **University of California, Riverside**: Graduate Assistant/ Researcher. Taught General Chemistry Recitations and Organic Chemistry Labs.

2006-2008 **Villanova University**: Graduate Assistant & Teaching Assistant for Advanced Inorganic Laboratory and General Chemistry I & II Laboratories. Developed and implemented experiments for the Advanced Inorganic Lab. Privately tutored students in General, Inorganic I and Inorganic II chemistry classes.

Presentations

2014 **American Chemical Society 247th National Meeting**, Dallas, TX.
Oral Presentation

2014 **University of California, San Diego-Inorganic Seminar**
Oral Presentation

2013 **American Chemical Society 245th National Meeting**, New Orleans, LA.
Oral Presentation

2010 **University of California, Riverside – Departmental Research Review**
Oral Presentation

2009 **University of California, Riverside – Departmental Literature Review**
Oral Presentation

2006 **American Chemical Society 231st National Meeting,**
Atlanta, GA.
Poster Presentation

Publications

1. **Isolation of Neutral Mono- and Dinuclear Gold Complexes of Cyclic (Alkyl) (amino) carbenes.**
Weinberger, D.S.; Melaimi, M.; Bertrand, G. *Angew. Chem. Int. Ed.,* **2013**, 52, 8964-8967.
***** Highlighted: **24-carat chemistry.** Doherty, R. *Nature Chemistry*. **2013**, 5, 728.

2. **Isolation of a Carborane-Fused Triazole Radical Anion.**
Asay, M.; Kefalidis, C.E.; Estrada, J.; **Weinberger, D.S**.; Wright, J.; Moore, C.E.; Rheingold, A.L.; Lavallo, V. *Angew. Chem. Int. Ed*. **2013**, 52, 11560-11563.

3. **Ruthenium Olefin Metathesis Catalysts Supported by Cyclic Alkyl Amino Carbenes (CAACs).**
Weinberger, D. S.; Lavallo, V. *Handbook of Metathesis (2nd ed.)* German: Wiley-VCH. *Accepted.*

4. **Isolation of Neutral Mononuclear Copper Complexes Stabilized by Two Cyclic (Alkyl)(amino)carbenes**
Weinberger, D.S.; Sk, N. A.; Chandra, K. C.; Melaimi, M.; Bertrand, G. Stuckl, A. C.; Roesky, H. W.; Dittrich, B.; Demeshko, S.; Schwederski, B.; Kaim, W.; Jerabek, P.; Frenking, G. *J Am. Chem. Soc.* **2014**, 136, 6235-6238.

5. **Trinuclear Gold Clusters Supported by CAAC Ligands, Mimics for Gold Heterogeneous Catalysts**
Jin, L.; **Weinberger, D. S.**; Melaimi, M.; Moore, C. E.; Rheingold, A. L.; Bertrand, G. *Angew. Chem. Int. Ed*. **2014**, *Accepted*

6. **Reactivity of Dinuclear Gold And Copper Complexes With a Variety of Substrates and Metals.**
Weinberger, D.S.; Melaimi, M.; Bertrand, G. *Manuscript in Progress*.

Analysis Techniques

1D and 2D NMR spectroscopy of common nuclei (^{1}H, ^{13}C, ^{11}B, ^{19}F, ^{31}P), Infrared spectroscopy, Gas chromatography, Cyclic Voltammetry, EPR, Gaussian calculations, X-ray diffraction (crystal mounting, data acquisition and structure solving)

ABSTRACT OF THE DISSERTATION

Stabilization of Coinage Metals With an Oxidation State of Zero

by

David S. Weinberger

Doctor of Philosophy in Chemistry

University of California, San Diego, 2014

Professor Guy Bertrand, Chair

Cyclic (alkyl) (amino)carbenes (CAACs) are highly nucleophilic and electrophilic species. By utilizing these properties, neutral mono- and di-nuclear coinage metal complexes have been stabilized and represent the first complexes of their kind. These complexes are readily available by one-electron reduction from the corresponding $(CAAC)_2Metal^+X^-$ and (CAAC)Metal chloride complexes, respectively. The $(CAAC)_2M^0$ complexes have been studied by X-ray diffraction and electron paramagnetic resonance, demonstrating that the additional electron is located on both the metal and ligand. In

addition to synthesizing the diamagnetic (CAAC)M-M(CAAC) complexes, interesting reactivity has been shown by the addition of alkynes, alkenes, CO_2, P_4, isocyanides and $Fe(CO)_5$ to the dimeric complexes. Attempts to isolate the larger neutral trinuclear gold complex were unsuccessful, but led to the isolation of the mixed valence Au(0)/Au(I)/Au(0) complex supported by three CAAC ligands, which proved to be a catalyst for the carbonylation of amines under mild conditions.

Introduction

The utilization of gold clusters has been traced to as early as the 4th-century when the Lycurgus cup was made of colloidal gold and silver to give a dichroic red or green depending on the lighting.[1] For nearly fourteen centuries, gold nanoparticles were used in stained glass to produce a deep-ruby color.[2] Without understanding, at the time, tin(II) chloride was used to reduce gold salts to produce gold colloids.[3] It wasn't until 1857 when Faraday reported the synthesis of red solutions of colloidal gold by the reduction of chloroauric acid ($HAuCl_4$) with white phosphorus in CS_2 that it was realized that the color was a consequence of the size of the gold particles.[4]

In the 157 years since the seminal work of Faraday, the process to make gold nanoparticles has not changed greatly. Essentially, the gold precursor is reduced in a solution. Varying the reducing agent, solvent, and the ligands leads to dramatic differences in the size and structure of the resulting particle. One of the conventional methods developed in 1951 by Turkevich for the synthesis of gold nanoparticles is the reduction of chloroauric acid with sodium citrate in water.[5] The original particles were *ca*. 20 nm, and further development by changing the ratio of citrate to gold changed the average size between 16 and 147 nm.[6] While the average size could be predicted, the bulk material still had large particle size dispersity and since the citrates only loosely bind the nanoparticles, after time the particles would agglomerate. In 1994, the Brust-Schiffrin method was published, which entailed the reduction of a Au(III) precursors with $NaBH_4$ in the presence of thiols.[7] The particles produced tend to have both a narrower size distribution than previously made particles and can be isolated and redissolved in organic solvents without irreversible aggregation. Small nanoparticle cores (< 2 nm) can be isolated with the fast addition of a reductant to a cooled solution of gold and thiol. By

utilizing a two-phase system, similar to the work by Faraday, this synthesis laid ground for further progress in designing nanoparticles with varying sizes and with different thiol/gold ratios.

The pivotal work by Haruta *et. al*. in 1987 paved the way for gold nanoparticle reactivity.[8] Previously, it was believed that gold was inert and could not be used for catalysis, but Haruta showed that coprecipitation of gold particles (~2-4 nm) with metal oxides were effective for the oxidation of carbon monoxide. Further studies have indicated that there is a large size threshold effect for gold particles.[9] Correspondingly, nanoparticles become catalytically active with diameters less than ~3.5 nm. Several groups have investigated the ability for 55-atom gold clusters (~1.4 nm) to catalytically oxidize substrates, particularly the selective oxidation of styrene by dioxygen.[10] Interestingly, the catalytic activity diminishes when the size of the particle is larger than ~2 nm.

Small gold clusters ranging in size between 4 and 55 atoms have been prepared in methods similar to the Brust-Schiffrin method. By using $(R_3P)AuX$ as a starting material, the general procedure is the reduction of the precursor with $NaBH_4$ in an organic solvent. Groups have found that by simply changing the R substituents and changing the anion from bonding to non-bonding, the size of the cluster is greatly influenced. For example, by using $(p\text{-tolyl})_3PAuBF_4$ instead of $(Ph_3P)AuNO_3$, the resulting clusters are either $Au_6(P(p\text{-tolyl})_3)_6[BF_4]_2$ or $Au_9(PPh_3)_8[NO_3]_3$[11], respectively (**Figure I.1**).[12]

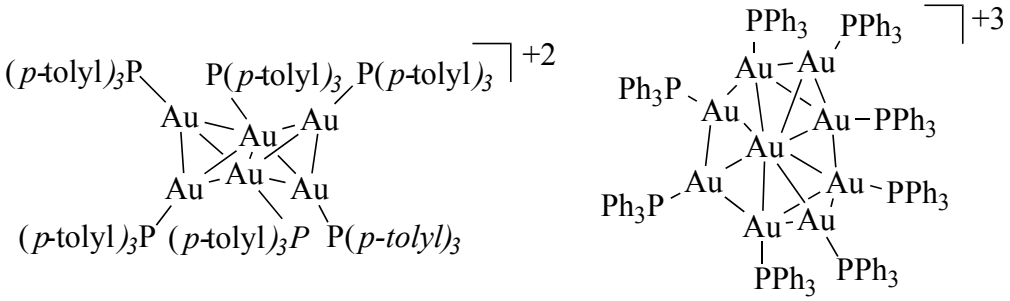

Figure I. 1: Au_6 and Au_9 clusters from the reduction of $(R_3P)AuX$ starting materials.

While the $Au_9(PPh_3)_8[NO_3]_3$ is the major product in the reduction of $(Ph_3P)AuNO_3$ with $NaBH_4$, these reactions are almost never clean, and other clusters can also be crystallized such as $Au_{14}(PPh_3)_8[NO_3]_4$[13]. Due to the nature of these reactions, it's nearly impossible to predict the size of the cluster before doing the reaction. Even when using a precursor such as $\{(t\text{Bu})_3\text{PAu}]_3\text{O}\}^+\text{BF}_4^-$ (**Scheme I.1**), which already has Au-Au aurophilic interactions, and reducing it with $(Me_3Si)_3P$ did not afford the straight forward complex $\{(t\text{Bu})_3\text{PAu}]_3\}^+\text{BF}_4^-$; instead, $\{(t\text{Bu})_3\text{PAu}]_4\}^{2+}[\text{BF}_4]_2^-$ was obtained. While it is not the Au_3 cluster that was predicted, it is the smallest gold cluster that only includes phosphine and gold.[14]

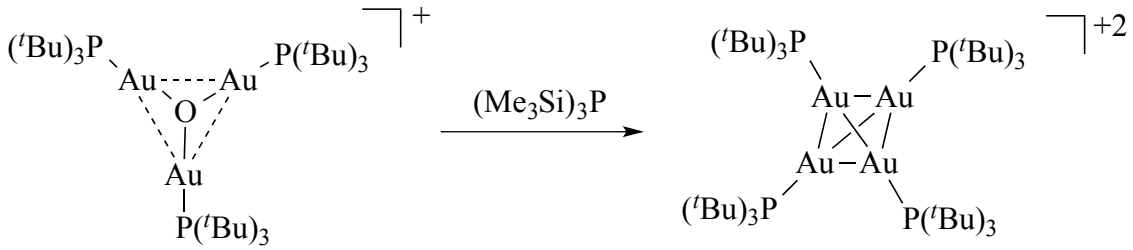

Scheme I. 1: Synthesis of $\{(t\text{Bu})_3\text{PAu}]_4\}^{2+}$ by the addition of $(Me_3Si)_3P$ to $\{(t\text{Bu})_3\text{PAu}]_3\text{O}\}^+$.

The group of Konishi has had luck with designing different sized clusters starting from smaller clusters. For instance when $[Au_6(dppp)_4](NO_3)_2$ is reacted with 2 equivalents of $(Ph_3P)AuCl$, $[Au_8(dppp)_4Cl_2]^{2+}$ is obtained (dppp: 1,3-

bis(diphenylphosphino)propane).[15] After anion exchange with hexafluorophosphate, crystals of $[Au_8(dppp)_4Cl_2]^{2+}$ were obtained showing an edge sharing bi-tetrahedral core of gold atoms with 2 pendant AuCl moieties. This is a rare example of being able to cleanly obtain one cluster from the addition of gold to another cluster. Several groups have discussed the prevalence of "magic-number" clusters, which seem to be more stable than other clusters and have intrinsic properties that are unique. For example, after the reduction of $Au_2(dppe)Cl_2$ (dppe: 1,2-bis(diphenylphosphino) ethane) with $NaBH_4$, a mixture of Au_9, Au_{11}, Au_{12}, and Au_{15} clusters are obtained and characterized by electrospray ionization mass spectrometry (ESIMS). However, treatment of this polydispersed sample with HCl results in a 30 % yield of the $[Au_{13}(dppe)_5Cl_2]Cl_3$ cluster.[16] The Au_{13} clusters are expected to be thermodynamically stable due to the closed shell geometry, and are believed to be subunits of larger gold clusters such as Au_{25} and Au_{38}. It was found experimentally that the "magic-number" Au_{20} was stable due to the large HOMO-LUMO gap of 1.77 eV, which is the largest among all coinage-metal clusters.[17] These clusters also tend to have increased luminescent properties, which have become a large area of research in the last several years. [18]

The bonding in the core of these clusters is best described as very strong aurophilic interactions. These type of bonds originate from the closed-shell metal centers, $5d^{10}$, with the overlap of the 6s valence orbital.[19] The 6p valence orbitals have been calculated to be too high in energy to significantly contribute to the bonding. Typical aurophilic interactions tend to be between 2.60 and 3.50 Å. These interactions are well below the sum of the van der Waals radii (3.80 Å).[20] The geometry of gold clusters have been classified as either spherical polyhedral or elliptical polyhedral clusters, which have

12*n*+8 or 12*n*+6 number of valence electrons, respectively (n is equal to the number of peripheral gold atoms).

Unlike the methods described above which reduce gold (I) and gold (III) precursors to gold clusters, other methods such as laser ablation allow for the deposition of small clusters (Au atoms<10) onto supports. By changing the support, it was found that these clusters were active for the partial oxidation of propene with water vapor.[22] Computational studies have probed the effect of the support, and found that the ability of the support to accept electron density away from the gold cluster directly influences the capability of the cluster to bind propene.[23] Consistently, it has been found experimentally that propene binds to the gold more strongly when an electron donating support is utilized.

In the gold clusters with less than 10 gold atoms, the charge of the clusters prepared by reduction of a gold (I) precursor are mixed valence with a charge between 0 and 1. With the example of gold clusters made by laser ablation, the cluster itself is neutral, but becomes charged depending on the support. Therefore, efforts have been made to isolate small gold complexes, which can be isolated and characterized by X-ray diffraction and NMR spectroscopy.

Many groups are also investigating the catalytic ability of very small clusters, which are not made by the laser ablation method. In 2012, Corma *et. al.* have shown that gold clusters ranging in number between 3 and 13 could be formed from the addition of gold(I) or gold(III) precursors in propargyl alcohol.[24] Impressively, it was shown that these small clusters were even more catalytically active than the larger gold nanoparticles and also more active than mononuclear homogenous gold catalysts for the ester assisted hydration of alkynes. Turnover numbers of ~10^7 were achieved at concentrations of only

10 ppb (**Scheme I.2**). From mass spectrometry, it was found that the highest turnover numbers occurred when the active catalyst was between 3 and 5 gold atoms. Elucidation of the gold cluster formation found that the Au_3-Au_5 clusters came from the degradation of the larger Au_5-Au_9 clusters, which instantaneously form after the addition of propargyl alcohol. The Au_5-Au_9 clusters were completely inactive for the hydration of alkynes, but active for the bromination of *p*-dimethoxybenzene. All activity decreased once the Au_3-Au_5 cluster concentration increased for the second reaction. For both reactions, the catalysis terminated once the Au_{13} cluster, which is the thermodynamically stable product, formed.

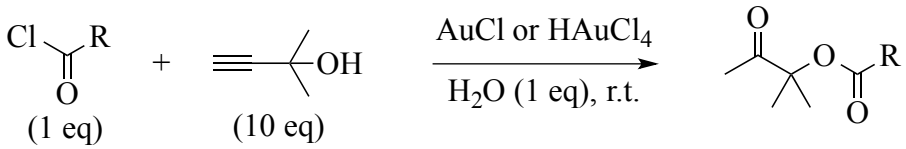

Scheme I.2: Ester assisted hydration of alkynes using AuCl precursors.

Unlike the discrete complexes formed and characterized by reducing $(R_3P)AuCl$, the clusters formed by Corma *et. al.* could not be isolated. When taken out of solution the clusters agglomerate to form large nanoparticles. While the active catalyst has been narrowed to a range of gold atoms, nothing is actually known about the active species. The structures of small gold clusters have been predicted by calculations, but vary greatly. The charge on these active clusters are believed to be neutral, which is also unlike any of the structures formed from the reduction of $(R_3P)AuCl$. Therefore, it is of great interest to isolate and characterize neutral small gold clusters.

When phosphine-gold complexes such as $(R_3P)AuCl$ are reduced further with stronger reducing agents, the complexes decompose to often form metallic gold, large

nanoparticles, or black precipitate that can not be characterized. It seems clear from the literature that stronger ligand-metal bonds are needed to stabilize these electron-rich complexes so they don't agglomerate or just simply fall apart. It has been well demonstrated that singlet carbenes make stronger ligand-metal bonds than phosphines; therefore, is it possible to use carbenes to stabilize small clusters? Carbenes have been shown to stabilize large gold nanoparticles (~2 nm), but never small clusters (Au<10).[25]

Carbenes are neutral molecules that contain a divalent carbon atom, which possesses only six electrons in its valence shell.[26] Starting as far back as 1835 with the attempts of Dumas to generate the simplest carbene ($:CH_2$) from the dehydration of methanol, generating carbenes has been of great interest.[27] Revolutionary work by Curtius[28] and Staudinger[29] at the end of the 19th and the very beginning of the 20th century showed that carbenes could be generated from diazo compounds and proved to be extremely reactive species (**Scheme I.3**). It wasn't until the middle of the 20th century that carbenes became useful as transient species in the discovery of the cyclopropanation reaction by Doering.[30]

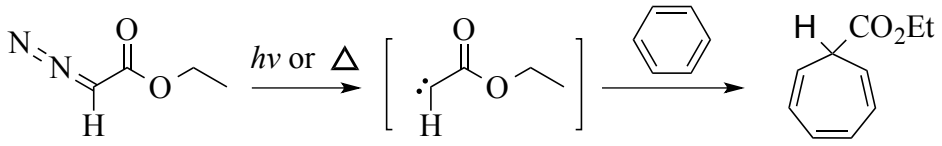

Curtius, 1885

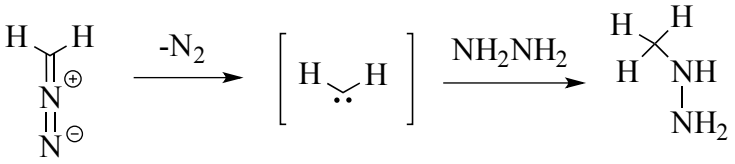

Staudinger, 1912

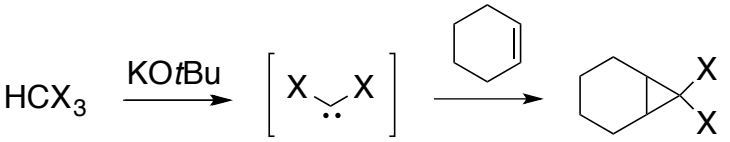

Doering, 1954

Scheme I.3: Organic reactivity utilizing transient carbene species.

It became clear that the extreme reactivity of carbenes came from the fact that they defied the octet rule. Breslow[31] and Wanzlick[32] demonstrated that the stability of carbenes was drastically improved by the presence of nitrogen groups alpha to the carbene center. The synthesis to make the carbene entailed the pyrolysis of the corresponding $HCCl_3$ adduct. Although the stability was improved from the lone pairs on the nitrogen donating into the empty p-orbital of the carbene, monomeric carbenes could not be isolated or characterized. (**Scheme I.4**) However, they did prove to be useful as organocatalysts for the benzoin condensation reaction.

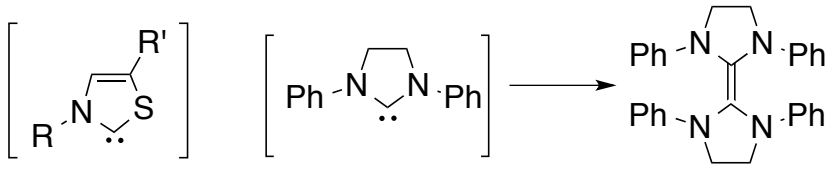

Breslow, 1958 Wanzlik, 1962

Scheme I.4: Early singlet carbenes.

Carbenes have played a prominent role in transition-metal catalysis, and given the work presented within this thesis, it would be remiss to not include the first carbene transition-metal complexes by Tschugajeff,[33] Fischer,[34] Ofele,[35] Wanzlick,[36] and Schrock.[37] While none of the carbenes were isolated, the corresponding metal complexes proved to be accessible (**Figure I.2**).

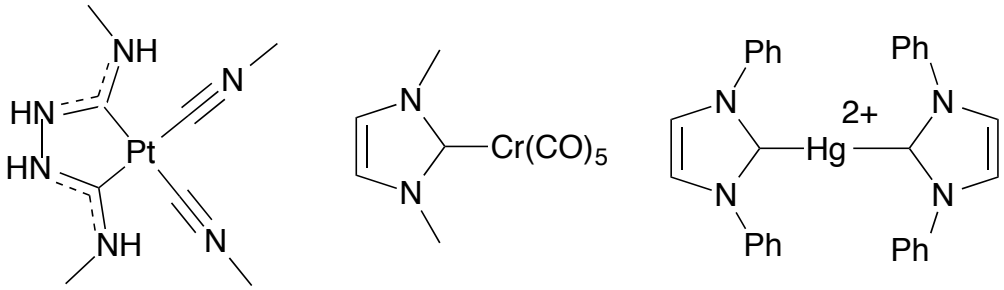

Tschugajeff, 1925 Ofele, 1968 Wanzlick, 1968

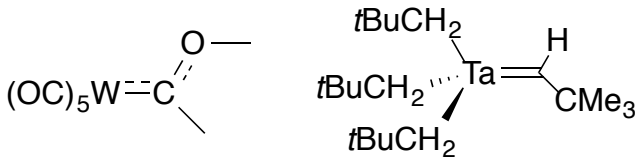

Fischer, 1964 Schrock, 1974

Figure I. 2: The first five examples of carbene-metal complexes.

In 1988, Bertrand and coworkers reported the synthesis of the first stable carbene, namely the (phosphino)(silyl) carbene (**Scheme I.5**).[38] This compound was prepared

similarly to the previously described transient carbenes by the decomposition of the corresponding diazo compound. In 1980, Pauling predicted this type of push-pull carbene with the idea that by preserving the neutrality of the carbene center the free carbene could be isolated.[39] In this case, the phosphorus is "pushing" electron density to the carbon center via p to p π-interaction, and the silyl group is "pulling" electron density away from the carbon's σ to the silyl σ*. While the original carbene in 1988 could not be crystallized, a similar carbene with a 2,6-bis(trifluoromethyl)benzene substituent instead of a trimethylsilyl substituent was prepared and crystallized.[40]

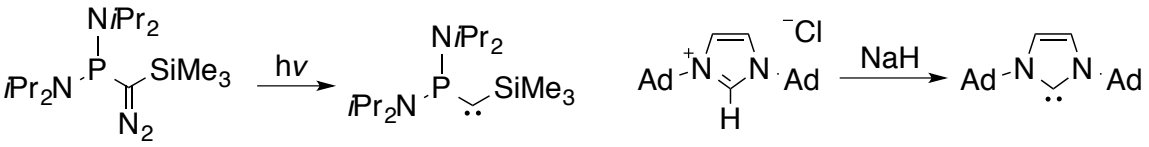

Bertrand, 1988 Arduengo, 1991

Scheme I.5: Synthesis of the first isolable carbene and the first crystalline carbene.

Three years later, Arduengo published the imidazole-2-ylidene or N-heterocyclic carbene (NHC), which was prepared by deprotonating the corresponding imidazolium salt (**Scheme I.5**).[41] This general method of deprotonating the imidazole has given yield to an enormously large number of carbenes. Unlike the push-pull carbenes, which have a relatively obtuse angle of 162° around the carbene carbon and do not make stable transition metal complexes, the incorporation of the carbene into a ring like the Arduengo carbene gives an N-C-N bond angle of 102.2° and very stable transition metal complexes.[42] Transition metal-NHC complexes have proven to be incredibly useful in catalysis as exemplified by the 2nd generation Grubbs catalyst for olefin metathesis.[43]

In 2005, the (cyclic)(alkyl)(amino) carbene (CAAC) was first synthesized from the addition of an epoxide to an azzalyl anion (**Scheme I.6, Route 1**), with the limitation that the sp^3-hybridized carbon center be sterically uncongested. In 2007, a second route utilizing alkylation with an allyl halide as an electrophile allowed for the introduction of large sterically hindering groups (**Scheme I.6, Route 2**).[44] By replacing the π-donating and σ-withdrawing electronegative nitrogen with a quaternary carbon atom incapable of π donating increases both the nucleophilicity and electrophilicity of the carbene compared to the NHC, as demonstrated by examining the HOMO and LUMO (**Figure I.3**).[45] The addition of the carbon instead of nitrogen also allows for the steric environment around the carbene to be changed in addition to positioning a chiral center alpha to the carbene center.

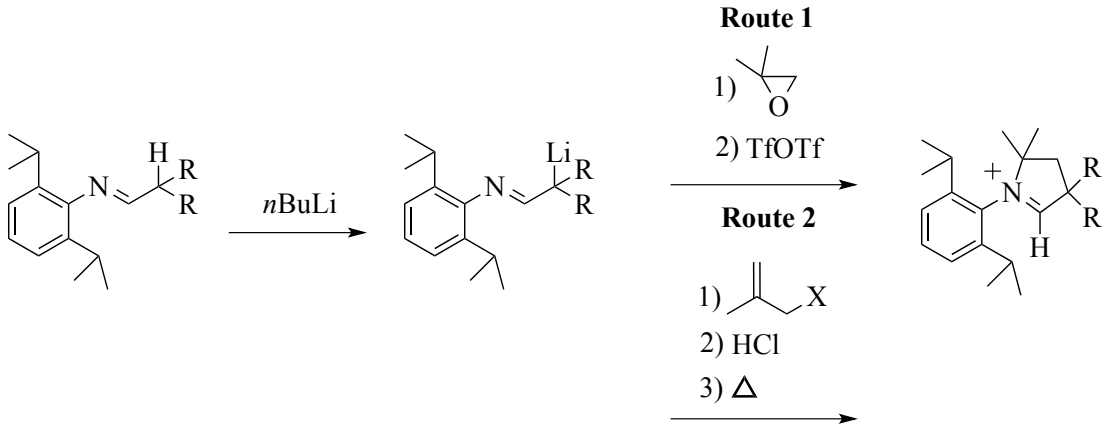

Scheme I.6: Two synthetic routes to (cyclic)(alkyl)amino carbenes CAACs.

Since the development of the NHC and CAAC, several other groups have experimented with the ability to tune carbenes. In 2009, Bielawski showed that by including a bis-diamido functionality in the imidizolium ring decreases both the

nucleophilicity of the carbene, but also generates a carbene that is more electrophilic than the CAACs (**Figure I.3**).[46]

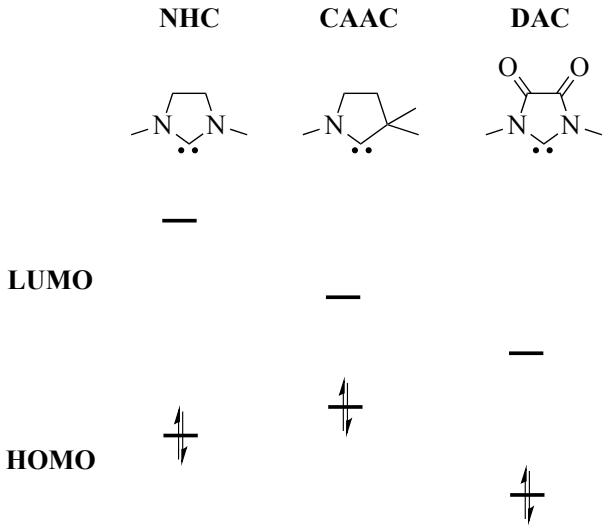

Figure I. 3: Comparison of the HOMO and the LUMO for carbenes.

The unusual electronic nature of CAACs is best demonstrated by the fact that CAACs react with H_2, whereas NHCs do not. Very similar to the mechanism for the activation of H_2 by frustrated Lewis pairs, the CAAC donates electrons into the σ* of the H-H bond and the σ bond donates into the partially vacant p-orbital on carbon resulting in the formal oxidative addition of the carbene with H_2.[47]

Given the high nucleophilicity and strong electrophilic character of CAACs they have been used to isolate and stabilize main group elements, in particular boron and phosphorus, in both interesting geometries and oxidation states. Prior to 2011, borylenes had only been spectroscopically characterized in a solid inert argon matrix or as part of transition metal complexes.[48] By utilizing the CAAC's donor abilities to decrease the Lewis acidity at the boron and the CAAC's electrophilicity to decrease the Lewis basicity of boron, **I.1** (Scheme 1.7) is reduced to the corresponding borylene **I.2**.[49] In comparison,

when the analogous NHC complex is reduced the diborene is isolated, which is the dimer of the borylene.[50] Interestingly, **I.2** behaves as a Lewis base and can be oxidized by one elctron up reacting with $GaCl_3$ yielding **I.3**.

The boryl anion **I.5** was also recently isolated by deprotonating the corresponding borohydride.[51] Due to both the electrophilic nature of the carbene and the electron withdrawing cyanide groups, the borohydride becomes acidic enough to be deprotonated with a strong base. The noteworthy shortening of the carbene-boron bond in **1.5 (**1.473Å) compared to **I.4** (1.617 Å) is indicative of significant delocalization of the electron density to the carbene.

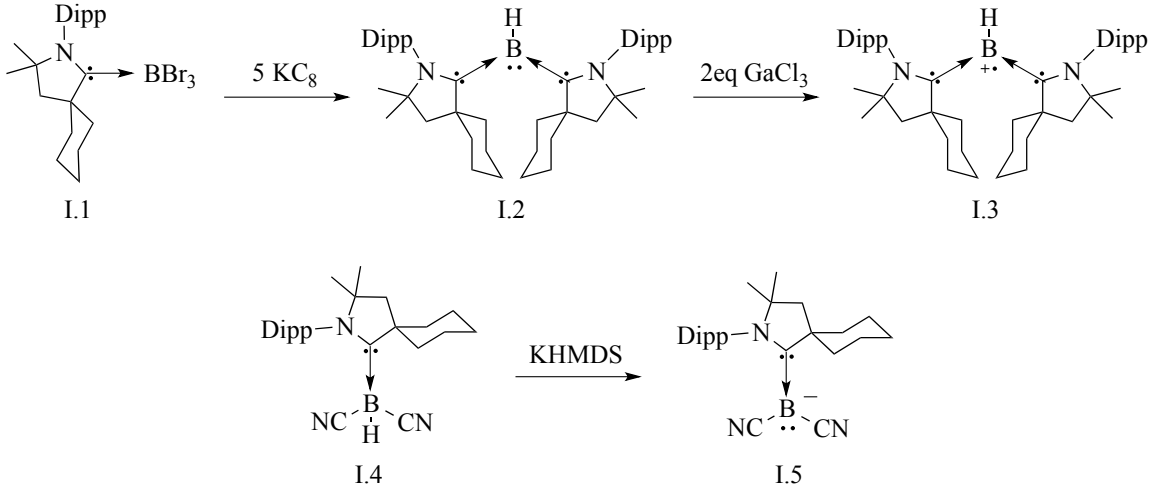

Scheme I.7: Synthesis of the CAAC stabilized borylene and boryl anion.

It has also been shown that both NHCs and CAACs react with P_4 to yield new phosphorus allotropes in the zero oxidation state. For example, the linear P_4 chain **I.6** was isolated by adding 2eq of the bulky menthyl-CAAC to white phosphorus (**Scheme I.8**).[52] However, by altering the stoichiometry so that there is an excess of white phosphorus and decreasing the steric bulk of the CAAC, the P_8 cluster with four CAACs **I.7** is accessible.[53] Moreover, by changing carbenes to the less electrophilic NHC, the P_{12}

allotrope can be isolated.[54] Further work by the Bertrand lab has shown that by changing the solubility of P_4 and the ensuing products, different carbene P_4 and P_2 allotropes can be crystallized.[55] The P_2 fragment **I.8** can undergo a one electron oxidation with the trityl cation to afford the radical cation **I.9**.[56] While identical results have been found with the analogous NHC complexes instead of CAACs, the NBO analysis shows the P_2 fragment to be significantly more positive in **I.9** than with the NHCs due to the ability of the CAAC to accept electron density from the P_2 fragment. Experimentally, it was shown that the NHC analogue of **I.8** can be oxidized twice to the dication, further showing that the P_2 fragment is more electron rich in the NHC case. These few examples demonstrate the interest of using different carbenes for promoting the aggregation of P_4 to neutral phosphorus allotropes, and the ability of carbenes to stabilize both electron rich and electron-poor fragments.

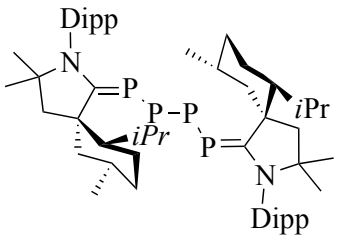

I.6

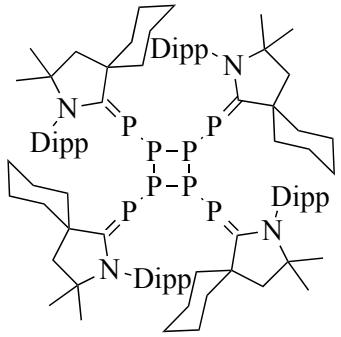

I.7

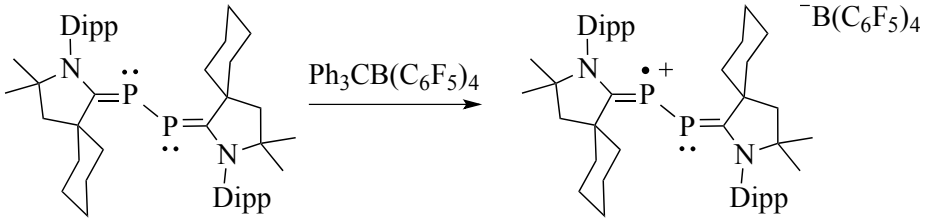

I.8 I.9

Scheme I.8: Carbene stabilized allotropes of P_2, P_4 and P_8.

Most recently, the Bertrand lab has shown that mono, di and tri (amino)(carboxy)radicals **I.11-I.13** utilizing a CAAC backbone could be isolated and characterized structurally for the first time by reducing the corresponding iminium salt **I.10**.[57] The spin density was calculated to be 40% on the carbene carbon, 24% on the nitrogen and 34% on the benzoyl oxygen and carbon. The similar benzoyl radical with a thiazolyidene scaffold could be identified by EPR (Electron Paramagnetic Resonance), and was persistent for several hours, but could not be isolated and fully characterized by X-ray crystallography, demonstrating the need for the electrophilic CAAC support.

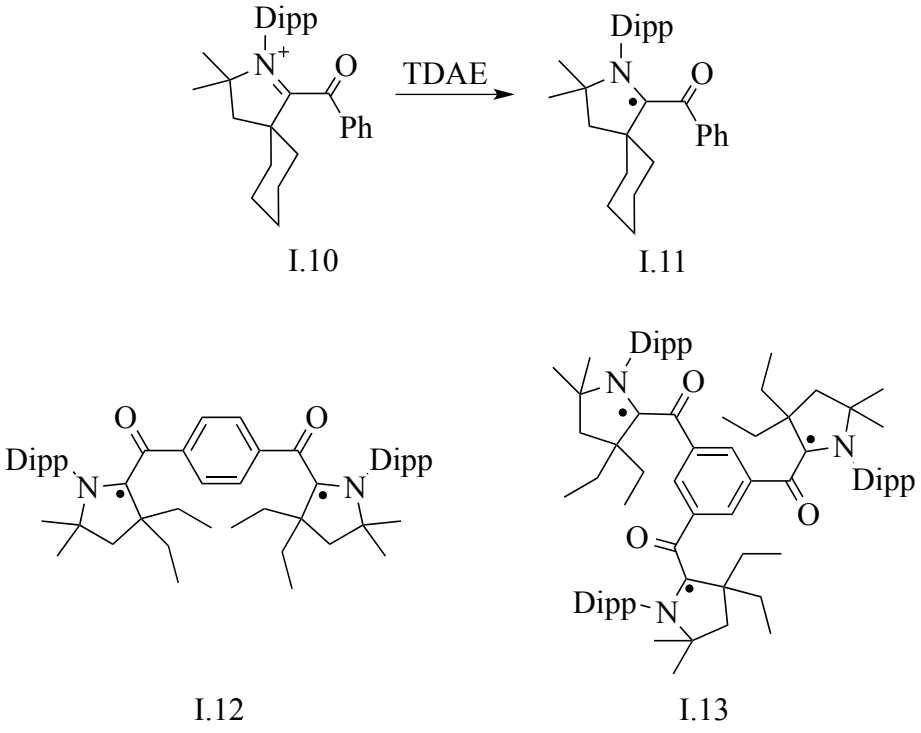

Scheme I.9: Using a CAAC support, the mono-, di, and tri- (amino)(carboxy)radicals could be isolated.

Another known example of CAACs stabilizing main group elements in the zero oxidation state is from the group of Roesky. They have shown that Si(0) **I.15** can be stabilized and isolated by the two electron reduction of the corresponding silicon (II)

dihalide **I.14**.[58] The resulting computational bonding scenario equates to a C-Si-C π-orbital in which 40% of the electron density is located at the silicon atom and the remaining spin density is located at the two carbons. Although the group of Frenking calculated similar systems to be possible with NHCs, it is clear that the use of NHCs in such a system would not be stable due to their inability to accept the required electron density.[59]

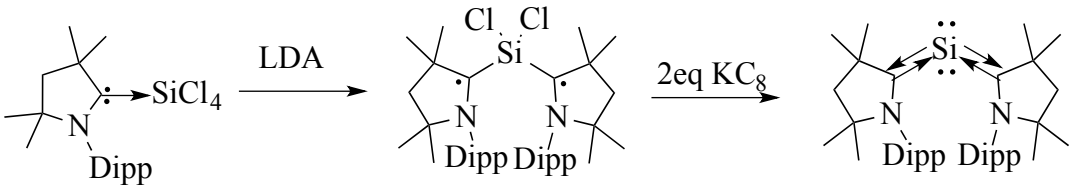

I.14 I.15

Scheme I.10: Isolation of a Si(0) species from the reduction of the Si(II) dihalide.

Concomitant to the research presented in this thesis, Roesky showed CAACs can be used for the isolation of transition metals in the zero oxidation state, specifically manganese (**Scheme I.11**).[60] The two electron reduction of CAAC-$MnCl_2$ **I.16** with 2eq of KC_8 in the presence of free carbene yielded the linear Mn(0) complex **I.17** stabilized with two carbenes. Addition of H_2 to the biscarbene Mn(0) complex yielded hydrogen splitting with the hydrogens becoming attached to the carbene carbons **I.18**.[61] While there is precedent of H_2 activation with metal complexes, the hydrogen is usually split at the metal center; for example, the addition of H_2 to unsaturated Cr, Mo, W complexes.[62] Calculations on **I.17** show the electronic configuration of the manganese to be d^6 with one radical electron delocalized over the two-carbene carbons giving explanation to the reactivity with H_2.

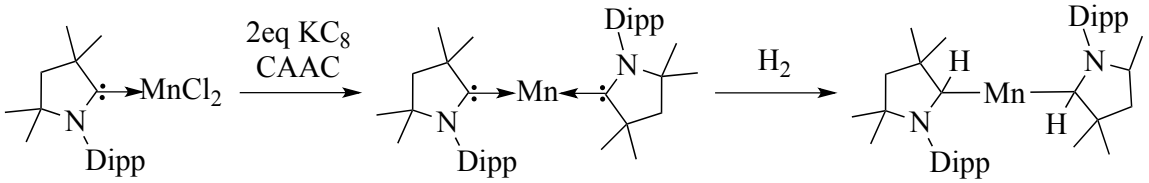

I.16 I.17 I.18

Scheme I.11: Isolation of a Mn(0) species and reactivity with H_2.

Similar to the previous example with manganese, Roesky has also shown that the reduction of CAAC-$ZnCl_2$ **I.19** with 2eq of KC_8 results in the bis CAAC-Zn complex **I.20** with zinc in the zero oxidation state.[63] The spin state of this complex is best described as a singlet biradicaloid **I.21**.

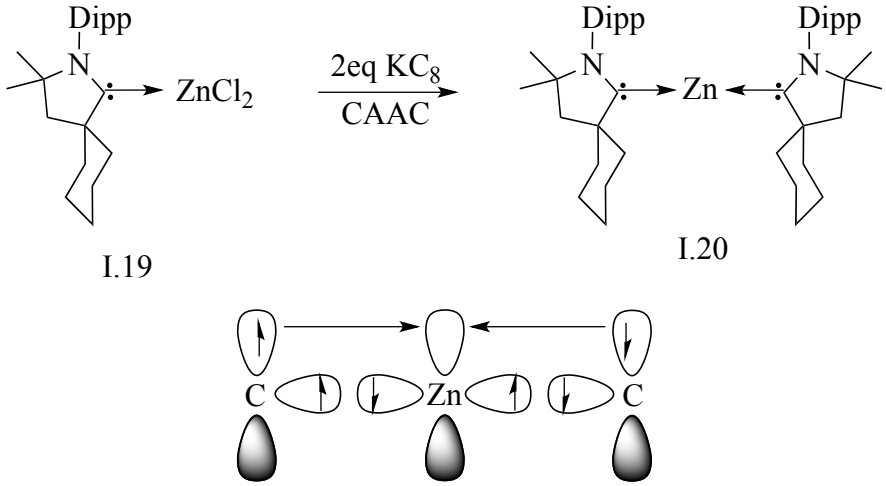

I.19 I.20

I.21

Scheme I.12: Isolation of a bis-CAAC Zn(0) species.

By utilizing the CAAC's ability to both make strong bonds with transition metals and accept electron density, the chemistry described herein represents the first reduced coinage metal complexes with CAAC ligands. Chapter 1 will be dedicated to the isolation and characterization of the first monomeric gold(0) species. By utilizing what we learned from the monomeric gold(0) species, chapter 2 will focus on the synthesis of a neutral

(CAAC)Au-Au(CAAC) complex. This chapter will also focus on the reactivity of the gold dimer with a variety of organic molecules. Chapter 3 will focus on making a neutral $(CAACAu)_3$ species and the reactivity of $(CAACAu)_3^+$. The chemistry developed with gold is then incorporated with copper leading to a copper(0) species, chapter 4, and a Cu-Cu dimer, chapter 5.

References

[1] Ueda, J., Samusawa, M., Kumagai, K., Ishida, A., Tanabe, S., *J. Mater. Sci.* **2014**, *49*, 3299-3304.

[2] Colomban, P., Tournié, A., Ricciardi, P., *J. Raman Spectrosc.* **2009**, *40*, 1949-1955.

[3] Mulvaney, P., *MRS Bulletin* **2001**, *26*, 1009-1014.

[4] a)Faraday, M., *Philosophical Transactions of the Royal Society of London* **1857**, *147*, 145-181; b)Schmid, G., Fenske, D., *Philosophical Transactions of the Royal Society A: Mathematical, Physical and Engineering Sciences* **2010**, *368*, 1207-1210.

[5] Turkevich, J., Stevenson, P. C., Hillier, J., *Discussions of the Faraday Society* **1951**, *11*, 55-75.

[6] Frens, G., *Nature Physical Science* **1973**, *241*, 20-22.

[7] a)Brust, M., Fink, J., Bethell, D., Schiffrin, D. J., Kiely, C., *J. Chem. Soc., Chem. Commun.* **1995**, 1655-1656; b)Brust, M., Walker, M., Bethell, D., Schiffrin, D. J., Whyman, R., *J. Chem. Soc., Chem. Commun.* **1994**, 801-802.

[8] Haruta, M., Kobayashi, T., Sano, H., Yamada, N., *Chem. Lett.* **1987**, *16*, 405-408.

[9] Turner, M., Golovko, V. B., Vaughan, O. P., Abdulkin, P., Berenguer-Murcia, A., Tikhov, M. S., Johnson, B. F. G., Lambert, R., *Nature* **2008**, *454*, 981-983.

[10] Gao, W., Chen, X. F., Li, J. C., Jiang, Q., *J. Phys. Chem. C* **2009**, *114*, 1148-1153.

[11] Wen, F., Englert, U., Gutrath, B., Simon, U., *Eur. J. Inorg. Chem.* **2008**, *2008*, 106-111.

[12] a)Bellon, P., Manassero, M., Sansoni, M., *J. Chem. Soc., Dalton* **1973**, 2423-2427; b)Briant, C. E., Hall, K. P., Mingos, D. M. P., *J. Organomet. Chem.* **1983**, *254*, C18-C20.

[13] Gutrath, B. S., Oppel, I. M., Presly, O., Beljakov, I., Meded, V., Wenzel, W., Simon, U., *Angew. Chem., Int. Ed.* **2013**, *52*, 3529-3532.

[14] Zeller, E., Beruda, H., Schmidbaur, H., *Inorg. Chem.* **1993**, *32*, 3203-3204.

[15] Kamei, Y., Shichibu, Y., Konishi, K., *Angew. Chem., Int. Ed.* **2011**, *50*, 7442-7445.

[16] Shichibu, Y., Konishi, K., *Small* **2010**, *6*, 1216-1220.

[17] Li, J., Li, X., Zhai, H.-J., Wang, L.-S., *Science* **2003**, *299*, 864-867.

[18] Gade, L. H., *Angew. Chem., Int. Ed.* **1997**, *36*, 1171-1173.

[19] Dyson, P. J., Mingos, D. M., in *Gold, Progress in Chemistry, Biochemistry and Technology* (Ed.: H. Schmidbaur), Wiley, Chichester, UK, **1999**, pp. 511-556.

[20] Schmidbaur, H., Schier, A., *Chem. Soc. Rev.* **2012**, *41*, 370-412.

[21] Hall, K. P., Mingos, D. M. P., in *Prog. Inorg. Chem.*, John Wiley & Sons, Inc., **2007**, pp. 237-325.

[22] Lee, S., Molina, L. M., López, M. J., Alonso, J. A., Hammer, B., Lee, B., Seifert, S., Winans, R. E., Elam, J. W., Pellin, M. J., Vajda, S., *Angew. Chem., Int. Ed.* **2009**, *48*, 1467-1471.

[23] Chrétien, S., Gordon, M. S., Metiu, H., *J. Chem. Phys* **2004**, *121*, 3756-3766.

[24] a)Oliver-Meseguer, J., Cabrero-Antonino, J. R., Domínguez, I., Leyva-Pérez, A., Corma, A., *Science* **2012**, *338*, 1452-1455; b)Oliver-Meseguer, J., Leyva-Pérez, A., Corma, A., *ChemCatChem* **2013**, *5*, 3509-3515.

[25] Vignolle, J., Tilley, T. D., *Chem. Commun.* **2009**, 7230-7232.

[26] For reviews, see for example: a)Bourissou, D., Guerret, O., Gabbaï, F. P., Bertrand, G., *Chem. Rev.* **1999**, *100*, 39-92; b)Díez-González, S., Marion, N., Nolan, S. P., *Chem. Rev.* **2009**, *109*, 3612-3676; c)Dröge, T., Glorius, F., *Angew.e Chem., Int.l Ed.* **2010**, *49*, 6940-6952; d)Hahn, F. E., Jahnke, M. C., *Angew. Chem., Int. Ed.* **2008**, *47*, 3122-3172; e)Lin, J. C. Y., Huang, R. T. W., Lee, C. S., Bhattacharyya, A., Hwang, W. S., Lin, I. J. B., *Chem. Rev.* **2009**, *109*, 3561-3598; f)Martin, C. D., Soleilhavoup, M., Bertrand, G., *Chemical Science* **2013**, *4*,

3020-3030; g)Melaimi, M., Soleilhavoup, M., Bertrand, G., *Angew. Chem., Int. Ed.* **2010**, *49*, 8810-8849; h)Poyatos, M., Mata, J. A., Peris, E., *Chem. Rev.* **2009**, *109*, 3677-3707; i)Tapu, D., Dixon, D. A., Roe, C., *Chem. Rev.* **2009**, *109*, 3385-3407; j)Vignolle, J., Cattoën, X., Bourissou, D., *Chem. Rev.* **2009**, *109*, 3333-3384; k)Canac, Y., Soleilhavoup, M., Conjero, S., Bertrand, G., *J. Organomet. Chem.* **2004**, *689*.

[27] Dumas, J. B., Peligot, E., *Ann. Chim. Phys* **1835**, *58*, 5.

[28] Buchner, E., Curtius, T., *Ber. Dtsch. Chem. Ges* **1885**, *8*, 2377.

[29] Staudinger, H., Kupfer, O., *Ber. Dtsch. Chem. Ges* **1912**, *45*, 501.

[30] Doering, W. v. E., Hoffmann, A. K., *J. Am. Chem. Soc* **1954**, *76*, 6162.

[31] Breslow, R., *J. Am. Chem. Soc* **1958**, *80*, 3719.

[32] Wanzlik, H. W., *Angew. Chem.* **1962**, *74*, 129.

[33] Tschugajeff, L., Skanawy-Grigorjewa, M., Posnjak, A., Skanawy-Grigorjewa, M., *Z. Anorg. Allg. Chem.* **1925**, *148*, 37-42.

[34] Fischer, E. O., Maasböl, A., *Angew. Chem., Int. Ed.* **1964**, *3*, 580-581.

[35] Öfele, K., *J. Organomet. Chem.* **1968**, *12*, P42-P43.

[36] Wanzlick, H. W., Schönherr, H. J., *Angew. Chem., Int. Ed.* **1968**, *7*, 141-142.

[37] Schrock, R. R., *J. Am. Chem. Soc.* **1974**, *96*, 6796-6797.

[38] Igau, A., Grutzmacher, H., Baceiredo, A., Bertrand, G., *J. Am. Chem. Soc.* **1988**, *110*, 6463-6466.

[39] Pauling, L., *J. Chem. Soc., Chem. Commun.* **1980**, 688-689.

[40] Buron, C., Gornitzka, H., Romanenko, V., Bertrand, G., *Science* **2000**, *288*, 834-836.

[41] Arduengo, A. J., Harlow, R. L., Kline, M., *J. Am. Chem. Soc.* **1991**, *113*, 361-363.

[42] Crudden, C. M., Allen, D. P., *Coord. Chem. Rev.* **2004**, *248*, 2247-2273.

[43] Vougioukalakis, G. C., Grubbs, R. H., *Chem. Rev.* **2009**, *110*, 1746-1787.

[44] a)Jazzar, R., Bourg, J.-B., Dewhurst, R. D., Donnadieu, B., Bertrand, G., *J. Org. Chem* **2007**, *72*, 3492-3499; b)Jazzar, R., Dewhurst, R. D., Bourg, J.-B., Donnadieu, B., Canac, Y., Bertrand, G., *Angew. Chem., Int. Ed.* **2007**, *46*, 2899-2902.

[45] Martin, D., Lassauque, N., Donnadieu, B., Bertrand, G., *Angew. Chem., Int. Ed.* **2012**, *51*, 6172-6175.

[46] Hudnall, T. W., Bielawski, C. W., *J. Am. Chem. Soc.* **2009**, *131*, 16039-16041.

[47] Frey, G. D., Lavallo, V., Donnadieu, B., Schoeller, W. W., Bertrand, G., *Science* **2007**, *316*, 439-441.

[48] a)Bettinger, H. F., *J. Am. Chem. Soc.* **2006**, *128*, 2534-2535; b)Hassanzadeh, P., Andrews, L., *J. Phys. Chem.* **1993**, *97*, 4910-4915.

[49] Kinjo, R., Donnadieu, B., Celik, M. A., Frenking, G., Bertrand, G., *Science* **2011**, *333*, 610-613.

[50] a)Wang, Y., Quillian, B., Wei, P., Wannere, C. S., Xie, Y., King, R. B., Schaefer, H. F., Schleyer, P. v. R., Robinson, G. H., *J. Am. Chem. Soc.* **2007**, *129*, 12412-12413; b)Wang, Y., Quillian, B., Wei, P., Xie, Y., Wannere, C. S., King, R. B., Schaefer, H. F., Schleyer, P. v. R., Robinson, G. H., *J. Am. Chem. Soc.* **2008**, *130*, 3298-3299.

[51] Ruiz, D. A., Ung, G., Melaimi, M., Bertrand, G., *Angew. Chem., Int. Ed.* **2013**, *52*, 7590-7592.

[52] Masuda, J. D., Schoeller, W. W., Donnadieu, B., Bertrand, G., *Angew. Chem., Int. Ed.* **2007**, *46*, 7052-7055.

[53] Martin, C. D., Weinstein, C. M., Moore, C. E., Rheingold, A. L., Bertrand, G., *Chem. Commun.* **2013**, *49*, 4486-4488.

[54] Masuda, J. D., Schoeller, W. W., Donnadieu, B., Bertrand, G., *J. Am. Chem. Soc.* **2007**, *129*, 14180-14181.

[55] Back, O., Kuchenbeiser, G., Donnadieu, B., Bertrand, G., *Angew. Chem., Int. Ed.* **2009**, *48*, 5530-5533.

[56] Back, O., Donnadieu, B., Parameswaran, P., Frenking, G., Bertrand, G., *Nat Chem* **2010**, *2*, 369-373.

[57] Mahoney, J. K., Martin, D., Moore, C. E., Rheingold, A. L., Bertrand, G., *J. Am. Chem. Soc.* **2013**, *135*, 18766-18769.

[58] a)Mondal, K. C., Roesky, H. W., Schwarzer, M. C., Frenking, G., Niepötter, B., Wolf, H., Herbst-Irmer, R., Stalke, D., *Angew. Chem., Int. Ed.* **2013**, *52*, 2963-2967; b)Mondal, K. C., Samuel, P. P., Tretiakov, M., Singh, A. P., Roesky, H. W., Stückl, A. C., Niepötter, B., Carl, E., Wolf, H., Herbst-Irmer, R., Stalke, D., *Inorg. Chem.* **2013**, *52*, 4736-4743.

[59] a)Takagi, N., Shimizu, T., Frenking, G., *Chem.—Eur. J.* **2009**, *15*, 3448-3456; b)Takagi, N., Shimizu, T., Frenking, G., *Chem.—Eur. J.* **2009**, *15*, 8593-8604; c)Takagi, N., Tonner, R., Frenking, G., *Chemistry – A European Journal* **2012**, *18*, 1772-1780.

[60] Samuel, P. P., Mondal, K. C., Roesky, H. W., Hermann, M., Frenking, G., Demeshko, S., Meyer, F., Stückl, A. C., Christian, J. H., Dalal, N. S., Ungur, L., Chibotaru, L. F., Pröpper, K., Meents, A., Dittrich, B., *Angew. Chem., Int. Ed.* **2013**, *52*, 11817-11821.

[61] Kubas, G. J., *J. Organomet. Chem.* **2014**, *751*, 33-49.

[62] Bullock, R. M., in *Catalysis without Precious Metals*, Wiley-VCH Verlag GmbH & Co. KGaA, **2010**, pp. 51-81.

[63] Singh, A. P., Samuel, P. P., Roesky, H. W., Schwarzer, M. C., Frenking, G., Sidhu, N. S., Dittrich, B., *J. Am. Chem. Soc.* **2013**, *135*, 7324-7329.

CHAPTER 1:

Isolation of a neutral $CAAC_2Au$ complex

Adapted from:

D. S. Weinberger, M. Melaimi, C. E. Moore, A. L. Rheingold, G. Frenking, P. Jerabek, G. Bertrand*, Angew. Chem. Int. Ed.* **2013**, *52*, 8964-8967.

Introduction

The common oxidation states of gold are –I, +I, and +III, with rare complexes featuring a gold +II, +IV, and +V.[1] To date, apart from elemental gold, the zero oxidation state has been mentioned in mixed gold(0)/gold(I) complexes.[2] However, mononuclear (L_nAu), binuclear (LAu-AuL) and polynuclear [(LAu)n] neutral complexes in which atoms of gold are coordinated end-on by L ligands have never been fully characterized.[3] In 1976 Ozin reported the synthesis of Au carbonyl species by the deposition of Au and CO at 10-12 K. The resulting Au(CO), $Au(CO)_2$ and Au(CO)(OC) products were only detected by infrared spectroscopy and elegant isotopic labeling experiments at very low temperatures, but the products were too unstable at room temperature to be further characterized.[4]

In 1999, Le Floch reasoned that the σ-donating and π-accepting properties of phosphines could be used to stabilize reduced transition metal species. With the addition of silacalix[4]phosphinine to [$AuCl(SMe_2)$] followed by the addition of $GaCl_3$ to abstract the chloride the Au(I) complex **1.1** was obtained. Further reduction of this complex with an alkali metal mirror in a sealed tube at -80 °C gave rise to complex **1.2.** The EPR spectrum, recorded at -80 °C, consists of 20 lines resulting from coupling with both the gold and the four phosphines. However, after warming the tube to -73 °C, the signal decreases in intensity after one hour and completely disappears at -43 °C. Due to the instability of the reduced gold species, an X-ray diffraction study was not obtained.

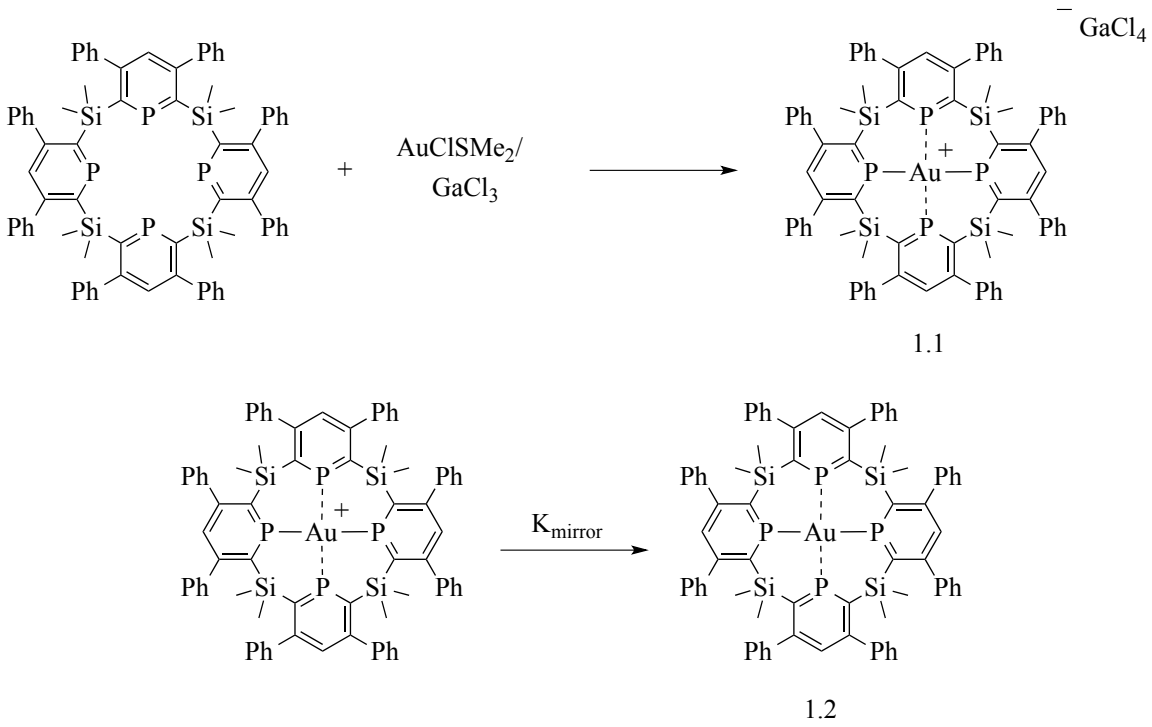

Scheme 1.1: Synthesis of a Au(0) complex with 4 phosphines only detectable at -80°C.

We reason that in order to stabilize the electron rich gold(0) center, the most suitable ligands should be good electron π-acceptors, which are also capable of forming robust bonds with gold. Cyclic (alkyl)(amino)carbenes (CAACs) feature the desired properties; additionally, they have been shown to strongly stabilize paramagnetic centers as outlined in the general introduction.

$CAAC_2Au(0)$ Synthesis and Characterization.

The $CAAC_2Au(I)$ complex **1.3** was prepared according to a modified literature procedure.[5] Instead of the disproportionation of CAACAuCl to $CAAC_2Au(I)$ and $AuCl_2$, two equivalents of the cyclohexyl-CAAC is used to prepare **1.3**. This procedure both increases the yield and ensures the anion to be chloride and not $AuCl_2$.

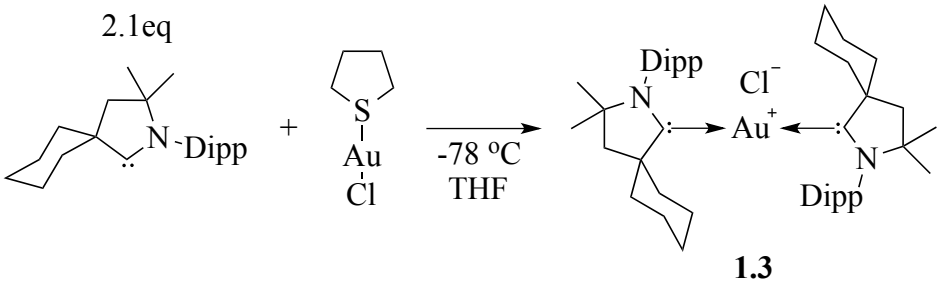

1.3

Scheme 1.2: Synthesis of $(CAAC)_2Au(I)$ from modified literature procedure.

To check our hypothesis that CAACs are able to stabilize gold in the zero oxidation state, we first carried out the cyclic voltammogram (CV) of a THF solution of $(CAAC)_2Au(I)$ complex **1.3**, containing 0.1 M n-Bu_4NPF_6 as the electrolyte (**Figure 1.1**). A reversible one-electron reduction was observed at $E_{½}$ = –2.24 V versus Fc+/Fc, which prompted us to perform the chemical synthesis of $(CAAC)_2Au$ complex **1.4**.

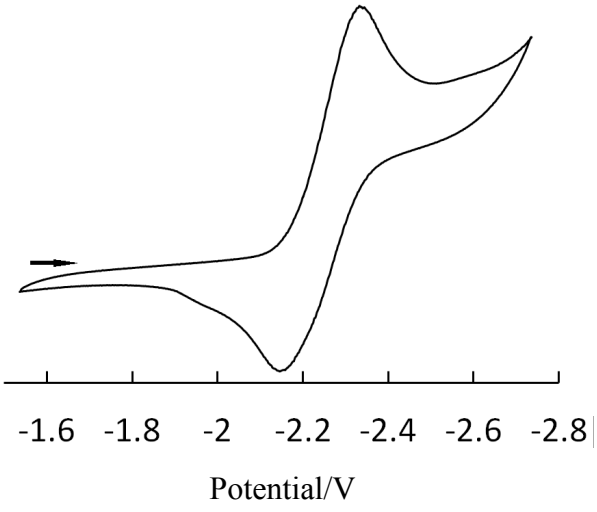

Figure 1.1: Cyclic voltammogram of $(CAAC)_2Au(Cl)$.

A benzene solution of **1.3** was stirred at room temperature for 4 hours in a Schlenk flask coated with a potassium mirror. After filtration and evaporation of the solvent under vacuum, a green solid was obtained (**Scheme 1.3**). The green solid was soluble in non-polar solvents such as hexane and diethyl ether, and this indicated that the

resulting complex was in fact neutral. **1.4** is stable for weeks at room temperature, both in solution and in the solid state.

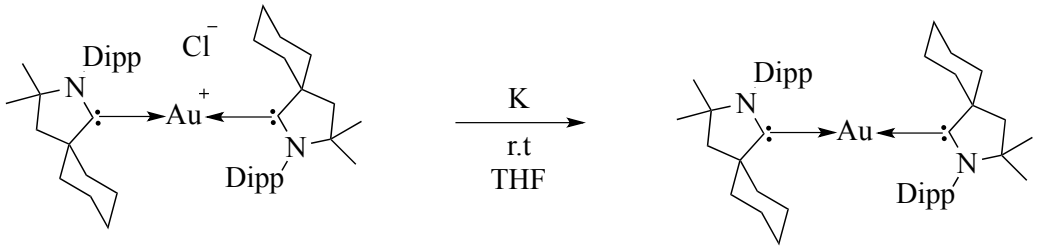

1.3 **1.4**

Scheme 1.3: Synthesis of $(CAAC)_2Au(0)$.

An X-ray diffraction study (**Figure 1.2**) first confirmed that the neutral is complex **1.4**, and features a linear geometry [C1-Au-C1': 180.0°], with the five-membered ring ligands being co-planar (N1-C1-C1'-N1' dihedral angle: 180 °). The Au-C1 [1.991 (2) Å] and C1-N1 [1.344 (3) Å] bond lengths of **1.4** are slightly shorter and longer, respectively, than in the gold(I) precursor **1.3** [2.032 (11) and 1.304 (2) Å], indicating a significant π-backdonation of the unpaired electron from gold to the ligands.

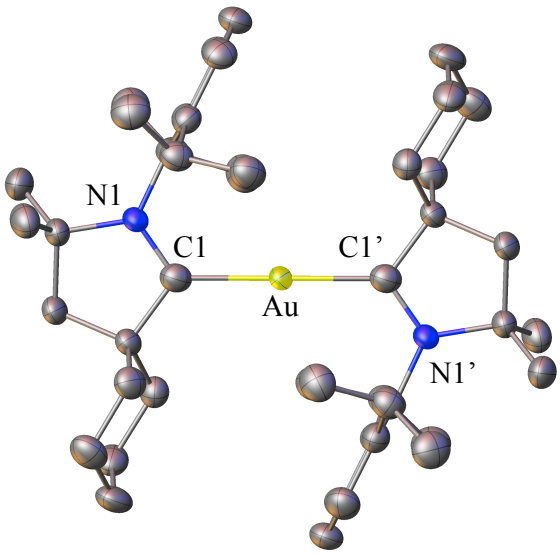

Figure 1.2: X-ray crystal structure of $CAAC_2Au(0)$. Thermal ellipsoids shown at 50% probability and hydrogens omitted for clarity.

As expected, solutions of **1.4** are NMR (Nuclear Magnetic Resonance) silent and EPR active. The room temperature EPR spectrum of **2** in benzene (**Figure 1.3, B)** displays a broad signal at g = 1.9607, while in the solid state (**Figure 1.3, A**), the anisotropic tensors are g_{xx} = 1.9410, g_{yy} = 1.9543 and g_{zz} = 1.9864.

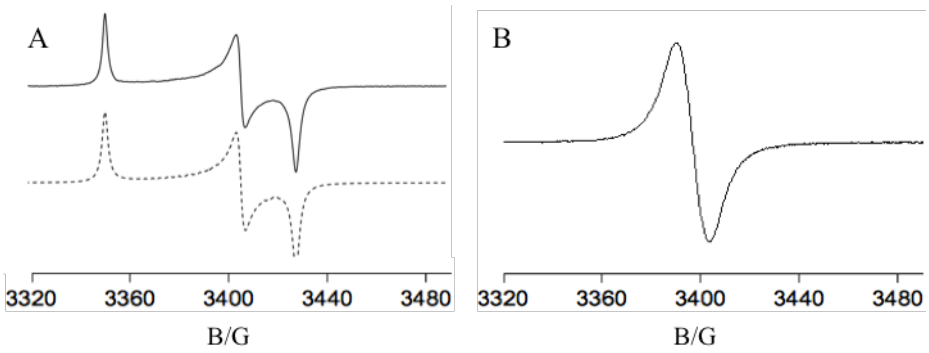

Figure 1.3: EPR of complex **1.4**. A) Frozen benzene solution at 253 K, simulated (---), experimental(—). B) Benzene solution at 298 K.

Additionally, the cyclohexene-CAAC reacts very similarly to the cyclohexyl-CAAC. The $(CAAC)_2AuCl$ with cyclohexene instead of cyclohexyl groups was prepared according to an adapted literature procedure. The reduction with potassium metal yielded the Au(0) species, which was detected by EPR (**Figure 1.4**).

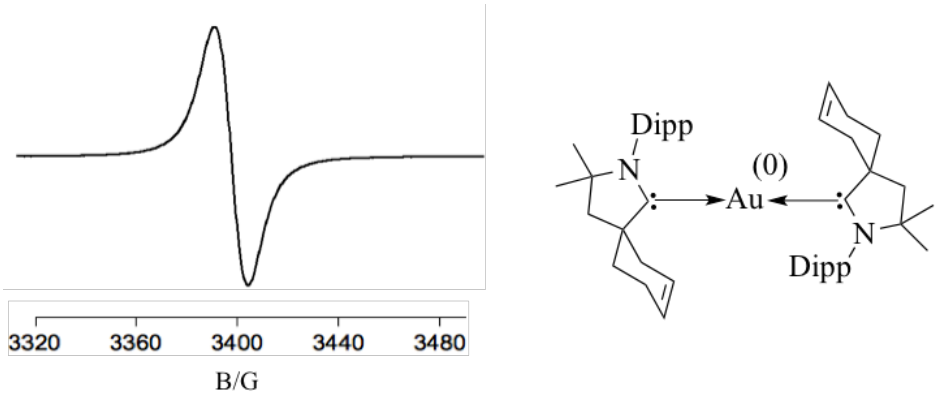

Figure 1.4: EPR of cyclohexeneCAACAu(0).

Calculations at the (U)M05-2X/def2-SVP level, using the NBO method, showed that the spin density in **1.4** is mainly localized at the carbene carbons (60 %) and the nitrogen atoms (20 %), while only 17 % stays at gold. The shape of the SOMO (**Figure 1.5**) shows that the unpaired electron is delocalized over the p(π) AOs of the carbene ligand and the p(π) AO of Au. This means that the electronic reference configuration for the bonding in $Au(CAAC)_2$ is $d^{10}s^0p^1$ and not the ground state configuration $d^{10}s^1 p^0$.

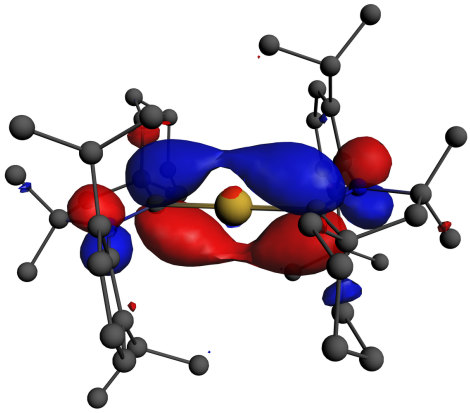

Figure 1.5: Graphical representation of the SOMO of **1.4**.

The NBO results also show a partial positive charge on the gold atom, which is surprising due to the fact that CAACs have been shown to be excellent donors. The EDA-NOCV results also show that the strongest orbital interactions leading to bonding are from the combination of the lone pair molecular orbital of the CAAC into the empty s orbital of the gold (**Figure 1.6, a**). The next strongest interaction is the π-back donation from the p(π) orbital of the gold into the p orbital of the carbene carbon, (**Figure 1.6, b**). The last two major bonding energy contributions are from the d(π) orbital on the gold into the p orbital of the carbene (**Figure 1.6, c**) and the lone pair molecular orbital of the carbene into the p(σ) atomic orbital of gold (**Figure 1.6, d**). These interactions are illustrated in **Figure 1.6** which show the NOCV deformation and the electron density

flow from red to blue. Therefore, the calculated bond dissociation energies for breaking both Au-C bonds into Au and 2CAACs in **1.4** is 91.2 kcal mol^{-1}.

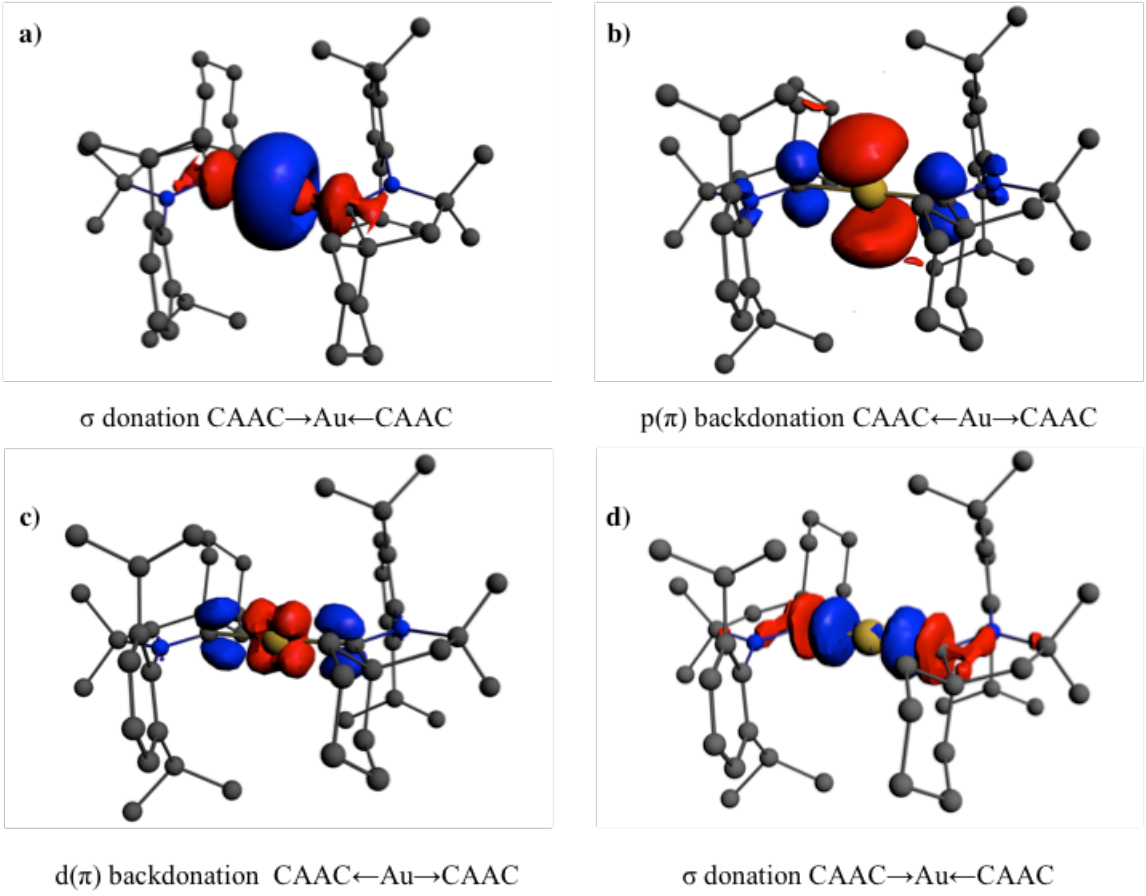

Figure 1.6: EDA-NOCV results showing the highest four bonding interactions.

$(CAAC)_2Au(0)$ Reactivity

It was found that **1.4** is extremely air and moisture sensitive; upon opening a solution of **1.4** in benzene, hexane or THF to air even for a minute time, the EPR signal for **1.4** completely disappears, and becomes NMR active. The $CAAC_2Au(I)$ complex is obtained, and is easily distinguishable in the ^{13}C NMR spectrum with the carbene peak appearing at 251 ppm. Upon addition of dried O_2 to complex **1.4**, clean conversion to the $CAAC_2Au(I)$ complex (**Scheme 1.4)** occurs**.**. Both the ^{1}H and ^{13}C NMR were identical

to that of **1.3**. Unfortunately, crystals of the resulting Au(I) complex could not be grown, so the anion could not be identified.

After examining the literature, there is only one example of monomeric gold being in the +2 oxidation state reported by Kirmse, in which $KAuCl_4$ is reduced in the presence of hexathia-18-crown-6 and nonathia-27-crown-9 (**Figure 1.7**). The Au(II) complex was identifiable by EPR, but could not be crystalized or isolated as a solid.[6]

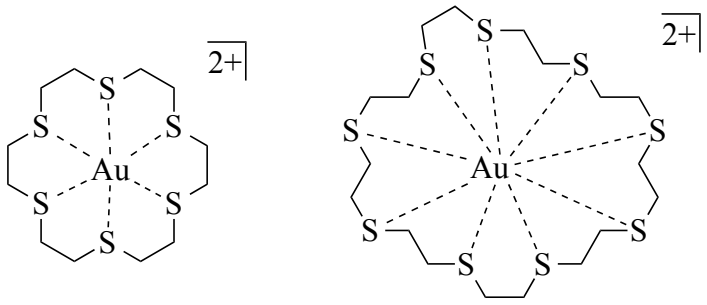

Figure 1.7: Kirmse's Au(II) example with crown thiols.

The only other examples with gold in the (+2) oxidation state are in complexes where there are two Au(II) atoms bonded to each other.[7] These complexes can be written as both in the Au(II) oxidation state, or as a mixed valence Au(I)-Au(III).

Due to the fact that Au(I) complexes can undergo oxidative addition to Au(III), it was of interest to see if the Au(0) complex **1.4** can undergo oxidative addition to give the elusive Au(II) species. Unfortunately, addition of 1 or ½ an equivalent of diphenyl disulfide to **1.4** resulted in the $(CAAC)_2Au(I)$ species which is EPR silent and NMR active (**Scheme 1.4**).

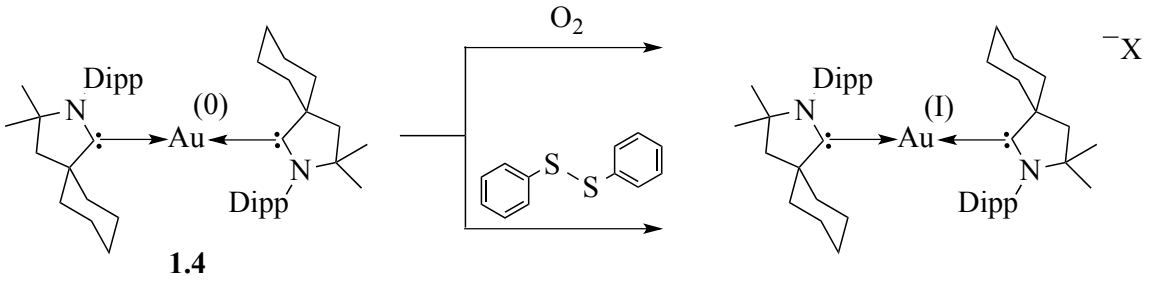

Scheme 1.4: Addition of O_2 and diphenyldisulfide to **1.4**.

Unluckily, crystals could not be grown of this complex; therefore, we could only hypothesize that the anion is phenyl sulfide. Addition of dihalides (Cl_2, Br_2 and I_2) resulted in mixtures of the Au(I) and Au(III) complexes even with stoichiometric addition. EPR studies of the resulting complexes were silent and gave no proof to any Au(II) complex formation.

Given that complex **1.4** can be considered the smallest neutral gold species, and carbon monoxide has been shown to react with gold nanoparticles,[8] we were interested in testing its reactivity. Unfortunately, upon addition of CO both by bubbling and at higher pressures (~2 atm) no reaction could be seen, and the EPR spectrum was identical to that of **1.4** and NMR silent.

Similarly, no change was seen with the addition of substituted alkynes such as diphenylacetylene. However, with the addition of phenylacetylene the dark green solution slowly turned yellow. After 3 hours, the EPR showed no signal and the NMR showed multiple different products. One of these products was crystalized from benzene and proved to be complex **1.5**. This reaction appears to not be so interesting since it is only one of several products detected by NMR. Additionally the mechanism isn't completely understood; however, it most likely goes through the one electron reduction of the

phenylacetylene followed by disproportionation. Then, a second equivalent of **1.4** reduces a second equivalent of phenylacetlyne, which forms the crystallized complex **1.5**.

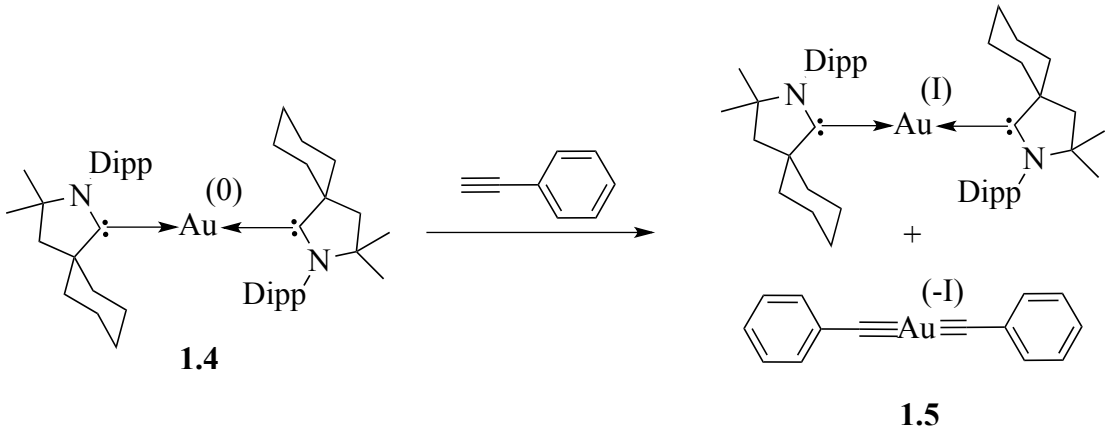

1.4 **1.5**

Scheme 1.5: Addition of phenylacetylene to **1.4** to form **1.5**.

Attempts to make analogous Au(0) complexes.

To prove the necessity of using a π-accepting carbenes, the analogous bis-benzoimidazol-2-ylidene Au(I) $(NHC_2Au)^+$ complex was prepared from a literature procedure.[9] When comparing the π-accepting ability of this NHC versus the CAAC, the benzoimidazol-2-ylidene **1.6** is significantly less accepting.[10] This is demonstrated by the ^{31}P NMR shifts for the corresponding carbene-phosphinidene adducts (**1.8** and **1.9**), the benzoimidazol-2-ylidene (**1.6**) is significantly less π-accepting than the CAACs, but more accepting than other unsaturated NHCs with alkyl substituents. Given the single bond character in **1.8**, the ^{31}P NMR δ for the **1.6**-phosphinidene adduct is -34.6 ppm. In contrast, the cyclohexyl-CAAC adduct **1.9**, has more C=P double bond character which gives a ^{31}P NMR δ = 68.9 ppm. Therefore, it can be concluded that **1.6** is less π-accepting than the previously used CAACs.

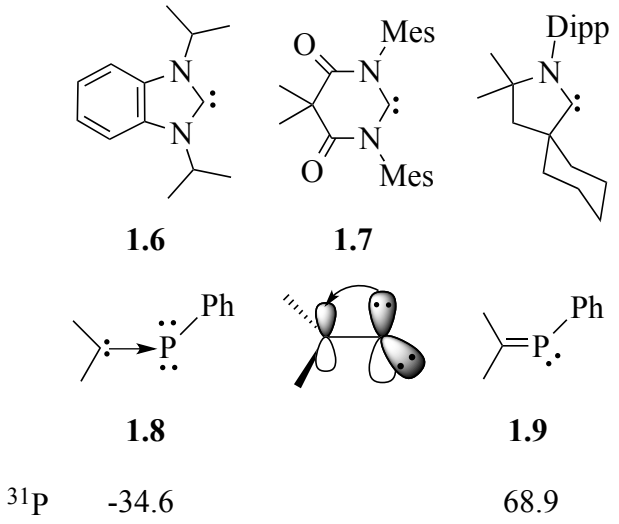

Figure 1.8: π-accepting ability by examining corresponding phosphinidene adducts.

To test the ability of the benzoimidazol-2-ylidene (**1.6**) to stabilize a neutral Au(0) species, **1.10** was reduced under several different conditions.

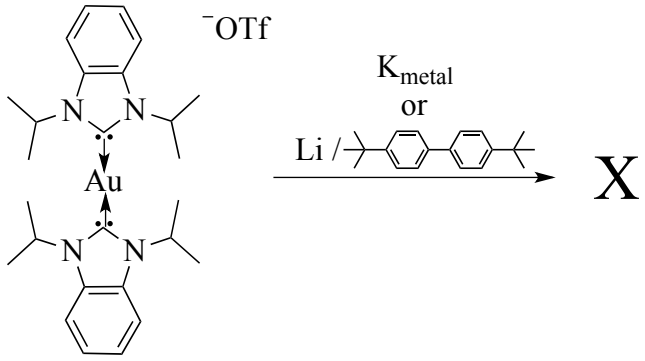

Scheme 1.6: Reduction of bis-benzoimidazol-2-ylidene Au(I)

As expected, it was not possible to prepare the desired Au(0) species. In each case an insoluble red/brown solid was obtained. EPR of the solid showed no signal, and the solid was completely insoluble in all organic solvents.

In the general introduction, the diamido-carbene(DAC) is shown to have a calculated LUMO lower in energy than that of the CAACs;[11] therefore, one might think

that DAC **1.7** and the monoamido-carbenes (MAC) should also be able to stabilize gold in the zero oxidation state. Therefore, the corresponding bis-carbeneAu(I) complexes were prepared.

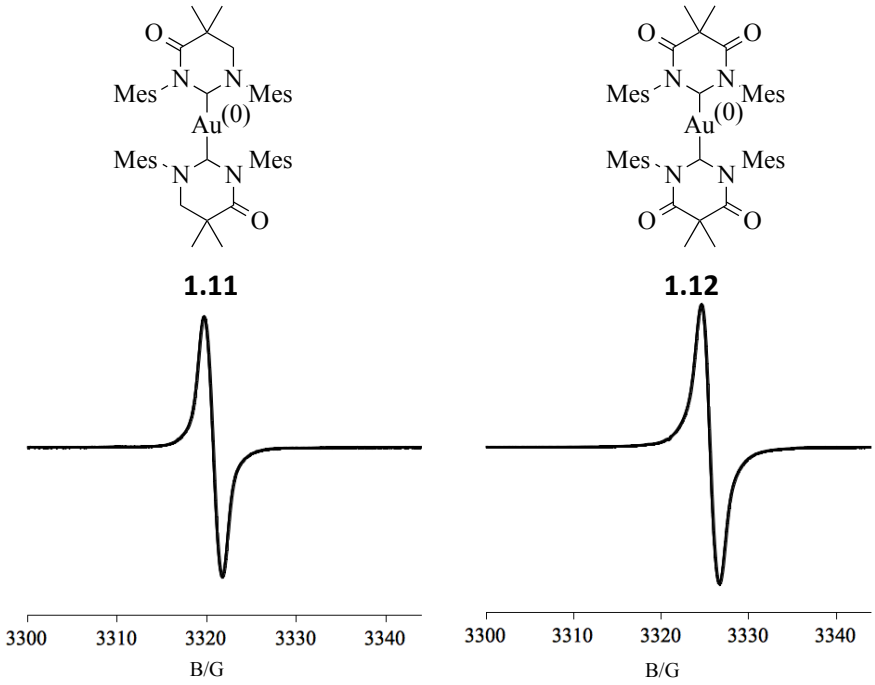

Figure 1.9: EPR and proposed structure for the reduced bis-amido-carbene Au complexes.

Upon addition of potassium to a stirring solution of the bis-carbeneAu(I), the solutions turned reddish brown over the course of a few hours. EPR of **1.11** and **1.12** in solution at room temperature are very similar to the $(CAAC)_2Au(0)$. However, after removing the solvent, the solids are yellow and NMR active; unfortunately, the NMR shows several different products. In contrast to the $CAAC_2Au(0)$ complex, the Au(0) complexes of the MAC and DAC are not stable.

From these results, it can be concluded that electrophilic carbenes are necessary to delocalize the electron density from the gold to stabilize the Au(0) species; however,

stability of these reduced complexes rely heavily on the nature of the carbene. Therefore, the subsequent question is whether a mixed CAAC-Au(0)-L complex could be isolated. Therefore, the Au(I) complexes with both triphenylphosphine and carbon monoxide were prepared. For this study, the CAAC with an adamantyl substituent was chosen since addition of only one ligand to THTAuCl is possible due to increased sterics **1.13**. Subsequently, the chloride was removed with $AgSbF_6$ in methylene chloride to give the cationic complex **1.14**. Addition of a large excess of triphenylphosphine and carbonmonoxide provided the desired Au(I) complexes **1.15** and **1.16**, respectively.

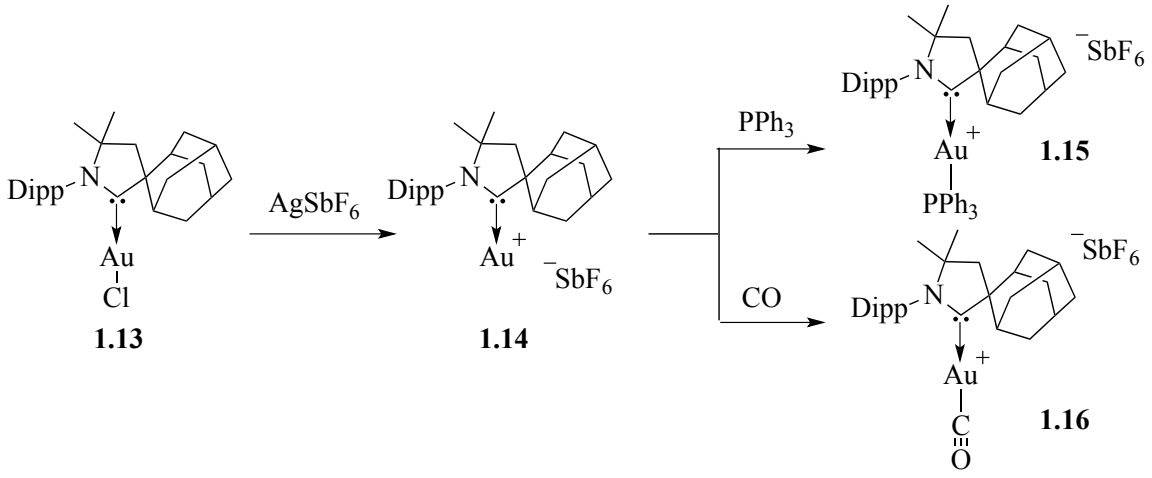

Scheme 1.7: Synthesis of mixed CAAC-Au-L complexes.

The reduction of complex **1.15** with potassium metal in THF resulted in a black precipitate, which was completely insoluble in all organic solvents and even water. The EPR of the solid was silent. The use of weaker reducing agents led to no reaction with **1.15**.

Even though the CAAC-Au-CO **1.16** adduct was fully characterized and crystallized in methylene chloride and chloroform, in THF, acetonitrile or benzene the complex would instantaneously expel carbon monoxide after addition. Due to the fact

that the CO is highly labile, it proved impossible to reduce this species with the CO still bound.

Conclusion

In this chapter, we demonstrated that a formal Au(0) complex could be prepared from the reduction of the Au(I) precursor when stabilized by two CAACs. The Au(0) complex was fully characterized by EPR and X-ray crystallography affording the first example of a stable and isolable Au(0) compound. Given the π-accepting ability of the CAAC, the electron density is delocalized both onto the carbene carbon and the nitrogen atoms of the CAAC. Therefore, approximately 17 % of the electron density is at the Au atom.

The Au(0) complex proved to be extremely air and water sensitive and very hard to handle. Reactivity studies showed the inability of the Au(0) to undergo oxidative addition at the metal with a variety of oxidants; instead, resulting in the one electron reduction of the oxidant to give back the Au(I) species and a variety of counter anions.

Through attempted reductions of a NHC_2-Au(I) complex and a variety of CAAC-Au-L complexes, we showed that it is necessary to have two CAACs attached to the Au in order to isolate the monomeric Au(0) species.

Chapter 1 has been adapted from materials published in D. S. Weinberger, M. Melaimi, C. E. Moore, A. L. Rheingold, G. Frenking, P. Jerabek, G. Bertrand, *Angew. Chem. Int. Ed.* **2013**, 52, 8964-8967. The dissertation author was the primary investigator of this paper and the reactivity discussed above.

Appendix: Experimental Section

General: All manipulations were performed under an inert atmosphere of dry argon, using standard Schlenk techniques. Dry, oxygen-free solvents were employed. EPR spectra were recorded on Bruker EMX. ^{1}H and ^{13}C spectra were recorded on Bruker Avance 300 (^{1}H=300.13 MHz, ^{13}C=75.48 MHz) or Varian Inova 500 (^{1}H=500.1 MHz, ^{13}C=125.8 MHz). All spectra were obtained in the solvent indicated at 25 °C. Chemical shifts are given in ppm and are referenced to residual protonated solvent. Melting points were measured with a Buchi melting point apparatus system. **1.10**[9] and **1.14**[5] were prepared from the previously published literature procedures.

1.3

Free cyclohexyl CAAC (500 mg, 1.536 mmol) and THTAuCl (221 mg, 6.911 x10^{-1} mmol) were loaded into a Schlenk flask in the glove box. At -78 °C, 30 mL of THF was added and the solution was allowed to slowly warm up to room temperature over 14 h. The solvent was evaporated and the slightly yellow solid washed with 3 x 15 mL *n*-hexane. The solid was then extracted with 3 x 5 mL of methylene chloride and dried under vacuum. ^{1}H NMR (CD_3CN) d 7.50 (dd, ^{3}J = 8.4 Hz, ^{3}J = 7.0 Hz, 2H, $H_{p,ar}$), 7.39 (d, ^{3}J = 7.0 Hz, 4H, $H_{m,ar}$), 2.71 (sept, ^{3}J = 6.7 Hz, 4H, CH), 2.10 (s, 4H, CH_2), 1.63 – 1.52 (m, 8H), 1.37 (s, 12H, $C(CH_3)_2$), 1.31 (br s, 12 H, $C(CH_3)_2$), 1.26 – 1.21 (m, 24H, $CH(CH_3)_2$). $^{13}C\{^{1}H\}$NMR (CD_3CN) 251.2 ($C_{carbene}$), 146.1 ($C_{o,ar}$), 135.8 ($C_{m,ar}$), 131.1 ($C_{p,ar}$), 126.3 ($C_{m,ar}$), 82.7 (C_{quat}), 60.2 (C_{quat}), 45.3 (CH_2), 36.3 (CH_2), 29.8, 29.6, 27.3, 25.8 (CH_2), 23.6, 22.2 (CH_2).

1.4

Gold complex **1.3** $[(CyCAAC)_2Au]^{+}Cl^{-}$ (200 mg) was added to a flame dried Schlenk flask previously coated with a potassium mirror (~ 50mg). 30 mL of THF was added, and the solution was stirred for 4 hours at room temperature. Subsequently, the solution was filtered and the solvent was removed under vacuum. The residue was extracted with 3 x 20 mL of benzene and the solvent was removed to yield a green solid. Crystals suitable for X-ray diffraction were grown at -30 °C from a concentrated THF solution. Yield: 85 mg (44 %). Mp: 110 °C.

Crystal data and structure refinement for **1.4**

Identification code	DW_04_06_2012bi
Empirical formula	$C_{46}H_{70}AuN_2$
Formula weight	848.00
Temperature/K	100(2)
Crystal system	triclinic
Space group	P-1
a/Å	9.5989(9)
b/Å	10.6415(10)
c/Å	11.8800(14)

α/°	105.645(2)
β/°	112.0460(10)
γ/°	103.0030(10)
Volume/Å^3	1008.16(18)
Z	1
ρ_{calc}mg/mm^3	1.397
m/mm^{-1}	3.681
F(000)	439.0
Crystal size/mm^3	0.28 × 0.16 × 0.10
Radiation	MoKα (λ = 0.71073)
2Θ range for data collection	4.688 to 51.998°
Index ranges	-11 ≤ h ≤ 10, -11 ≤ k ≤ 13, -14 ≤ l ≤ 10
Reflections collected	3884
Independent reflections	3884 [R_{int} = 0.0316, R_{sigma} = 0.0189]
Data/restraints/parameters	3884/0/230
Goodness-of-fit on F^2	1.026
Final R indexes [I>=2σ (I)]	R_1 = 0.0150, wR_2 = 0.0389
Final R indexes [all data]	R_1 = 0.0150, wR_2 = 0.0389
Largest diff. peak/hole / e Å^{-3}	0.55/-0.47

1.4 + diphenyldisulfide

In the glove box, diphyenlydisulfide (19 mg, 8.844 x 10^{-5} mol) was added to a stirring solution of **1.4** (150mg, 1.768 x 10^{-4} mol) in 5 mL of THF. The solution instantly turned yellow. The solution was evaporated to dryness and washed with 3 x 3 mL of *n*-hexane. $^{13}C\{^1H\}$NMR (CD_3Cl) 251.4 ($C_{carbene}$), 144.4 ($C_{o,ar}$), 129.8, 128.7, 127.0, 124.8, 116.4, 81.4 (C_{quat}), 59.0 (C_{quat}), 44.5 (CH_2), 35.2 (CH_2), 30.8, 29.0, 28.4, 26.3, 25.1, 24.5, 22.7, 20.9.

1.5

In the glove box, **1.4** (139 mg, 1.639 x 10^{-4} mol) was dissolved in 40 mL of benzene. Phenylacetylene (0.04ml, 2 eq, 3.280x10^{-4} mol) was added and the solution was allowed to stir for 3 h. After evaporating the solvent, a yellow/green solid was obtained. The NMR in C_6D_6 was indicative of at least 4 different products. A few crystals suitable for X-ray diffraction were grown from slow evaporation of a concentrated benzene solution.

Crystal data and structure refinement for **1.5.**

Identification code	davidw_05_17_2012_0m
Empirical formula	$C_{80}H_{98}Au_2N_2$
Formula weight	1481.54
Temperature/K	100 (2)
Crystal system	monoclinic
Space group	$P2_1/n$

a/Å	12.109(7)
b/Å	41.92(2)
c/Å	14.316(8)
α/°	90.00
β/°	106.524(7)
γ/°	90.00
Volume/$Å^3$	6968(7)
Z	4
$\rho_{calc}mg/mm^3$	1.412
m/mm^{-1}	4.249
F(000)	3000.0
Radiation	MoKα (λ = 0.71073)
2Θ range for data collection	3.54 to 46.46°
Index ranges	$-13 \leq h \leq 13$, $-38 \leq k \leq 46$, $-15 \leq l \leq 15$
Reflections collected	37875
Independent reflections	9915 [R_{int} = 0.1551, R_{sigma} = 0.1593]
Data/restraints/parameters	9915/658/769
Goodness-of-fit on F^2	1.055
Final R indexes [I>=2σ (I)]	R_1 = 0.0896, wR_2 = 0.1942
Final R indexes [all data]	R_1 = 0.1605, wR_2 = 0.2320
Largest diff. peak/hole / e $Å^{-3}$	1.82/-2.65

1.11 & 1.12

In the glove box, DAC_2AuCl or MAC_2AuCl (65-100 mg) and potassium metal (~50 mg) were loaded into a Schlenk flask. 8 mL of THF were added and the solution was stirred for 1 h to yield a dark red solution. After filtration, the solution was transferred into an EPR tube, and the EPR was collected. The remaining solution was evaporated to give a yellow solid which was EPR silent and NMR active. The ^1H and ^{13}C NMR spectra contained many products and the spectra could not be explained.

1.15

In the glove box, AdCAAC-Au-Cl **1.14** (310 mg, $5.082x10^{-4}$ mol) and $AgSbF_6$ (210 mg, 1.2 eq, $6.098x10^{-4}$ mol) were loaded in a Schlenk flask. 10 ml of methylene chloride was added at room temperature and stirred for 14 h. The solution was then filtered and PPh_3 (266 mg, 10 eq, $1.016x10^{-3}$ mol) was added and stirred overnight. The solution was evaporated under vacuum and the solid washed with 5 x 10 mL n-hexanes. The solid was extracted with 3 x 3 mL of methylene chloride and then the solvent evaporated. Yield: 374 mg (88%). Crystals suitable for X-ray diffraction were grown from slow evaporation of concentrated methylene chloride solution. $^{13}C\{^1H\}$NMR (CD_2Cl_2) 256.0 ($C_{carbene}$), 255.0 ($C_{carbene}$), 145.0 ($C_{o,ar}$), 135.4 ($C_{m,ar}$), 133.7 ($C_{m,\ ar}$), 133.5 ($C_{m,\ ar}$) 132.3 ($C_{p,ar}$), 129.1 ($C_{p,ar}$), 128.6 ($C_{m,ar}$), 125.5 ($C_{m,ar}$) 125.5 ($C_{m,ar}$), 79.9 (C_{quat}), 65.3 (C_{quat}), 53.5 (CH_2), 48.2 (CH_2), 38.5, 36.9, 36.1, 34.0, 29.2, 29.0, 27.9, 26.7, 23.0

Crystal data and structure refinement for **1.15**.

Identification code	GB_DSW_004_0m
Empirical formula	$C_{45}H_{54}AuF_6NPSb$
Formula weight	1072.58
Temperature/K	100 (2)
Crystal system	triclinic
Space group	P-1
a/Å	9.7455(3)
b/Å	11.7514(4)
c/Å	19.4752(7)
α/°	106.3390(10)
β/°	97.9460(10)
γ/°	97.3040(10)
Volume/Å^3	2087.14(12)
Z	2
ρ_{calc}mg/mm^3	1.707
m/mm^{-1}	4.256
F(000)	1060.0
Radiation	MoKα (λ = 0.71073)
2Θ range for data collection	4.44 to 50.8°
Index ranges	$-10 \leq h \leq 11$, $-14 \leq k \leq 14$, $-23 \leq l \leq 23$
Reflections collected	26990
Independent reflections	7642 [R_{int} = 0.0211, R_{sigma} = 0.0197]
Data/restraints/parameters	7642/0/505
Goodness-of-fit on F^2	0.669
Final R indexes [I>=2σ (I)]	R_1 = 0.0185, wR_2 = 0.0611
Final R indexes [all data]	R_1 = 0.0214, wR_2 = 0.0734
Largest diff. peak/hole / e Å^{-3}	1.53/-0.93

1.16

In the glove box, AdCAAC-Au-Cl **1.14** (310 mg, 5.082x10^{-4} mol) and $AgSbF_6$ (210 mg, 1.2 eq, 6.098x10^{-4} mol) were loaded in a Schlenk flask. 10 ml of methylene chloride was added at room temperature and stirred for 14 hours. The solution was then filtered and CO was bubbled through the solution for 5 min to form a white precipitate. The solution was evaporated under vacuum. Yield: 300 mg (77%). Crystals suitable for X-ray diffraction were grown from slow evaporation of concentrated methylene chloride solution. Yield: 220 mg (51.6 %). ^{1}H NMR (CD_3CN) 7.54 (t, ^{3}J = 8.19 Hz, 1H, $H_{p,ar}$), 7.41(d, ^{3}J=8.19 Hz, 2H, $H_{m,ar}$), 3.64 (d, ^{3}J = 12.1 Hz, 2H). 2.78 (sept, ^{3}J = 6.44 Hz, 2H, CH), 2.48 (s, 2H, CH_2), 2.16 (s, 2H), 2.11 (br, 2H), 2.07 (br, 4H),1.84 (br, 6H), 1.37 (s, 4H), 1.34 (d, ^{3}J=3.87 Hz, 6H), 1.32 (d, ^{3}J=3.86 Hz, 6H). ^{13}C{^{1}H}NMR (CD_2Cl_2) 241.7

($C_{carbene}$), 182.9 (CO), 145.3 ($C_{o,ar}$), 134.8 ($C_{m,ar}$), 131.7 ($C_{p,ar}$), 126.2 ($C_{m,ar}$), 81.3 (C_{quat}), 65.9 (C_{quat}), 48.3 (CH_2), 39.0 (CH_2), 37.4, 37.2, 34.3, 29.5, 28.2, 27.6, 27.2, 23.2.

Crystal data and structure refinement for **1.16.**

Identification code	gb_dsw_002_0m
Empirical formula	$C_{25}N_9O_2ClAuSb_{0.5}F_{0.5}H_{0.5}$
Formula weight	840.34
Temperature/K	100 (2)
Crystal system	triclinic
Space group	P-1
a/Å	11.1584(18)
b/Å	11.9182(19)
c/Å	12.2017(19)
α/°	83.993(7)
β/°	65.814(6)
γ/°	77.161(7)
Volume/$Å^3$	1443.1(4)
Z	2
$\rho_{calc}mg/mm^3$	1.9338
m/mm^{-1}	6.075
F(000)	809.7
Crystal size/mm^3	0.20 × 0.15 × 0.10
Radiation	(λ = 0.71073)
2Θ range for data collection	3.5 to 53.04°
Index ranges	$-14 \leq h \leq 14$, $-14 \leq k \leq 14$, $-15 \leq l \leq 15$
Reflections collected	19291
Independent reflections	5927 [R_{int} = 0.0214, R_{sigma} = 0.0227]
Data/restraints/parameters	5927/0/343
Goodness-of-fit on F^2	1.967
Final R indexes [I>=2σ (I)]	R_1 = 0.0234,
Final R indexes [all data]	R_1 = 0.0277, wR_2 = 0.2170
Largest diff. peak/hole / e $Å^{-3}$	1.52/-1.68

References

[1] Pyykkö, P., *Angew. Chem., Int. Ed.* **2004**, *43*, 4412-4456.

[2] a)Serpell, C. J., Cookson, J., Thompson, A. L., Brown, C. M., Beer, P. D., *Dalton Trans.* **2013**, *42*, 1385-1393; b)Vignolle, J., Tilley, T. D., *Chem. Commun.* **2009**, 7230-7232; c)Weidner, T., Baio, J. E., Mundstock, A., Große, C., Karthäuser, S., Bruhn, C., Siemeling, U., *Aust. J. Chem.* **2011**, *64*, 1177-1179; d)Zhukhovitskiy, A. V., Mavros, M. G., Van Voorhis, T., Johnson, J. A., *J. Am. Chem. Soc.* **2013**, *135*, 7418-7421.

[3] Raubenheimer, H. G., Schmidbaur, H., *Organometallics* **2011**, *31*, 2507-2522.

[4] McIntosh, D., Ozin, G. A., *Inorg. Chem.* **1977**, *16*, 51-59.

[5] Frey, G. D., Dewhurst, R. D., Kousar, S., Donnadieu, B., Bertrand, G., *J. Organomet. Chem.* **2008**, *693*, 1674-1682.

[6] Kampf, M., Griebel, J., Kirmse, R., *Z. Anorg. Allg. Chem.* **2004**, *630*, 2669-2676.

[7] Mohr, F., Sanz, S., Tiekink, E. R. T., Laguna, M., *Organometallics* **2006**, *25*, 3084-3087.

[8] a)Li, L., Chai, S.-H., Binder, A., Brown, S., Veith, G., Dai, S., *Catal. Lett.* **2014**, *144*, 912-919; b)Taketoshi, A., Haruta, M., *Chem. Lett.* **2014**, *43*, 380-387.

[9] Sivaram, H., Tan, J., Huynh, H. V., *Organometallics* **2012**, *31*, 5875-5883.

[10] Back, O., Henry-Ellinger, M., Martin, C. D., Martin, D., Bertrand, G., *Angew. Chem., Int. Ed.* **2013**, *52*, 2939-2943.

[11] Martin, D., Lassauque, N., Donnadieu, B., Bertrand, G., *Angew. Chem., Int. Ed.* **2012**, *51*, 6172-6175.

CHAPTER 2:

Isolation of a neutral (CAAC)Au-Au(CAAC) complex and its reactivity

Adapted from:

D. S. Weinberger, M. Melaimi, C. E. Moore, A. L. Rheingold, G. Frenking, P. Jerabek, G. Bertrand*, Angew. Chem. Int. Ed.* **2013**, *52*, 8964-8967.

Introduction

As illustrated in the previous chapter, it is necessary to have two CAACs to stabilize a gold atom in the zero oxidation state. Therefore, the next obvious question is whether it is possible to isolate a Au-Au dimer using the same CAAC ligands. Besides the mixed valence gold clusters discussed in the general introduction, there are also a few examples of multinuclear mixed-metal clusters, such as [cis-η^2-(Ph_3P)Au-Au(PPh_3)}$Ph_3PCr(CO)_4$] **2.1** in which the Au atoms can be considered to have an oxidation state of zero.[1] Early claims by Mingos in 1980 on the preparation of [(PPh_3)Au-Au(PPh_3) **2.2** have not been confirmed,[2] and calculations by Schwerdtfeger and Boyd on the model compound (H_3P)Au-Au(PH_3) **2.3** leave serious doubts about the structural assignment.[3] In fact, this type of dinuclear gold(0) species supported by phosphines has been postulated as intermediates to rationalize the formation of gold nanoparticles.[4] The differences between the calculations and the structure published by Mingos are very different. The Au-Au bond of Mingos is much more in the range of an aurophilic interaction rather than an actual Au-Au bond, which was calculated by Schwerdtfeger and Boyd. Moreover, if this was simply an aurophilic interaction between the d and s orbitals, this would also explain the large difference in the Au-Au-P bond angle compared to the calculated angle of 180°.

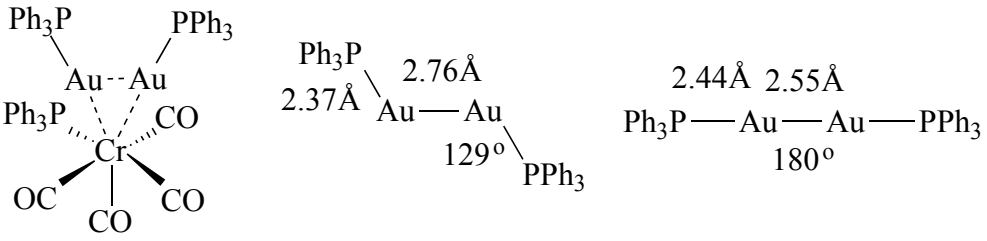

2.1 Raubenheimer, 2003 **2.2** Mingos, 1980 **2.3** Schwerdtfeger & Boyd, 1992

Figure 2.1: Previously published Au-Au dimers and relevant calculation.

Raubenheimer and Schmidbaur wrote that "*it is very likely that N-heterocyclic carbenes (NHCs) may be the right choice to prepare the much sought-after complexes of the Au_2 molecule*".[5] A study by Sadighi *et al*. sought to generate (NHC)Au-Au(NHC) **2.5** by the deprotonation of the corresponding cationic proton-bridged species **2.4**; however, they found that **2.5** could not even be detected and led to colloidal gold.[6]

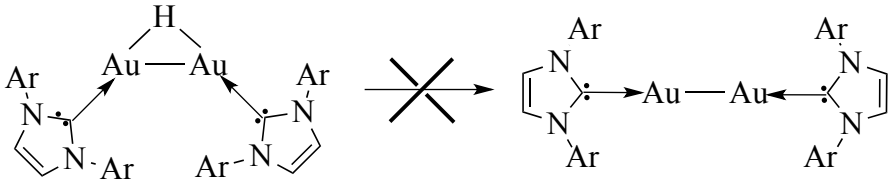

2.4 **2.5**

Scheme 2.1: Sadighi *et al.* proposed synthesis for Au-Au dimer stabilized with NHCs.

Given our previous success with stabilizing the monomeric Au(0) complex and other extremely reactive complexes with CAACs, described in detail in the general introduction, we sought to make the Au-Au dimer with CAACs.

(CAAC)Au-Au(CAAC) Synthesis and Characterization.

For this purpose, the bulky menthyl-substituted CAAC was chosen and the (CAAC)AuCl complex **2.6** was prepared.[7] Subsequently, the cyclic voltammogram

showed a quasi-reversible reduction at -2.8 V (versus Fc+/Fc). This was extremely surprising since we would have expected an irreversible reduction to occur due to formation of the dimer. Therefore we computed the energy to dimerization by varying the distance between two (CAAC)Au• radicals and found that there was no barrier to dimerization. Theoretically, once the gold radical is made it should recombine to form the dimer.

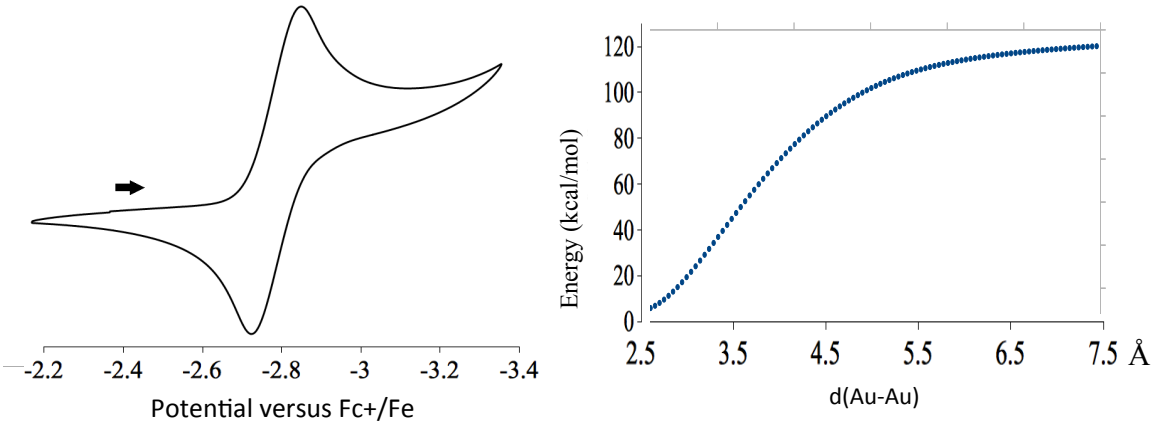

Figure 2.2: CV of complex **2.6** and calculated energy as two CAACAu• approaching each other showing no boundary to dimerization.

Consequently, **2.6** was reduced at room temperature with a suspension of lithium sand in THF. After work up, the dinuclear complex **2.7** was isolated in 20 % yield as a highly air- and water-sensitive brown solid. Its non-ionic character was indicated by its solubility in non-polar solvents, such as n-hexane, and its diamagnetic nature apparent from NMR spectroscopy.

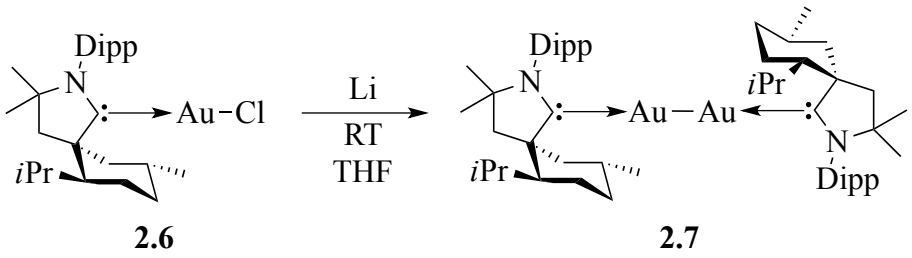

2.6 **2.7**

Scheme 2.2: Synthesis of CAACAu-AuCAAC.

Interestingly, a ^{13}C NMR signal was observed at δ = 286 ppm, downfield-shifted by δ = 50 ppm compared to the carbene gold(I) precursor **2.6**; a similar trend has been observed with a variety of metal-NHC complexes when comparing oxidation states zero and one. A single-crystal X-ray diffraction study confirmed the desired (CAAC)Au-Au(CAAC) structure. There are six molecules in the asymmetric unit, three of them are nearly identical, the others differ merely by the respective orientation of the two carbene ligands; in other words, these molecules are rotamers. When optimizing the structure, the same two minimum energy structures, which are 1.0 kcal/mol different, were found as the Au-Au bond is rotated **Figure 2.3**.

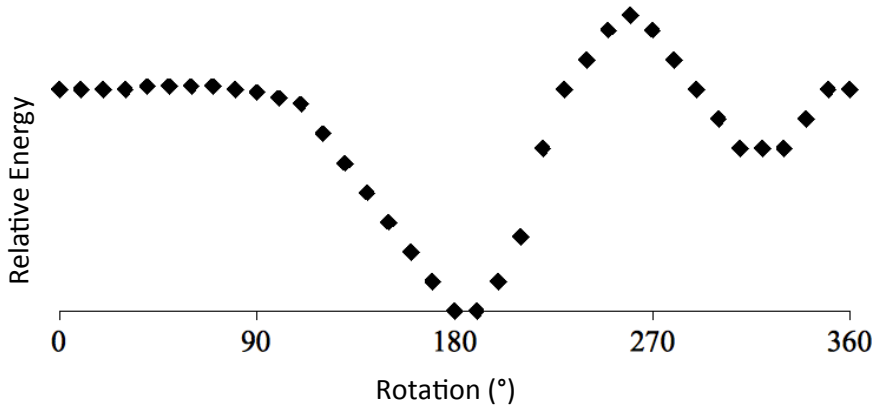

Figure 2.3: Relative energy calculated as Au-Au bond is rotated in (CAAC)Au-Au(CAAC).

As predicted by Scwerdtfeger and Boyd for $(H_3P)Au\text{-}Au(PH_3)$, the C1-Au1-Au2-C2 skeleton is almost linear (C1-Au1-Au2: 173.8(2), Au1-Au2-C2: 171.3(3)°), and the gold-gold bond is short (2.5520(6) Å) (**Figure 2.4**).

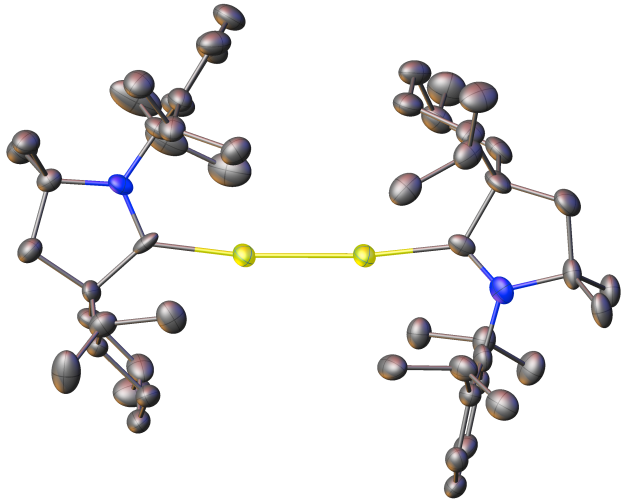

Figure 2.4: Crystal structure of just one of the rotamers for (CAAC)Au-Au(CAAC). Thermal ellipsoids are at 50 % probability and hydrogens are omitted for clarity.

Unlike the $(CAAC)_2Au(0)$ species where the gold atom carried a positive charge, the NBO calculations (M05-2X/SVP) for the Au-Au dimer show the gold atom to have a slightly negative charge (-0.05 e). As expected, the EDA-NOCV (M05-2X/SVP) results show that the Au-Au bond is the result of the coupling of the unpaired electrons in the valence s AO of the gold with minor contributions (~13%) from the d_z^2(**Figure 2.5 A**). Therefore, the gold reacts through its ground state configuration of $d^{10}s^1p^0$, compared to the $(CAAC)_2Au(0)$ which reacted through its excited $d^{10}s^0p^1$. Consequently, the strongest ligand-metal bond is between the CAAC's lone pair ligand orbitals which donate into the antibonding Au-Au σ* orbital. Accordingly, the Au-Au bond distance in elemental Au_2 is a little shorter (2.546 Å) compared to (CAAC)Au-Au(CAAC) (2.579 Å). The following strongest bonding interaction is the combination of the lone-pair ligand orbitals and the

p(σ) AOs of the gold (**Figure 2.5 B**). Subsequent interactions are from the back donation of the d-orbitals into the carbene p-orbitals (**Figure 2.5 C & D**). The sum of these bonding energies gives a bond dissociation energy (BDE) of 90.6 kcal•mol^{-1} for the cleavage of (CAAC)Au-Au(CAAC) into Au_2 + 2 (CAAC). As discussed in Chapter 1, this energy is very similar to (CAAC)Au(CAAC)→Au+2(CAAC).

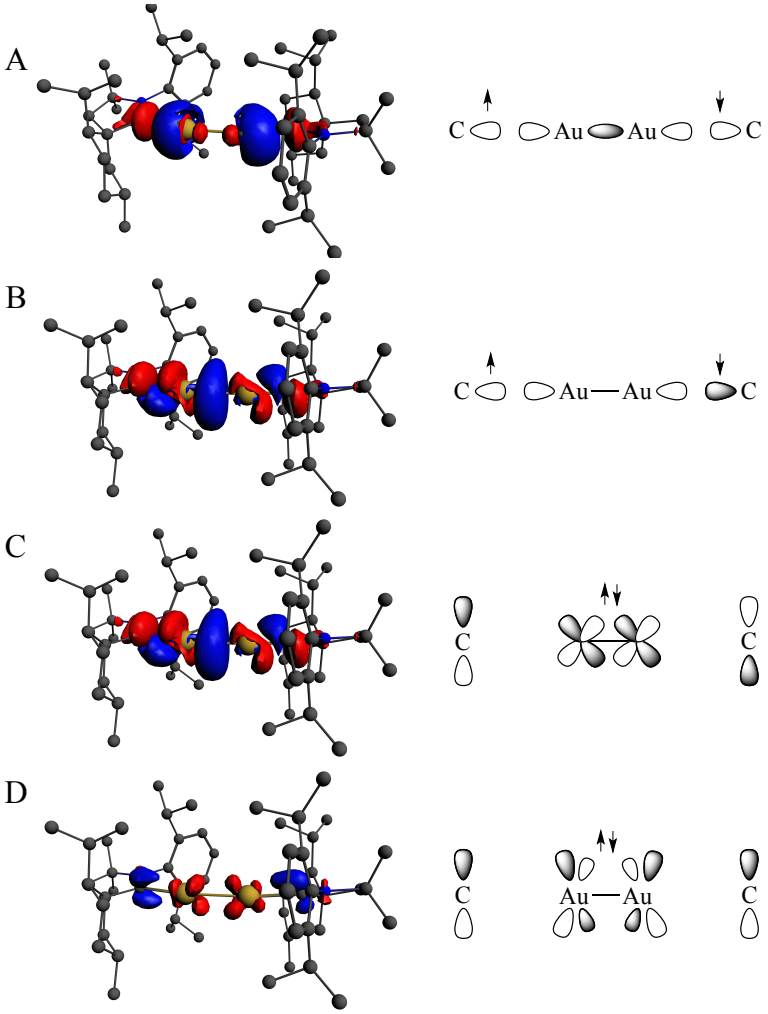

Figure 2.5: EDA-NOCV results for the four strongest ligand-metal bonding interactions.

These results demonstrate that Au_2 can be stabilized end-on with the addition of two CAACs, and given that the HOMO is calculated (**Figure 2.6**) to be almost entirely on the Au-Au bond, this complex should display interesting reactivity.

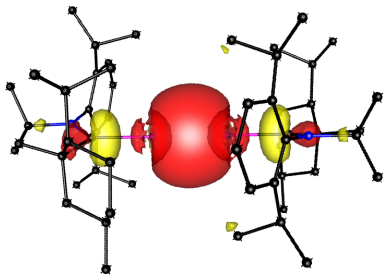

Figure 2.6: Calculated HOMO for CAACAu-AuCAAC.

(CAAC)Au-Au(CAAC) Reactivity.

Due to the fact that it's incredibly difficult to control the stoichiometry when using lithium powder (typical quantity of lithium needed is ~2 mg), one of the primary problems with performing the reduction as described above is the over-reduction of the (CAAC)AuCl to produce free carbene and colloidal gold. In addition, the yield (20 %) is very low to carry out subsequent reactions; therefore, a new method for the formation of **2.7** was needed. Instead of directly using Li powder, the lithium was used to reduce 4,4'-di-tert-butylbiphenyl (DBB) to make the corresponding aryl-radical.[8] By doing this in a nitrogen filled glove box instead of argon, the yield was increased to near quantitative conversion. The separation of **2.7** away from DBB proved to be challenging since **2.7** and DBB have very similar solubilities. Complex **2.7** could be isolated cleanly by washing several times with cold hexane; however, the yield once again would be very low (~20 %). Attempts to sublime the DBB away from **2.7** were unsuccessful due to the thermal instability of the Au-Au dimer. Therefore, for the reactivity described below, **2.7** was reacted in the presence of one equivalent of DBB. Interestingly, this preparation

does not work in an Argon filled glove box because it is believed the lithium is capable of reducing the DBB by more than one electron leading to unwanted impurities. It is speculated that in a N_2 filled glove box this second reduction is much harder since it is known that lithium can react with N_2.[9]

In Chapter 1, we demonstrated that $(CAAC)_2Au(0)$ was an excellent one-electron reducing agent; if we were to assume that the Au-Au dimer would have similar properties, then we can imagine doing one-electron reduction chemistry followed by addition of the Au-Au dimer to the substrate. Therefore, the first reactivity conducted was the addition of tetracyanoethylene (TCNE) to the Au-Au dimer. TCNE is well known to undergo one electron reduction to form $TNCE^-$.[10] However, instead of having the addition of the Au-Au dimer onto the carbon-carbon double bond of the TCNE, the crystal structure shows two independent molecules in the unit cell with the addition of the dimer onto a single CN^- with a $TNCE^-$ anion. As expected, the chemical shift for the carbene carbon in complex **2.8** is indicative of Au(I) with a ^{13}C NMR $\delta = 246$ ppm.

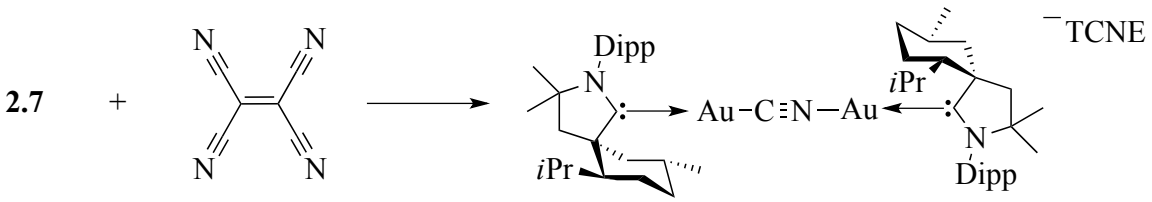

2.8

Scheme 2.3: Addition of tetracyanoethylene (TCNE) to (CAAC)Au-Au(CAAC).

We propose the mechanism to be a one-electron reduction of the TCNE followed by addition of the Au-Au dimer to the CN and C-C bond cleavage. The structure is nearly linear with Au-C-N and Au-N-C bond angles of 174.70° and 173.02°, respectively. The

C-N has an average bond distance of 1.131 Å (**Figure 2.7**), which is very typical for CN triple bonds.

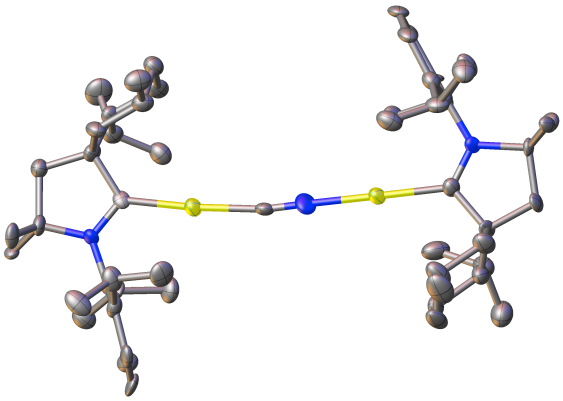

Figure 2.7: Crystal structure of (CAAC)Au-C-N-Au(CAAC) **2.8** . Ellipsoids shown at 50% probability. Hydrogens and TCNE anion are removed for clarity.

Since TCNE proved to be too reactive to do simple one-electron reduction and addition, we tried the addition of the gold dimer to a less redox-active alkene, diethyl fumarate (**Scheme 2.4**). As expected, **2.7** reacts cleanly with the alkene to afford **2.9**.

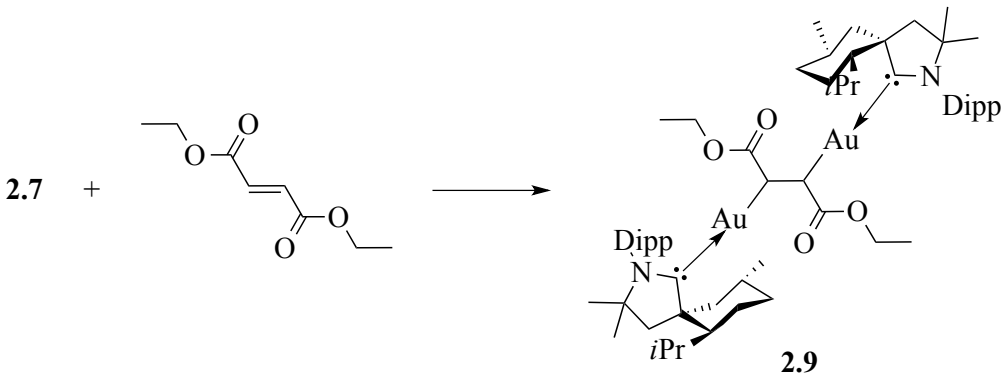

Scheme 2.4: Addition of diethyl fumarate to (CAAC)Au-Au(CAAC).

Crystals suitable for X-ray crystallography were grown from a concentrated hexane solution at -30°C.

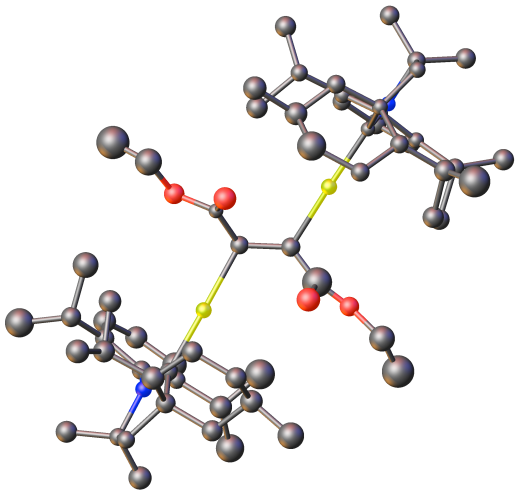

Figure 2.8: Crystal structure of the addition of **2.7** across the alkene of diethyl fumarate. Ellipsoids shown at 50% probability. Hydrogens were removed for clarity.

The C-C bond length of 1.456 Å (**Figure 2.8**) is indicative of reduction of the alkene to make a C-C single bond. Additionally, the ^{13}C NMR δ = 260 ppm is indicative of a CAACAu(I) with an alkyl group bound.[11]

Since it was shown that non-redox active alkenes reacted cleanly with the Au-Au dimer, the subsequent step was to test reactivity with alkynes. No reactions were observed with acetylene, diphenylacetylene, and 4-hexyne, indicating that an electrophilic alkyne was needed. Therefore, dimethyl acetylenedicarboxylate (DMAD) was reacted with **2.7**.

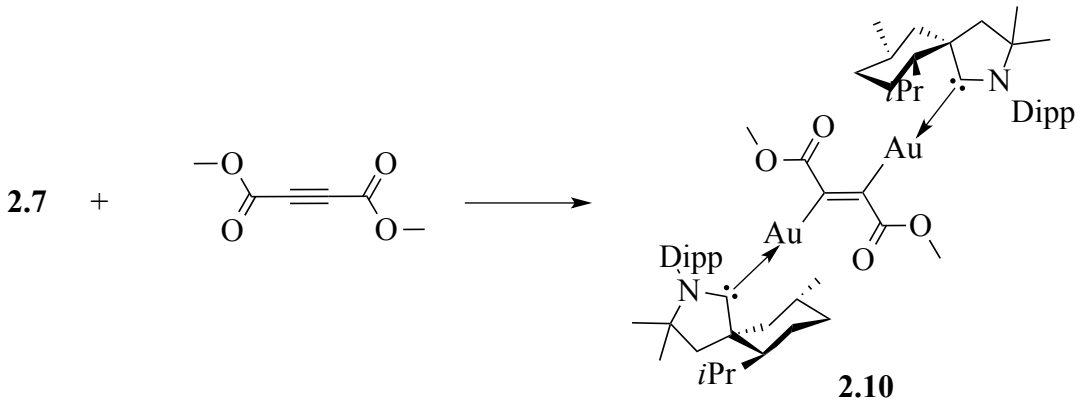

Scheme 2.5: Addition of DMAD to (CAAC)Au-Au(CAAC).

The crude NMR showed two sets of similar signals indicating the formation of two very similar products. However, after several washings with cold hexane, only **2.10** was isolated and crystallized. Interestingly, the expected geometry for the addition to the alkyne would have been cis; however, as shown in **Figure 2.9,** the crystallized species shows trans addition. Given that the crude NMR indicated two products, it could be rationalized that the other complex in solution is in fact the cis addition of the dimer to the alkyne.

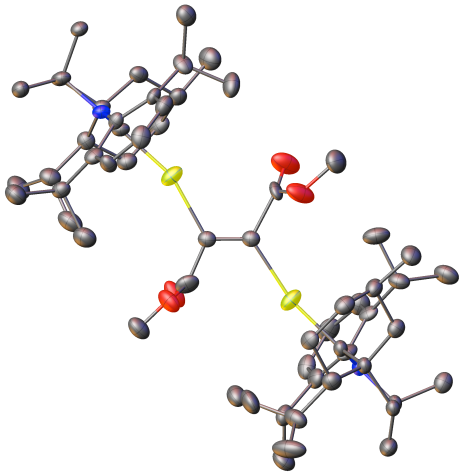

Figure 2.9: Crystal structure of the addition of **2.7** across DMAD. Ellipsoids shown at 50% probability. Hydrogens are removed for clarity.

From the X-ray crystal structure, the C=C bond length of 1.367 Å clearly shows that the carbon-carbon triple bond was reduced to a double bond. The dihedral angle (Au-C-C-Au) is 177.49°, which is very close to the expected 180.0°. Additionally the C-Au-C bond angle of 167.32° differs slightly from the expected linear geometry for CAACAu(I) complexes.

Given the white phosphorus (P_4)-metal complexes published by Scheer *et al.*,[12] we believed the Au-Au dimer could react with P_4 and result in similar complexes. Examination of the literature indicates that similar complexes with gold have never been reported.

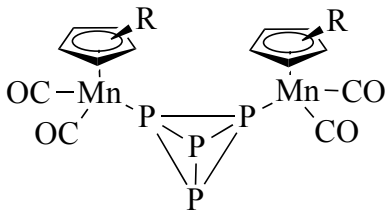

Figure 2.10: Structure of a bridging P_4 fragment between two Mn(I) centers published by Scheer *et al.* [11]

Therefore, P_4 was reacted in benzene with **2.7** to yield a yellow solid **2.11**.

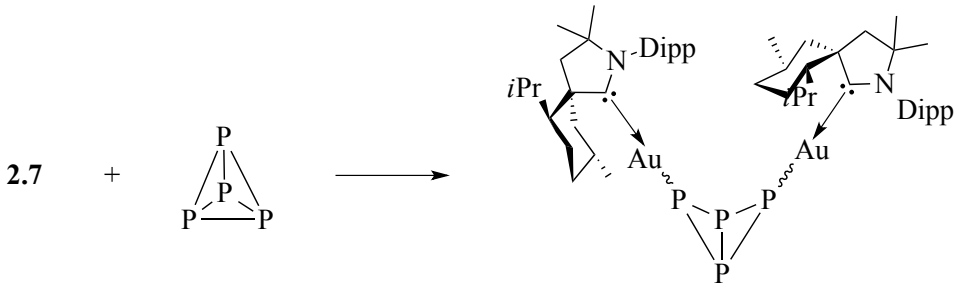

2.11

Scheme 2.6: Addition of white phosphorus (P_4) to (CAAC)Au-Au(CAAC).

The ^{31}P NMR of the solid showed three sets of signals (**Figure 2.11**). The chemical shifts in the down-field region (-286 ppm to -324 ppm) correlate well to the phosphorus atoms bound to the gold. Additionally, the up-field shifts (-26 ppm to -89 ppm) appear in the region expected for the other two phosphorus atoms.[13] The multiplicity, doublet and triplet, are expected for the $^{1}J_{p\text{-}p}$ and $^{2}J_{p\text{-}p}$ coupling. Since the three sets of signals in the NMR are so close, we believe they correspond to three different isomers.

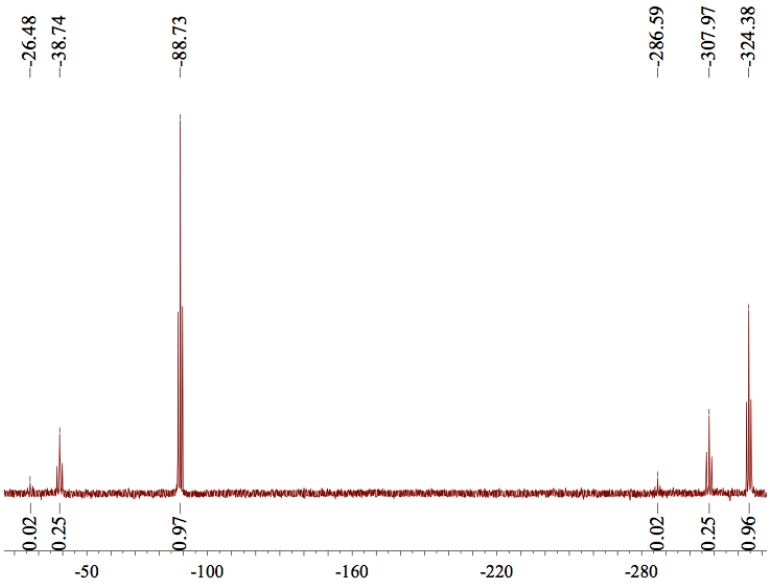

Figure 2.11: ^{31}P NMR for proposed structure **2.11**.

Unfortunately, this complex has not been crystallized, and the exact structure has not been determined.

Due to the intriguing reactivity with P_4, this led us to react **2.7** with other small molecules. Unfortunately, CO_2 showed no reactivity even when a Schlenk flask is pressurized with CO_2 for several days. Therefore, we next moved on to nitrogen dioxide (NO_2), believing that it would be possible to reduce the NO_2 to form a bridging ONO

fragment between the two gold atoms. There is a great interest in being able to reduce NO_2 cleanly to NO, and has been shown to work with the addition of NO_2 to a H/Au surface[14]. Upon bubbling NO_2 through a hexane solution of **2.7**, a white precipitate formed. The insolubility in non-polar solvents and the ^{13}C NMR of the carbene showed a chemical shift at 239 ppm is indicative of a CAACAu(I)X complex.

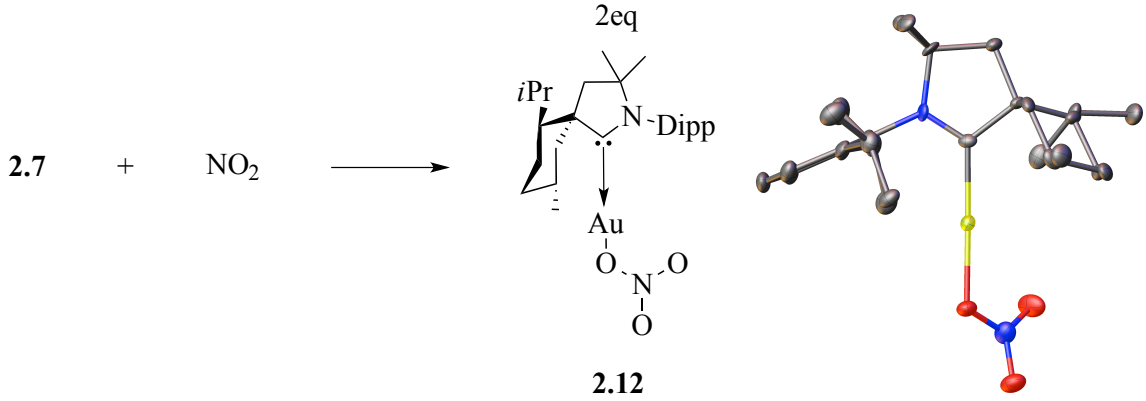

2.12

Scheme 2.7: (CAAC)$AuNO_3$ obtained by bubbling NO_2 through a solution of **2.7**.

X-ray diffraction quality crystals were obtained by layering a THF solution of **2.12** with n-hexanes. X-ray crystallography confirmed the structure of **2.12** with a C-Au-O bond of angle of 176.45°, which is to be expected for the divalent Au(I) complex. A possible mechanism is a one-electron reduction of the NO_2 and Au-Au cleavage followed by an outer sphere abstraction of an oxygen from an excess of NO_2 in solution to generate **2.12**.

The next small molecule that we reacted with **2.7** was O_2. The hypothesis was that the Au-Au dimer would be able to do a two-electron reduction of the O_2 to form a bridging peroxide, similar to K_2O_2. After bubbling O_2 through a solution of **2.7** in THF, an immediate color change occurred from brown to yellow. The ^{13}C NMR, δ = 237 ppm,

corresponds to a (CAAC)Au(I) species.. The crystals obtained from slow evaporation of a concentrated benzene solution were identified as complex **2.13**.

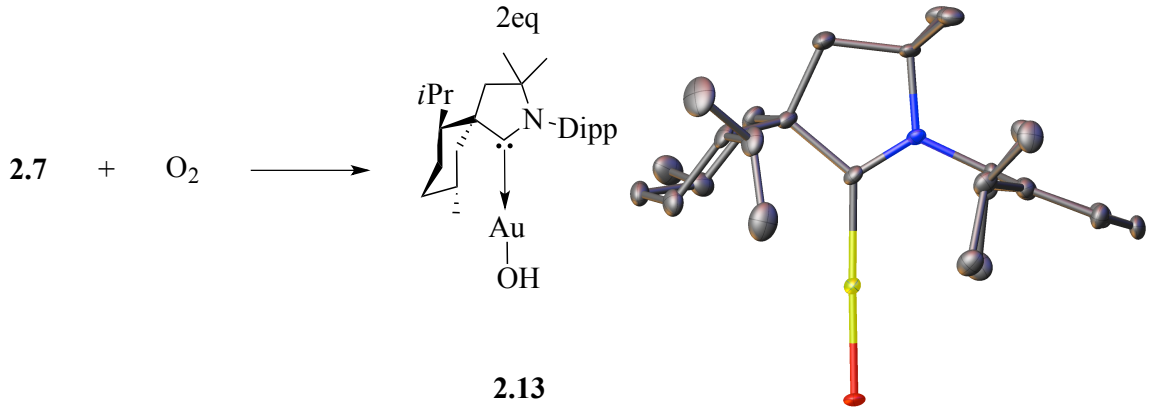

Scheme 2.8: (CAAC)AuOH from the addition of **2.7** and O_2.

The origin of the proton is unknown. The oxygen used is passed through CaH and subsequently passed through tubing cooled to -78°C to avoid any water. Varying the solvent in which **2.7** is dissolved and oxygen bubbled through does not have an impact on the formation of **2.13**. The C-Au-O bond angle is 176.76°, which is nearly identical to the unsaturated NHCAuOH complex **2.14** (C-Au-O: 177.13°) published by Nolan.[15]

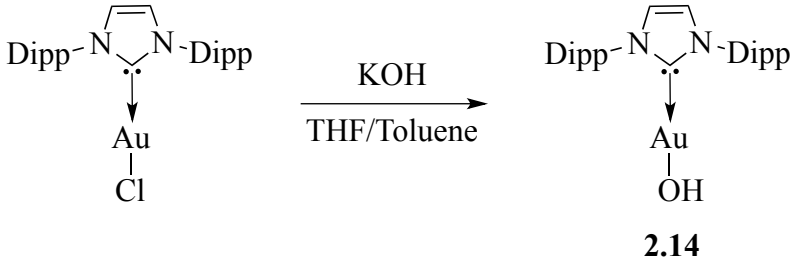

Scheme 2.9: Synthesis of (NHC)AuOH from (NHC)AuCl.

As an aside, attempts to prepare **2.13** with a CAAC instead of an NHC by Nolan's method (**Scheme 2.9**) failed even with the use of other metal hydroxide bases.

Due to the large interest in the catalytic oxidation of CO with O_2 to form CO_2 using gold nanoparticles, we tried the first step in this process, which is the absorption of CO onto the gold. Therefore, CO was bubbled through a THF solution of **2.7** for 17 hours to yield a new product by NMR. The ^{13}C NMR δ = 252 ppm for the carbene, and a new peak at δ = 218 ppm appeared. Given that it wasn't CO (free CO is at δ = 181 ppm in the carbon NMR) it was assumed that it was a bridging complex (Au-CO-Au). Additionally, the complex was soluble in non-polar solvents, which Au(I) complexes are not. However, crystals grown from a concentrated solution of hexane showed the structure to be **2.15** (**Figure 2.12**).

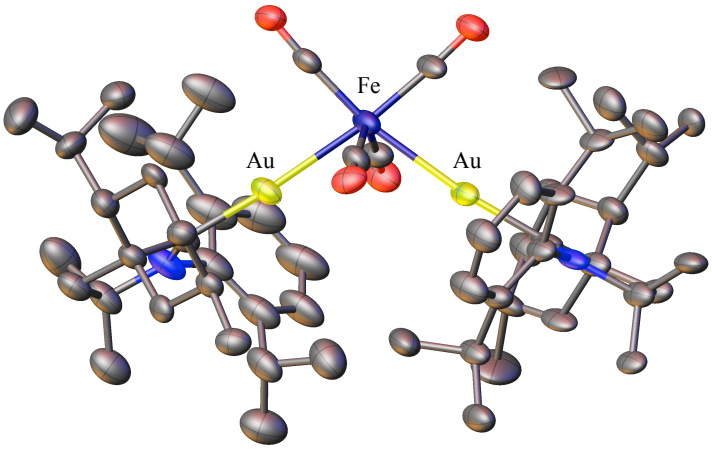

Figure 2.12: Crystal structure of (CAAC)Au-Fe(CO)$_4$-Au(CAAC).

The iron carbonyl in **2.15** most likely comes from the tank of carbon monoxide, which has been previously reported.[16] When a Schlenk charged with **2.7** is pressurized with carbon monoxide instead of allowed to bubble through the solution, no reaction occurs. However, when iron pentacarbonyl is added to a stirring solution of **2.7**, complex **2.15** is obtained cleanly **Scheme 2.10**.

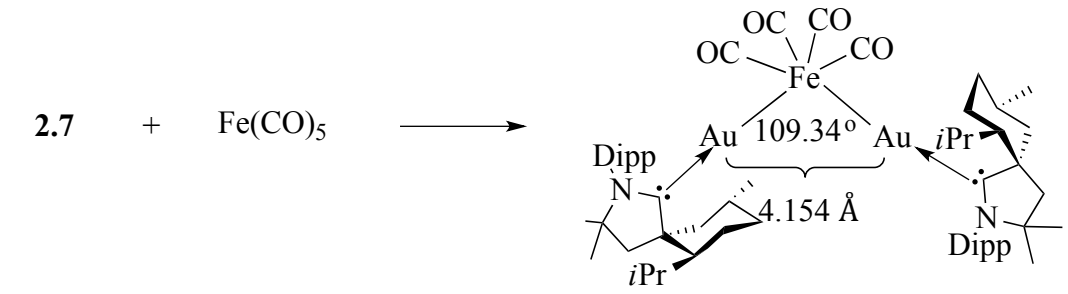

2.15

Scheme 2.10: Synthesis of (CAAC)Au-Fe(CO)$_4$-Au(CAAC).

Interestingly, complexes of the general formula Phosphine-Au-Fe(CO)$_4$-Au-Phosphine have been known since the work of Coffey in the early 1960s by reacting (Ph_3P)AuCl with disodium tetracarbonylferrate (Na_2FeCO_4) **Scheme 2.11**.[17] In 1993, Albano published the crystal structure of this complex **2.16**[18], and it's surprisingly very different than the structure of **2.15**.

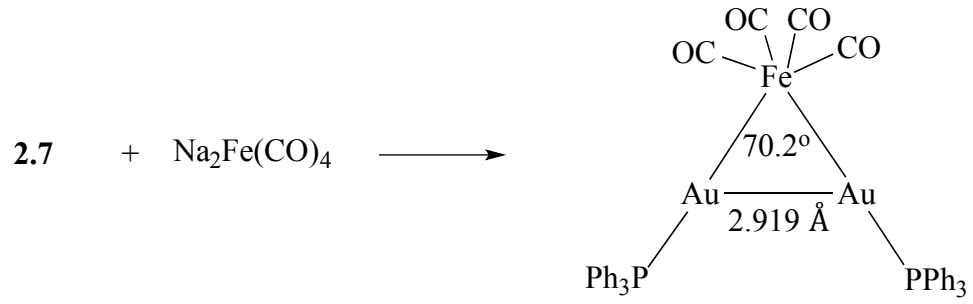

2.16

Scheme 2.11: Synthesis of (Ph_3P)Au-Fe(CO)$_4$-Au(PPh_3).

The Au-Au distance in **2.16** is 2.919 Å and within the range considered for aurophilic Au-Au bonding. In fact, it has been calculated that aurophilic attraction with this length of Au-Au bonding is between 29 and 46 kJ mol^{-1}, which seems to have a major contribution to the structure of **2.16** given the acute Au-Fe-Au angle of 70.2°. Therefore, it can be speculated that the oxidation state of the Au is in fact +1 to give rise

to the short Au-Au bond and the aurophilic interactions. In contrast, the complex with the CAACs **2.15** has a Au-Au distance of 4.154 Å which is much longer than any bonding interactions. Additionally, the Au-Fe-Au bond angle in **2.15** is 109.34°, which is significantly larger than in **2.16**. Even though the Au-Fe bond distances in both **2.15** and **2.16** are very close to the same, it's obvious that the bonding in these two-complexes are very different. Given that there are no aurophilic interactions, it can be speculated that the charge on the two gold atoms is not in fact in the +1 oxidation state but possibly between 0 and +1. Calculations on these two complexes are currently on going to elucidate the electronic structure.

Reduction of DAC-Au-Cl

As already discussed in the general introduction and Chapter 1, the diamido-carbene (DAC) is more electrophilic than the CAACs, but also less nucleophilic. Therefore, it was of interest to try to reduce the seven-membered DAC gold chloride **2.17**.[19]

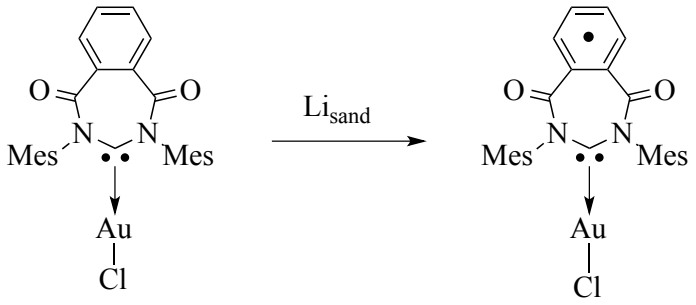

2.17 ***Proposed Structure***

Scheme 2.12: Reduction of 7DAAC-AuCl to form a radical species by EPR.

The reduction of **2.17** with lithium sand in THF produced a green solution, which was silent by NMR and EPR active. The EPR was collected (**Figure 2.13**, left) and

simulated using four different couplings each having a spin of ½ (**Figure 2.13**, right). This coupling could correlate to the four protons on the fused phenyl ring, which are inequivalent due to the non-planar geometry of the DAC. Unfortunately, crystals of the reduced product could not be obtained. Therefore, the actual structure is ambiguous and needs further investigation.

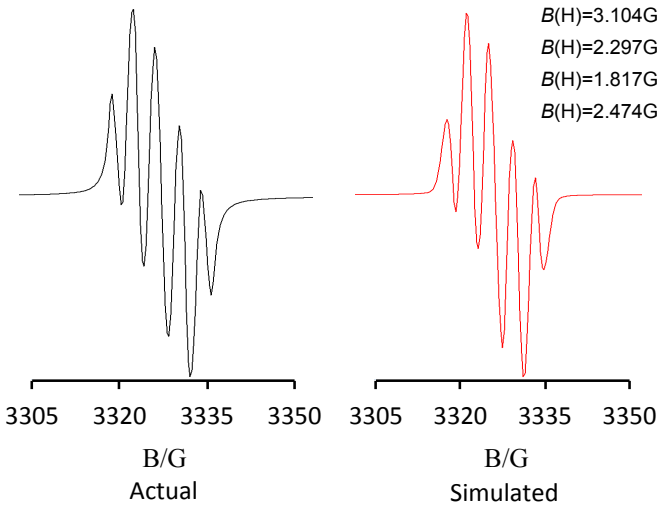

Figure 2.13: EPR spectrum of the reduction of **2.17**.

Conclusion

In this chapter, the synthesis and characterization of the first stable Au-Au dimer was presented. Despite the quasi-reversible reduction seen by cyclic voltammetry, the one-electron reduction of (CAAC)AuCl generates the dimer with an isolated yield of 20 % after workup. However, the dimer can be prepared cleanly and near quantitatively with one equivalent of 4,4'-di-tert-butylbiphenyl in the mixture.

Given that the HOMO resides primarily on the Au-Au bond, interesting reactivity was demonstrated with alkynes, alkenes and small molecules. The P_4 activation with the

dimer is hopefully the first step to prepare new and interesting gold and white phosphorus complexes.

Even though Au-$Fe(CO)_4$-Au complexes have been known for nearly half a century, the isolation of the reaction of $Fe(CO)_5$ with the Au-Au dimer shows a complex which has significantly different electronic properties that need to be investigated further. Preliminary results were obtained while investigating the reduction of (DAC)AuCl and requires further research.

Chapter 2 has been adapted from materials published in D. S. Weinberger, M. Melaimi, C. E. Moore, A. L. Rheingold, G. Frenking, P. Jerabek, G. Bertrand, *Angew. Chem. Int. Ed.* **2013**, 52, 8964-8967. The dissertation author was the primary investigator of this paper and the reactivity discussed above. The reactivity will be published in a future paper with the same set of authors.

Appendix: Experimental Section

General

All manipulations were performed under an inert atmosphere of dry Nitrogen, using standard Schlenk techniques. Dry, oxygen-free solvents were employed. EPR spectra were recorded on Bruker EMX. ^{1}H, ^{13}C, spectra were recorded on Bruker Avance 300 (300.13 MHz for 1H, 75.48 MHz for ^{13}C) and Varian Inova 500 spectrometers (500.1 MHz for ^{1}H, 125.8 MHz for ^{13}C). All spectra were obtained in the solvent indicated at 25 °C. Chemical shifts are given in ppm and are referenced residual protonated solvent. Melting points were measured with a Büchi melting point apparatus system. (CAAC)AuCl[7] **2.6** and (DAC)AuCl[19] **2.17** were prepared following literature procedures while all other starting materials were purchased from commercial sources.

2.7

In the glove box, (CAAC)AuCl **2.6** (150 mg) and lithium sand (4.5 mg) were stirred in 20 mL of THF for 1 h. The solution was subsequently filtered and dried *in vacuo*. The product was extracted with 3 x 20 mL of *n*-hexane, and evaporated. The solid was then washed with 3 x 0.5 mL of hexane to yield pure pale brown solid. Yield: 56 mg (20%). ^{1}H NMR (C_6D_6, 500 MHz) = 7.15 (m, 4H, $H_{m, ar}$), 7.07 (dd, ^{3}J = 6.68 Hz, ^{3}J = 6.38 Hz, 2H, $H_{p, ar}$), 3.54 - 3.67 (m, 4H), 2.96 (sept., ^{3}J = 6.7 Hz, 4H, C*H*$(CH_3)_2$), 2.11(m, 2H),

2.01 (d, ^3J = 12.92 Hz, 2H), 1.89- 1.93(m, 4H), 1.77 (br, 2H), 1.75 (d, ^3J = 7.06 Hz, 6H), 1.70 (d, ^3J = 5.89 Hz, 6H), 1.65 (m, 2H), 1.41 (d, ^3J = 7.05Hz, 6H), 1.39 (d, ^3J = 6.7 Hz, 2H) 1.34 (d, ^3J = 7.06 Hz, 6H), 1.26 (d, ^3J = 5.89 Hz, 6H), 1.18 (m, 2H), 1.08 (d, ^3J = 6.85, 6H), 1.08 (br, 2H), 1.07 (s, 10H), 1.05 (br, 2H), 0.89 (d, ^3J = 6.67, 6H). $^{13}C\{^1H\}$ NMR (C_6D_6, 125.8 MHz) = 287.2 ($C_{carbene}$), 145.8 (C_{ortho}), 145.5 (C_{ortho}), 136.0 (C_{ipso}), 128.6 (C_{para}), 124.2 (C_{meta}), 76.5 (C_{quat}), 66.7 (C_{quat}), 53.6 (CH_2), 52.48 (CH), 50.26 (CH_2), 36.9 (CH_2), 29.6, 29.3, 29.2, 29.1, 29.0, 28.6, 28.31, 27.3, 25.6, 25.0 ($CH2$), 23.48, 23.3, 23.2, 20.0. Mp: 98 °C(dec.).

Alternative synthesis of 2.7

In the glove box, 4,4' di-tert-butylbiphenyl (49.5 mg, 0.95eq, 1.856 x10^{-4} mol) was stirred with lithium powder (4 mg) in 10 mL of THF for 1 h to yield a dark blue solution. The excess lithium was filtered off and the solution was added drop wise to a solution of **2.6** (120 mg, 1.954 x 10^{-4} mol) in 10 mL of THF. After stirring for 20 min, the solution was evaporated and **2.7** and 4,4' di-tert-butylbiphenyl were extracted with 3 x 5 mL of *n*-hexane. The solution was dried *in vacuo* to yield **2.7** as a mixture with 4,4' di-tert-butylbiphenyl.

Crystal data and structure refinement for **2.7.**

Identification code	MM6
Empirical formula	$C_{54}H_{86}Au_2N_2$
Formula weight	1157.18
Temperature/K	100 (2)
Crystal system	monoclinic
Space group	$P2_1$
a/Å	19.1144(7)
b/Å	42.0545(16)
c/Å	20.3983(7)
α/°	90
β/°	107.6820(10)
γ/°	90
Volume/Å^3	15622.4(10)
Z	12
ρ_{calc}mg/mm^3	1.476
m/mm^{-1}	5.662
F(000)	6984.0
Crystal size/mm^3	0.217 × 0.181 × 0.112
Radiation	MoKα (λ = 0.71073)
2Θ range for data collection	4 to 61.13°
Index ranges	$-26 \leq h \leq 16$, $-46 \leq k \leq 60$, $-21 \leq l \leq 29$
Reflections collected	129560
Independent reflections	73310 [R_{int} = 0.0284, R_{sigma} = 0.0654]

Data/restraints/parameters	73310/6/3246
Goodness-of-fit on F^2	1.023
Final R indexes [I>=2σ (I)]	$R_1 = 0.0423$, $wR_2 = 0.0896$
Final R indexes [all data]	$R_1 = 0.0565$, $wR_2 = 0.0945$
Largest diff. peak/hole / e $Å^{-3}$	3.91/-1.65
Flack parameter	0.016(2)

2.8

In the glove box, tetracyanoethylene (23 mg, 1.856 $x10^{-4}$ mol) was added to a stirring solution of **2.7** (mixture with 4,4' di-tert-butylbiphenyl, 1.856 $x10^{-4}$ mol) in 5 mL of THF. The brown solution became lighter in color over the course of 3 h. The solution was evaporated under vacuum and subsequently washed with 3 x 5 mL of *n*-hexane to yield a yellow solid. (63 mg, 25.7 %) $^{13}C\{^1H\}$ NMR ($CDCl_3$, 125.8 MHz) = 246.9 ($C_{carbene}$), 233.3 (CN), 145.1 (C_{ortho}), 144.8 (C_{ortho}), 134.5 (C_{ipso}), 134.3 (C_{ipso}), 128.0 (C_{para}), 125.1 (C_{meta}), 77.2 (C_{quat}), 66.1 (C_{quat}), 64.05 (C_{quat}), 52.7 (CH_2), 51.3 (CH), 49.6 (CH_2), 49.3 (CH_2), 35.3 (CH_2), 30.9, 30.7, 29.0, 28.8, 27.7, 27.2, 26.7, 24.8, 24.6, 24.45, 22.9, 22.8, 20.0, 19.8.

Crystal data and structure refinement for **2.8.**

Identification code	gb_dsw_018
Empirical formula	$C_{33.5}H_{46}AuN_{3.5}$
Formula weight	879.89
Temperature/K	100 (2)
Crystal system	triclinic
Space group	P1
a/Å	9.3665(14)
b/Å	18.5633(18)
c/Å	19.981(2)
α/°	65.829(4)
β/°	80.551(6)
γ/°	85.206(4)
Volume/$Å^3$	3126.1(7)
Z	4
$\rho_{calc}mg/mm^3$	1.870
m/mm^{-1}	4.754
F(000)	1780.0
Radiation	MoKα (λ = 0.71073)
2Θ range for data collection	2.56 to 52.74°
Index ranges	$-5 \leq h \leq 11$, $-16 \leq k \leq 20$, $-23 \leq l \leq 17$
Reflections collected	13021
Independent reflections	8177 [$R_{int} = 0.0402$, $R_{sigma} = 0.0795$]
Data/restraints/parameters	8177/399/1405

Goodness-of-fit on F^2	1.012
Final R indexes [I>=2σ (I)]	$R_1 = 0.0374$, $wR_2 = 0.0795$
Final R indexes [all data]	$R_1 = 0.0592$, $wR_2 = 0.0996$
Largest diff. peak/hole / e $Å^{-3}$	0.88/-0.85
Flack parameter	0.016(13)

2.9

To a stirring solution of **2.7** (mixture with 4,4' di-tert-butylbiphenyl, 1.856 $x10^{-4}$ mol) in 5 mL of benzene, 5 drops of diethyl fumarate were added. The solution turned orange after 5 minutes, and was allowed to stir overnight. The solution was evaporated to dryness, and washed with 5 x 2 mL of cold hexane. The solid was then dried to give a white solid. Crystals suitable for X-ray crystallography were grown from a concentrated solution of hexane at -79°C. $^{13}C\{^1H\}$ NMR (C_6D_6, 125.8 MHz) = 260.6 ($C_{carbene}$), 180.4 (C_{quat}), 145.7 (C_{ortho}), 145.5 (C_{ortho}), 135.7 (C_{ipso}), 129.1 (C_{para}), 124.5 (C_{meta}), 124.6 (C_{meta}), 76.4 (C_{quat}), 65.4 (C_{quat}), 56.8, 53.4 (CH_2), 52.1 (CH), 49.9, 41.1, 36.4 (CH_2), 29.6, 29.4, 29.3, 28.4, 27.7, 26.8, 25.3, 24.5, 23.5, 23.0, 20.4, 15.4.

2.10

To a stirring solution of **2.7** (mixture with 4,4' di-tert-butylbiphenyl, 1.856 $x10^{-4}$ mol) in 5 mL of benzene, dimethyl acetylenedicarboxylate (10 mg, 7.021 x 10^{-4} mol) was added. The solution immediately turned yellow, and was stirred for an additional 2 h. Upon evaporation of the solvent, an orange oil was collected. Upon addition of 2 mL of cold *n*-hexane, a yellow solid precipitated. The solid was subsequently washed with 2 x 1 mL of cold *n*-hexane and dried *in vacuo*. (33 mg, 14 % yield) ^1H NMR (C_6D_6, 500 MHz) = 7.11 (d, ^3J = 7.63 Hz, 2H, $H_{p, ar}$), 6.99 (d, ^3J = 7.63 Hz, 1H, $H_{m, ar}$), 6.98 (d, ^3J = 7.63 Hz, 1H, $H_{m, ar}$), 6.96 (d, ^3J = 7.63 Hz, 1H, $H_{m, ar}$), 6.95 (d, ^3J = 7.63 Hz, 1H, $H_{m, ar}$), 3.37 (m, 4H), 3.25 (m, 4H), 2.68 (m, ^3J = 6.7 Hz, 4H), 2.32(br, 2H), 1.85 (d, ^3J = 13.43 Hz, 2H), 1.78 (d, ^3J = 13.11 Hz, 2H), 1.69 (m, 4H), 1.42 (d, ^3J = 7.19 Hz, 6H), 1.38 (d, ^3J = 6.66 Hz, 6H), 1.23 (br, 16H), 1.22 (d, ^3J = 6.87Hz, 6H), 1.07 (d, ^3J = 6.95 Hz, 6H) 0.93 (d, ^3J = 6.38 Hz, 6H), 0.91 (d, ^3J = 6.80 Hz, 6H), 0.84 (d, ^3J = 8.16 Hz, 12H). $^{13}C\{^1H\}$ NMR (C_6D_6, 125.8 MHz) = 263.3 ($C_{carbene}$), 179.2 (C_{quat}), 172.5 (C_{quat}), 149.9, 146.0 (C_{ortho}), 145.6 (C_{ortho}), 135.8 (C_{ipso}), 129.0 (C_{para}), 127.1, 126.02, 124.7 (C_{meta}), 124.6 (C_{meta}), 76.0 (C_{quat}), 65.5 (C_{quat}), 53.4 (CH_2), 52.6 (CH), 52.0, 49.8, 49.9, 36.4 (CH_2), 34.5 (CH_2), 31.5, 29.7, 29.5, 29.2, 28.5, 27.4, 26.7, 25.8, 25.2, 24.61, 23.5, 23.1, 20.3.

Crystal data and structure refinement for **2.10.**

Identification code	gb_dsw_016_0m
Empirical formula	$C_{78}H_{110}Au_2N_2O_4$
Formula weight	1292.96
Temperature/K	100 (2)
Crystal system	triclinic
Space group	P1
a/Å	9.6529(7)
b/Å	12.6289(9)

c/Å	15.1371(12)
α/°	90.595(2)
β/°	94.514(2)
γ/°	105.222(2)
Volume/Å^3	1774.1(2)
Z	1
ρ_{calc}mg/mm^3	1.210
m/mm^{-1}	4.211
F(000)	607.0
Radiation	MoKα (λ = 0.71073)
2Θ range for data collection	4.23 to 52.808°
Index ranges	-12 ≤ h ≤ 12, -14 ≤ k ≤ 15, -18 ≤ l ≤ 18
Reflections collected	29101
Independent reflections	11933 [R_{int} = 0.0359, R_{sigma} = 0.0526]
Data/restraints/parameters	11933/3/748
Goodness-of-fit on F^2	1.075
Final R indexes [I>=2σ (I)]	R_1 = 0.0307, wR_2 = 0.0558
Final R indexes [all data]	R_1 = 0.0392, wR_2 = 0.0582
Largest diff. peak/hole / e Å^{-3}	1.43/-2.21
Flack parameter	0.038(5)

2.11

In a vial, in the glove box, **2.7** (mixture with 4,4' di-tert-butylbiphenyl, 1.856 x10^{-4} mol) and white phosphorus (5 eq) were stirred together in 10 mL of benzene for 14 h. The solution was then removed *in vacuo* to obtain a yellow solid. The solid was then evacuated under vacuum for 14 h to remove excess P_4 and washed with 3 x 4 ml of *n*-hexane. The ^{31}P NMR was then collected in C_6D_6. **Figure 2.11**.

2.12

To a stirring solution of **2.7** (mixture with 4,4' di-tert-butylbiphenyl, 1.856 x10^{-4} mol) in 15 mL of *n*-hexane, NO_2 was bubbled through the solution for about 3 min. The solution turned orange and a white precipitate formed. The hexane was decanted and the solid washed with 3 x 3 mL of *n*-hexane to yield a white solid. (67 mg, 59 % yield) ^{1}H NMR (C_6D_6, 500 MHz) = 7.22 (t, ^3J = 7.37 1H, $H_{p, ar}$), 7.07 (d, ^3J = 7.37 Hz, 2H), 3.19 (m, 2H), 2.78 (sept., ^3J = 6.88 Hz, 2H, C*H*$(CH_3)_2$), 2.16 (d, ^3J = 13.27 Hz, 1H) 2.05 (d, ^3J = 11.05 Hz, 1H), 1.99 (d, ^3J = 13.27 Hz, 1H), 1.90 (m, 1H), 1.74 (d, ^3J = 13.81 Hz, 1H), 1.62 (d, ^3J = 13.81 Hz, 1H), 1.47 (d, ^3J = 6.67 Hz, 3H), 1.41 (d, ^3J = 6.56 Hz, 3H), 1.27 (d, ^3J = 6.68 Hz, 4H), 1.19 (d, ^3J = 8.01 Hz, 3H), 1.18 (d, ^3J = 7.10 Hz, 3H), 1.07 (s, 3H), 1.04 (s, 3H), 1.01 (d, ^3J = 6.56 Hz, 4H), 1.92 (d, ^3J = 6.10 Hz, 4H). ^{13}C{^{1}H} NMR (C_6D_6, 125.8 MHz) = 230.0 ($C_{carbene}$), 145.4 (C_{ortho}), 145.0 (C_{ortho}), 135.6 (C_{ipso}), 130.2 (C_{para}), 125.3 (C_{meta}), 125.2 (C_{meta}), 76.9 (C_{quat}), 64.0 (C_{quat}), 52.5 (CH_2), 51.3 (CH), 49.2 (CH_2), 35.7 (CH_2), 30.5, 29.5, 29.2, 28.2, 27.4, 26.7, 25.0, 24.4, 23.0, 22.9, 22.7, 20.3.

2.13

In the glove box, a solution of **2.7** (mixture with 4,4' di-tert-butylbiphenyl, 1.856 x10^{-4} mol) in 10 mL of THF was loaded into a schlenk. O_2, passed through a CaH column and tubing at -78 °C, was then bubbled through the solution. The color turned yellow almost immediately after bubbling O_2. The solution was subsequently evaporated and washed with 3 x 2 mL *n*-hexane. (54 mg, 48.8 % yield). Crystals were grown from a concentrated benzene solution. ^{1}H NMR (C_6D_6, 500 MHz) = 7.10 (d, ^3J = 7.12 1H, $H_{p,\,ar}$), 7.97 (dd, ^3J = 7.12 Hz, ^3J = 6.62 Hz, 2H, $Hm_{,\,ar}$), 3.35 (m, 1H), 3.27 (m, 1H), 2.78 (sept., ^3J = 7.02 Hz, 2H, C*H*$(CH_3)_2$), 1.90 (m, 1H), 1.85 (br, 1H), 1.77 (br, 1H), 1.55 (d, ^3J = 5.92 Hz, 3H), 1.48 (d, ^3J = 6.34 Hz, 3H), 1.39 (m, 3H), 1.30 (d, ^3J=7.19 Hz, 2H), 1.14 (d, ^3J = 6.7 Hz, 3H) 1.34 (d, ^3J = 7.06 Hz, 3H), 1.26 (d, ^3J = 5.89 Hz, 3H), 1.18 (m, 1H), 1.08 (d, ^3J = 7.17, 3H), 1.08 (d, ^3J = 6.68, 3H), 0.88 (br, 2H), 0.85 (br, 1H), 0.81 (d, ^3J = 6.44, 3H). ^{13}C{^{1}H} NMR (C_6D_6, 125.8 MHz) = 237.0 ($C_{carbene}$), 145.7 (C_{ortho}), 145.4 (C_{ortho}), 136.1 (C_{ipso}), 129.6 (C_{para}), 125.0 (C_{meta}), 128.88 (C_{meta}), 75.1 (C_{quat}), 64.1 (C_{quat}), 52.8 (CH_2), 51.5 (*C*H), 50.0 (CH_2), 35.9 (CH_2), 30.2, 29.5, 29.2, 28.3, 27.4, 26.9, 25.8, 25.3, 24.6, 23.1, 23.0, 22.8, 20.4.

Crystal data and structure refinement for **2.13**.

Identification code	GB_dsw022_0m
Empirical formula	$C_{30}NO_3Au_2Cl_{0.25}H_{0.25}F_{0.25}$
Formula weight	830.11
Temperature/K	100 (2)
Crystal system	orthorhombic
Space group	$P2_12_12_1$
a/Å	10.1676(4)
b/Å	15.3588(5)
c/Å	19.7057(7)
α/°	90.00
β/°	90.00
γ/°	90.00
Volume/Å^3	3077.28(19)
Z	4
ρ_{calc}mg/mm^3	1.792
m/mm^{-1}	9.573
F(000)	1503.0
Crystal size/mm^3	0.33 × 0.3 × 0.27
Radiation	MoKα (λ = 0.71073)
2Θ range for data collection	6.64 to 56.56°
Index ranges	$-13 \le h \le 8$, $-20 \le k \le 14$, $-26 \le l \le 23$
Reflections collected	16087
Independent reflections	7568 [R_{int} = 0.0315, R_{sigma} = 0.0588]
Data/restraints/parameters	7568/0/334

Goodness-of-fit on F^2	0.548^{-1}):
Final R indexes [I>=2σ (I)]	$R_1 = 0.0249$, $wR_2 = 0.0680$
Final R indexes [all data]	$R_1 = 0.0297$, $wR_2 = 0.0733$
Largest diff. peak/hole / e $Å^{-3}$	1.21/-0.70
Flack parameter	-0.006(8)

2.15

To a stirring solution of complex **2.7** (mixture with 4,4' di-tert-butylbiphenyl, 1.856 $x10^{-4}$ mol) in 6 ml of benzene, 6 drops of iron pentacarbonyl was added. The solution immediately turned yellow, and was allowed to stir for an additional 30 min. The benzene and excess iron pentacarbonyl was evaporated under vacuum. The solid was washed with 4 x 2 ml of cold *n*-hexanes. The remaining solid was extracted with 10 mL of *n*-hexane and evaporated to dryness. (41 mg, 17% yield). Crystals for x-ray diffraction were grown from a concentrated solution *n*-hexanes at -30 °C. ^{1}H NMR (C_6D_6, 500 MHz) = 7.14 (t, ^{3}J = 7.49 2H, $H_{p, ar}$), 7.04 (d, ^3J = 7.49 Hz, 4H, $H_{m, ar}$), 3.31 (br, 2H), 2.85 (m, 4H), 2.42 (d, ^3J = 11.26 Hz, 2H), 1.97 (br, 4H), 1.52 (d, ^3J = 6.53 Hz, 6H), 1.47 (d, ^3J = 6.53 Hz, 6H), 1.30 (d, ^3J = 6.93 Hz, 6H) 1.27 (d, ^3J = 14.00 Hz, 6H), 1.12 (d, ^3J = 6.53 Hz, 6H), 1.09 (d, ^3J = 7.06 Hz, 6H), 1.26 (d, ^3J = 5.89 Hz, 6H), 1.18 (m, 2H), 1.08 (d, ^3J = 6.88, 6H), 1.06 (d, ^3J = 6.37 Hz, 6H), 1.03 (d, ^3J = 6.83 Hz, 6H), 0.94 (br, 4H). $^{13}C\{^1H\}$ NMR (C_6D_6, 125.8 MHz) = 249.6 ($C_{carbene}$), 218.86 (CO), 145.6 (C_{ortho}), 145.1 (C_{ortho}), 135.7 (C_{ipso}), 129.7 (C_{para}), 125.2 (C_{meta}), 77.0 (C_{quat}), 65.7 (C_{quat}), 53.6 (CH_2), 52.6 (*C*H), 48.5 (CH_2), 36.6 (CH_2), 29.9, 29.6, 29.3, 28.1, 27.58, 26.6, 25.3, 24.3, 23.3, 23.2, 23, 20.7. IR CO Stretches (cm^{-1}): 1974, 1901, 1883, 1863.

Crystal data and structure refinement for **2.15**.

Identification code	Dsw_021_p1_ap21_sq
Empirical formula	$Au_4C_{116}Fe_2N_4O_8$
Formula weight	2653.16
Temperature/K	293(2)
Crystal system	monoclinic
Space group	$P2_1$
a/Å	10.543(3)
b/Å	18.823(5)
c/Å	33.311(9)
α/°	90
β/°	97.110(5)
γ/°	90
Volume/$Å^3$	6560(3)
Z	2
ρ_{calc}mg/mm^3	1.343
m/mm^{-1}	4.719
F(000)	2662.0

Radiation	MoKα (λ = 0.71073)
2Θ range for data collection	1.232 to 52.854°
Index ranges	$-13 \leq h \leq 13$, $-23 \leq k \leq 23$, $-41 \leq l \leq 36$
Reflections collected	49904
Independent reflections	25739 [R_{int} = 0.0559, R_{sigma} = 0.1099]
Data/restraints/parameters	25739/1159/1242
Goodness-of-fit on F^2	1.027
Final R indexes [I>=2σ (I)]	R_1 = 0.0580, wR_2 = 0.1486
Final R indexes [all data]	R_1 = 0.0933, wR_2 = 0.1670
Largest diff. peak/hole / e $Å^{-3}$	3.07/-1.33
Flack parameter	0.056(6)

Reduced DAC-Au-Cl
To a solution of **2.16** (120 mg, 1.966 x 10^{-4} mol) in 5 mL of THF, a solution of Lithium (4 mg) /4,4'- ditert-butylbiphenyl (47 mg, 1.773 x 10^{-4} mol, 0.95eq) in 10 mL of THF was added drop wise. The EPR spectra (**Figure 2.12**) was then acquired.

References

[1] Esterhuysen, M. W., Raubenheimer, H. G., *Acta Crystallogr., Sect. C* **2003**, *59*.

[2] Mingos, D. M. P., *Pure Appl. Chem.* **1980**, *52*.

[3] Schwerdtfeger, P., Boyd, P. D. W., *Inorg. Chem.* **1992**, *31*, 327-329.

[4] Labouille, S., Escalle-Lewis, A., Jean, Y., Mézailles, N., Le Floch, P., *Chem. – Euro. J.* **2011**, *17*, 2256-2265.

[5] Raubenheimer, H. G., Schmidbaur, H., *Organometallics* **2011**, *31*, 2507-2522.

[6] Tsui, E. Y., Müller, P., Sadighi, J. P., *Angew. Chem., Int. Ed.* **2008**, *47*, 8937-8940.

[7] Frey, G. D., Dewhurst, R. D., Kousar, S., Donnadieu, B., Bertrand, G., *J. Organomet. Chem.* **2008**, *693*, 1674-1682.

[8] Karaman, R., Fry, J. L., *Tetrahedron Lett.* **1989**, *30*, 6267-6270.

[9] Roy, D., Navarro-Vazquez, A., Schleyer, P. v. R., *J. Am. Chem. Soc.* **2009**, *131*, 13045-13053.

[10] Pokhodnya, K. I., Bonner, M., DiPasquale, A. G., Rheingold, A. L., Miller, J. S., *Chem. – Euro. J.* **2008**, *14*, 714-720.

[11] Ung, G., Bertrand, G., *Angew. Chem., Int. Ed.* **2013**, *52*, 11388-11391.

[12] a)Schwarzmaier, C., Bodensteiner, M., Timoshkin, A. Y., Scheer, M., *Angew. Chem., Int. Ed.* **2014**, *53*, 290-293; b)Heinl, S., Peresypkina, E. V., Timoshkin, A. Y., Mastrorilli, P., Gallo, V., Scheer, M., *Angew. Chem., Int. Ed.* **2013**, *52*, 10887-10891.

[13] Scherer, O. J., Hilt, T., Wolmershäuser, G., *Organometallics* **1998**, *17*, 4110-4112.

[14] Pan, M., Ham, H. C., Yu, W.-Y., Hwang, G. S., Mullins, C. B., *J. Am. Chem. Soc.* **2012**, *135*, 436-442.

[15] Gaillard, S., Slawin, A. M. Z., Nolan, S. P., *Chem. Commun.* **2010**, *46*, 2742-2744.

[16] Broida, H. P., Heath, D. F., *J. Chem. Phys.* **1957**, *26*, 1352-1352.

[17] a)Coffey, C. E., Lewis, J., Nyholm, R. S., *Journal of the Chemical Society* **1964**, 1741-1749; b)Gladysz, J. A., Tam, W., *J. Org. Chem.* **1978**, *43*, 2279-2280.

[18] Albano, V. G., Monari, M., Iapalucci, M. C., Longoni, G., *Inorg. Chim. Acta* **1993**, *213*, 183-190.

[19] Hudnall, T. W., Tennyson, A. G., Bielawski, C. W., *Organometallics* **2010**, *29*, 4569-4578.

CHAPTER 3:

Isolation and reactivity of a trinuclear gold cluster supported by CAAC ligands

Adapted from:

L. Jin, D. S. Weinberger, M. Melaimi, C. E. Moore, A. L. Rheingold, G. Bertrand *Angew. Chem. Int. Ed.* **2014**, *submitted*.

Introduction

In the general introduction, the work by Corma *et. al*. was discussed;[1] specifically the activity of their small metallic gold clusters (3 to 10 atoms) which show better catalytic reactivity than gold nanoparticles, as well as mononuclear homogeneous gold catalysts. Unfortunately, the clusters described by Corma *et al.* are still unidentified and are only known to be in a general range. It would be of great interest to investigate these reactions with well-defined clusters to elucidate the catalytic mechanisms.

As shown in the previous two chapters, CAAC ligands have been used to isolate both monomeric Au(0) and the dimeric gold complexes in the zero oxidation state. Due to the excellent σ-donating and π-accepting ability of the CAAC, these complexes were stable in the absence of traces of O_2 or H_2O. Therefore, the next step is to try to isolate a neutral tri-nuclear gold complex. In the literature, there is only one example described by Sadighi *et al.* of a cationic tris(gold) cluster (**Scheme 3.1**).[2]

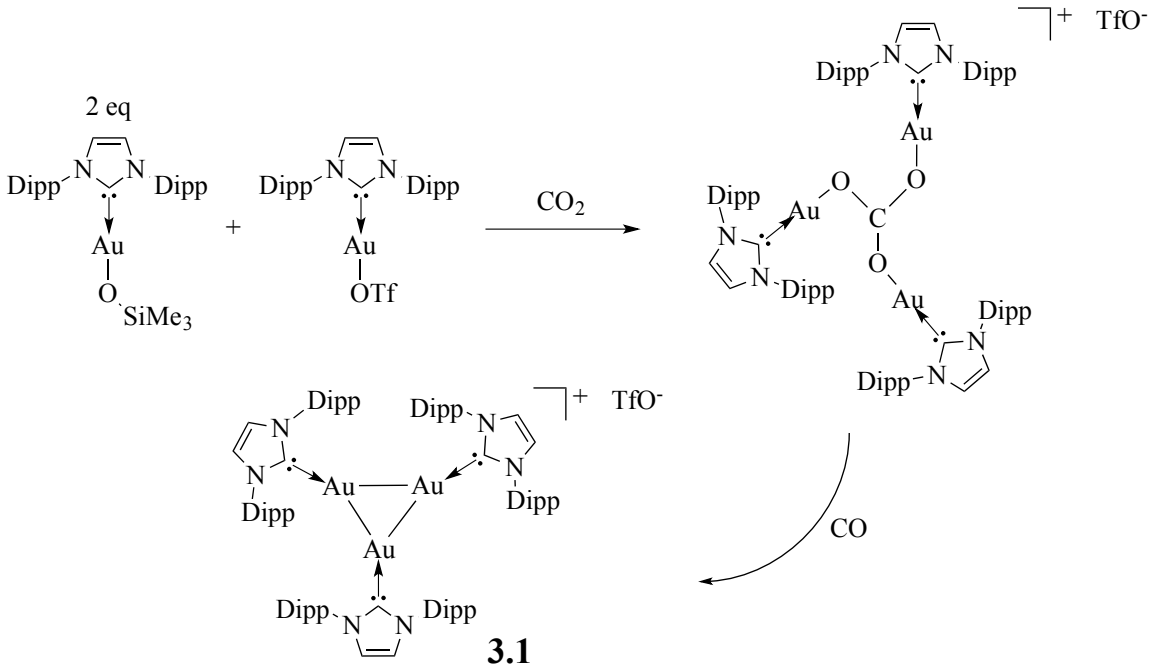

Scheme 3.1: Sadighi *et al*. synthesis of the first tris(gold) cluster.

One of the most classical routes for the preparation of small phosphine-supported gold clusters, such as $[(R_3PAu)_6]^{2+3}$, $[(R_3P)_6Au_8]^{2+4}$ and $[(R_3PAu)_4]^{2+}$,[5] is the reduction of the corresponding μ^3-oxo complexes $[(R_3PAu)_3O]^+X^-$, which was described in detail in the general introduction. In the same report that **3.1** is described, Sadighi *et al*. also reported their attempts to make the μ^3-oxo complexes with NHCs. These reactions failed and gave rise to a mixture of products.[2] However, Sadighi *et al.* were able to make **3.1** through an elegant route incorporating the reduction of a $[(NHC)Au]_3$ carbonate species with carbon monoxide. The cyclic voltammogram of **3.1** shows no reduction wave, which would have corresponded to the neutral gold trimer. Therefore, we decided to investigate whether using CAACs instead of NHCs would allow for the isolation of a trinuclear gold cluster in the zero oxidation state.

Preparation of a neutral Au_3 complex

The obvious synthesis would be to adapt a similar synthetic route to the one Sadighi *et al.* published (**Scheme 3.1**). Both the (CAAC)AuOTf[6] and (CAAC)AuOTMS could both be prepared according to the published synthesis for (NHC)AuOTf and (NHC)AuOTMS. However, the reaction with CO_2 to make the μ^3-carbonato species was unsuccessful. Therefore, since we had the (CAAC)Au-Au(CAAC) in hand, and knowing that this complex reacts well with electrophilic species, a third equivalent of cationic Au(I) could be introduced. During the synthesis of the (CAAC)Au-Au(CAAC) dimer, excess (CAAC)AuCl is present and no Au_3 species is detected. Therefore, the (CAAC)AuOTf and (CAAC)Au $BAr^F{}_4$ (tetrakis(pentafluorophenyl)borate) complexes, which only have loosely bound anions, were prepared and added to the dimer (**Scheme 3.2**). No reaction occurred with these complexes, probably due to the steric bulk of the menthyl substituents on the CAACs, which surround the dimer. Therefore, the dimer was reacted with other sources of Au(I) with smaller substituents including: (THT)AuCl, Ph_3PAuCl, $Ph_3PAu^I(SbF_6)^-$ (**Scheme 3.2**). Due to the reducing nature of the Au-Au dimer, all of these reactions proceeded with the precipitation of gold either as a gold film on the NMR tube or colloidal gold.

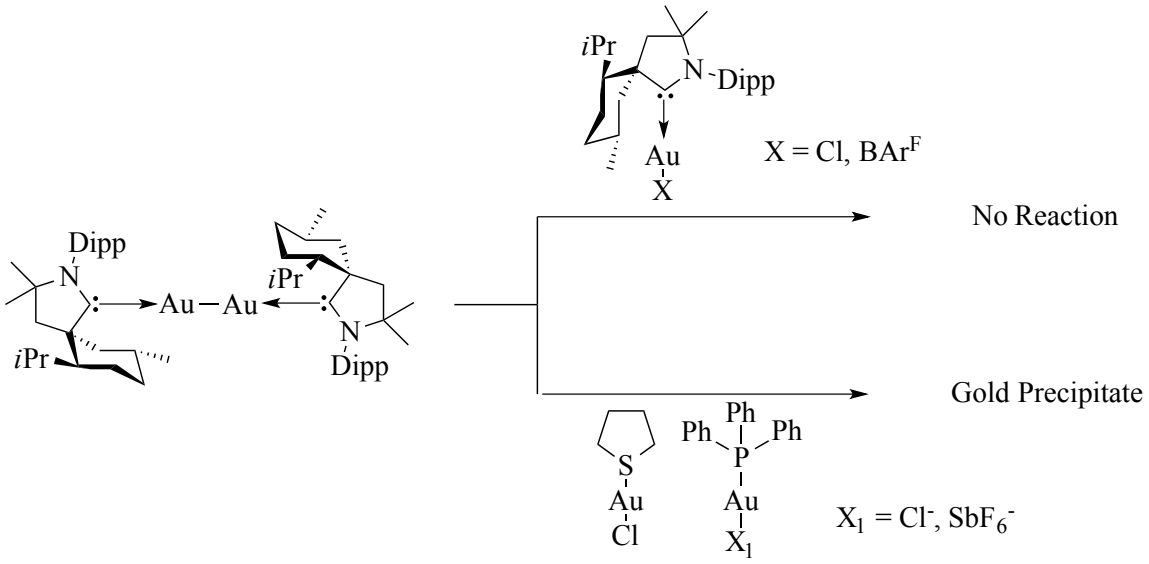

Scheme 3.2: Addition of Au(I) complexes to (CAAC)Au-Au(CAAC) in attempts to make a trinuclear complex.

Even though Sadighi *et al*. tried to prepare the NHC gold μ_3-oxo complex, the synthesis did not proceed cleanly;[2] however, the reaction of (Cy-CAAC)AuCl[7] **3.2** with silver oxide and sodium tetrafluoroborate did afford the corresponding μ^3-oxo complex $[(CAACAu)_3O]^+BF_4^-$ **3.3** as an off-white powder in 62 % yield (**Scheme 3.2**).

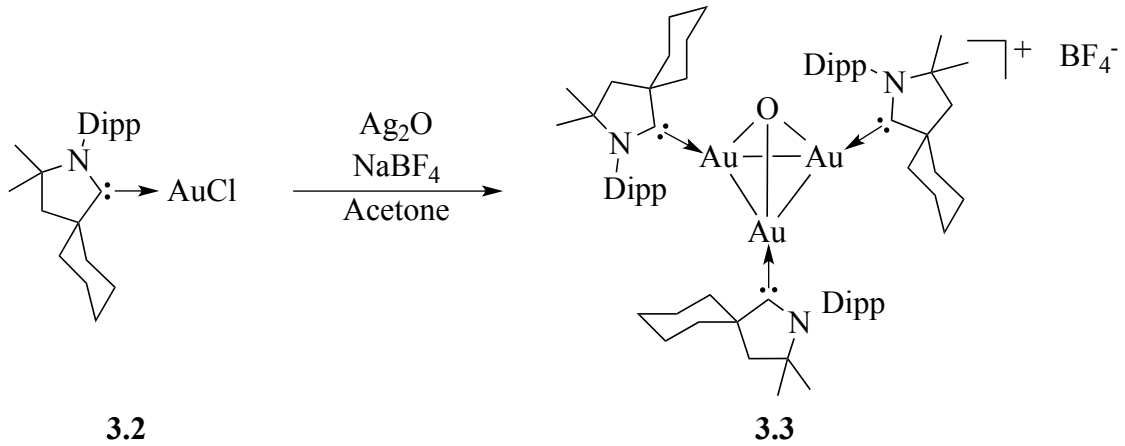

3.2 **3.3**

Scheme 3.3: Synthesis of $[(CAAC)Au]_3$-μ_3-oxo complex.

Subsequent reduction of **3.3** with 30 psi of carbon monoxide for 12 hours yielded the desired trinuclear gold complex **3.4**.[3] Complex **3.4** was characterized by ^1H and ^{13}C

NMR spectroscopies as well as by high-resolution mass spectrometry. The ^{13}C NMR signal corresponding to the carbene carbon appears at 262.5 ppm, which is halfway between those observed for gold(I) complexes **3.2** and **3.3** (237.4 and 230.4 ppm, respectively) and the (CAAC)Au-Au(CAAC) complex (287.2 ppm), as is expected for a mixed-valence gold(I)/gold(0) compound.

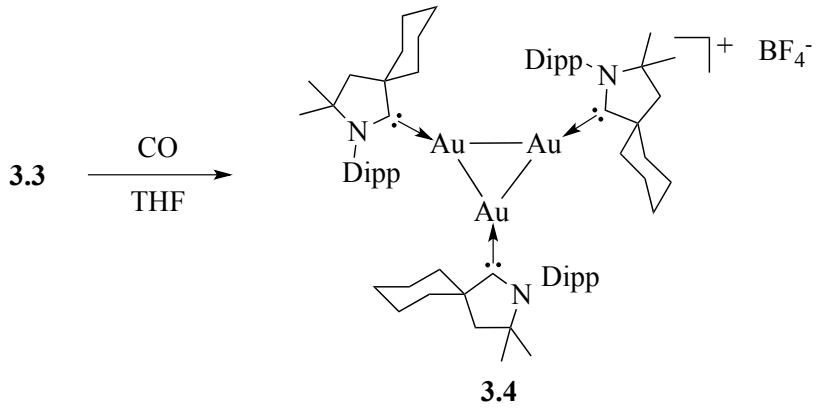

3.4

Scheme 3.4: Synthesis of $[(CAAC)Au]_3$ **3.4** by reduction of **3.3** with CO.

3.4 was found to be indefinitely stable in air and moisture both in the solid state and in solution; its melting point [240 ^oC (dec.)] is another indication of its high stability. Even though the reaction sequence from **3.2** to **3.4** proved to be efficient, the starting material **3.2** proved to be very difficult to purify due to its ability to rearrange to $(CAAC)_2Au(I)$ and $AuCl_2$.[7] Therefore, we decided to investigate the possibility of performing ligand exchange on the readily available phosphine-supported μ^3-oxo complex **3.5**. The addition of 3.5 equivalents of Et_2CAAC[8] to **3.5**[9] afforded the μ^3-oxo complex **3.6** in 86% yield as an off-white solid. Similar to **3.4,** treatment with carbon monoxide yielded the desired trinuclear gold complex **3.7** as a pale yellow solid in almost quantitative yield.

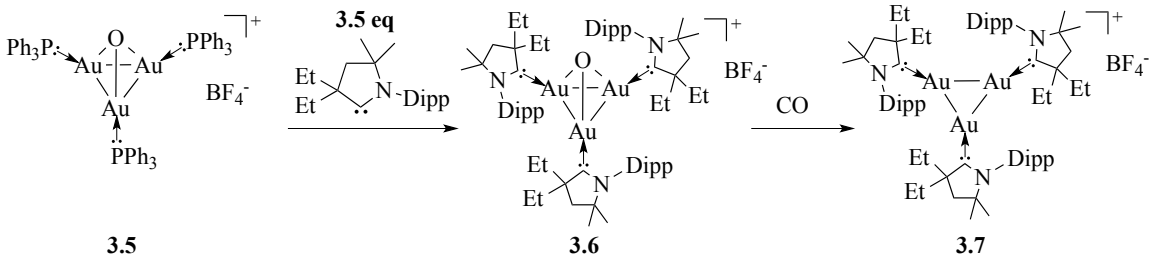

Scheme 3.5: Synthesis of $[((Et_2CAAC)Au)_3O]^+$ **3.6** and $[(CAAC)Au]_3$ **3.7**.

Very interestingly, this reaction sequence is very flexible and the number of CAAC ligands can be modulated with the stoichiometry. Indeed, the addition of two equivalents of Et_2CAAC to **3.5** allows, after reduction with CO, for the preparation of the mixed (CAAC)(phosphine)-supported complex **3.8**.

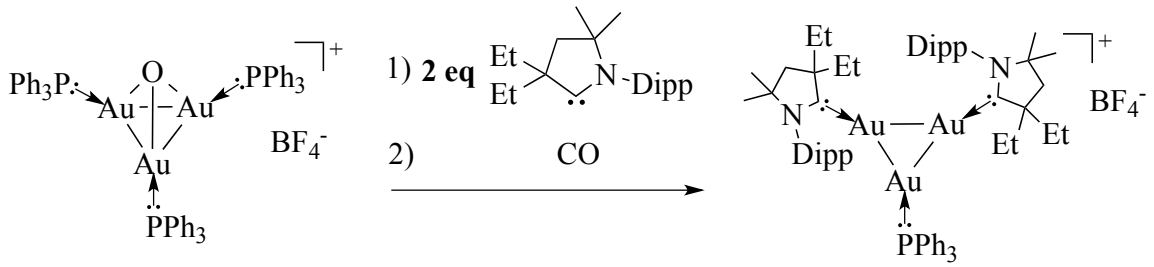

Scheme 3.6: Synthesis of $[(Et_2CAAC)_2(PPh_3)Au_3]^+$ **3.8.**

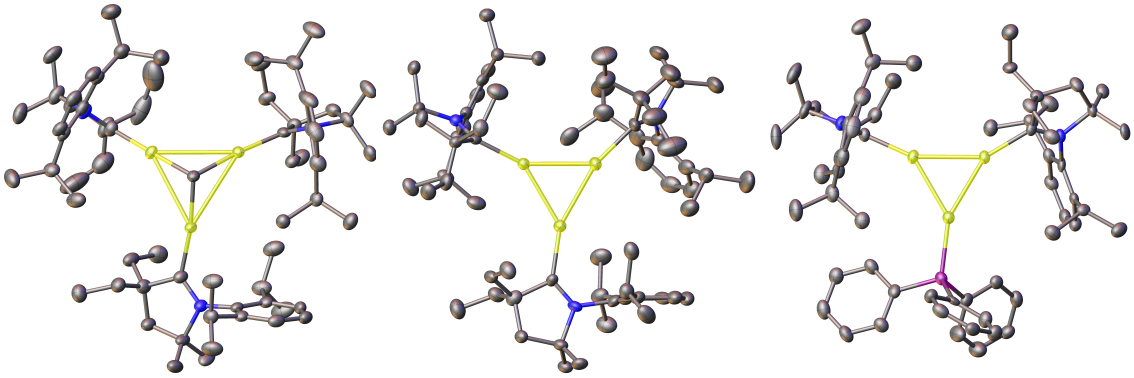

3.6 **3.7** **3.8**

Figure 3.1: X-ray crystal structure of **3.6**, **3.7** and **3.8**.

Single crystal X-ray diffraction studies of **3.6**, **3.7** and **3.8** were carried out (**Figure 3.1**). Similar to the analogous cluster bearing P(*o*-Tol)$_3$ ligands,[10] **3.6** has a pseudo-tetrahedral geometry, and can be viewed as three [CAAC-Au]$^+$ units, with strong aurophilic interactions,[11] bound to a central O^{2-}.

In **3.7**, the Au-Au distances [2.6324(8) - 2.6706(8) Å] are much shorter than in **3.6** [3.1669(3) – 3.3149(3) Å] indicative of true covalent bonds; for comparison, the Au-Au bond distance of 2.552 Å was observed for the neutral (CAAC)Au-Au(CAAC) complex described in Chapter 2. In **3.8**, the distance between the two gold atoms bearing CAACs [2.6604(4) Å] is slightly longer than the other Au-Au bonds [2.6191(4) and 2.6219(4) Å], arguing for the stronger σ-donor properties of CAACs, compared to triphenylphosphine.

As shown in **Figure 3.2**, the one-electron reversible reduction of **3.7** at $E_{1/2}$ = 2.05 V shows the possibility of forming the neutral gold trimer with three CAACs.

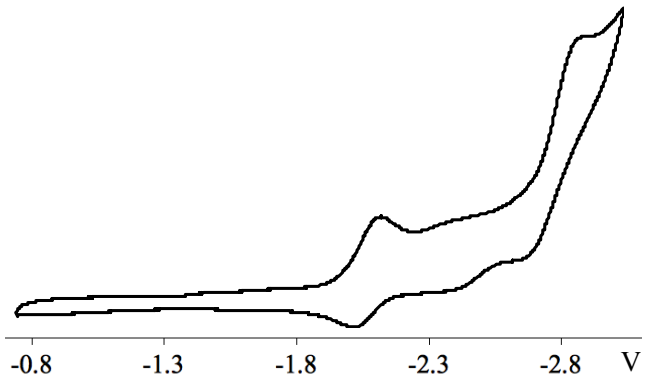

Figure 3.2: Cyclic Voltammogram of **3.7**.

Unfortunately, the attempted reduction of **3.7** failed despite the addition of several different reducing agents: Na, K, KC_8, Li $_{powder}$ and Li $_{4,4'Di\text{-}tertbutylbiphenyl}$. As illustrated in **Figure 3.2**, an irreversible reduction at $E_{1/2}$ = -2.8 V leads to unwanted over reduction products that could not be isolated.

Reactivity of Trinuclear Gold Cation

Due to the ongoing interest in gold-catalyzed functionalization of amines,[12] we chose to investigate the behavior of cluster **3.7** for the carbonylation of this class of compounds. Such a reaction is the simplest and most environmentally friendly route for the preparation of urea derivatives.[13]

Table 3.1: Catalytic carbonylation of cyclohexyl amine using **3.4** and **3.7**.

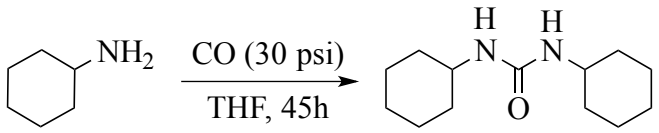

Entry	Catalyst	Temperature	O_2	Yield (%)
1	**3.7** (2.5 %)	70 °C	none	0
2	**3.7** (2.5 %)	70 °C	Air	30
3	**3.7** (2.5 %)	90 °C	Air	51
4	**3.7** (2.5 %)	90 °C	10 psi	69
5	**3.4** (2.5 %)	90 °C	10 psi	29

Surprisingly, we observed that with 2.5 mol % of **3.7**, cyclohexylamine did not react with carbon monoxide (30 psi) even after 4 days at 70 °C under strict anaerobic conditions (**Table 3.1**, **entry 1**). However, we quickly found that under the same experimental conditions, but in air, N,N'-dicyclohexylurea was formed in 30 % yield after two days (**Table 3.1**, **entry 2**).

Increasing the temperature to 90 °C appeared to be beneficial for the conversion (**Table 3.1**, **entry 3**), but further increase above 90 °C did not improve the yields, certainly due to the degradation of the catalyst. Interestingly, under 10 psi of oxygen, the yield improved drastically (**Table 3.1**, **entry 4**). Noteworthy, under the same conditions, the more bulky cluster **3.4** proved to be less efficient than **3.7** (**Table 3.1**, **entry 5**). As an aside, the $CAAC_{menthyl}$-AuCl complex failed to produce any N,N'-dicyclohexylurea.

Using the optimized conditions, we did preliminary experiments to study the scope of this catalytic process. As shown in **Table 2**, benzyl amine and 2-phenylethylamine could be converted to the corresponding urea in good yields of 74% and 72%, respectively (**Table 2, entries 1 and 3**). No decomposition of the catalyst could

be observed during the reaction with benzylamine as the substrate, which encouraged us to decrease the catalyst loading to 0.5 mol %; the urea was obtained with 52% yield after extending the reaction time to four days (**Table 2**, **entry 2**). In the case of more sterically hindered amines, the conversion was significantly decreased (**Table 2, entry 4-6**), while no reaction was observed with the less nucleophilic aniline (**Table 2, entry 7**).

Table 3.2: Catalytic production of urea using **3.7**, amines, CO and O_2.

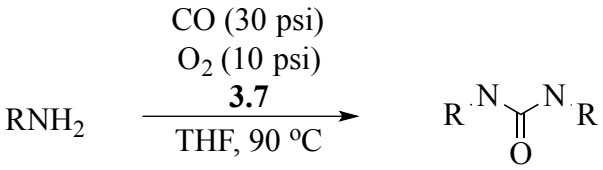

Entry	Substrate	**3.7** (mol %)	Time (h)	Yield (%)
1	Benzylamine	2.5	45	74
2	Benzylamine	0.5	96	52
3	2-Phenylethylamine	2.5	45	72
4	α-Methylbenzylamine	2.5	45	40
5	α-Methylbenzylamine	2.5	72	55
6	2-Adamantylamine	2.5	45	10
7	Aniline	2.5	45	0

Deduction of the Mechanism

Examination of the literature shows that several other transition metal catalysts are efficient for this transformation, but generally at higher CO pressures and temperatures.[14] More importantly, the well-defined nature of **3.7** allowed for an investigation of the intermediates involved in the catalytic process. We first found that **3.7** does not react with carbon monoxide (30 psi) at 90 °C. Similarly, in the absence of air,

no reaction occurs with cyclohexylamine at 90 °C. In contrast, in aerobic condition, or under 10 psi of oxygen, **3.7** reacts with cyclohexylamine leading, after two days at 70 °C, to the dinuclear complex **3.9a**, which was isolated in 63 % yield (**Scheme 3.7**).

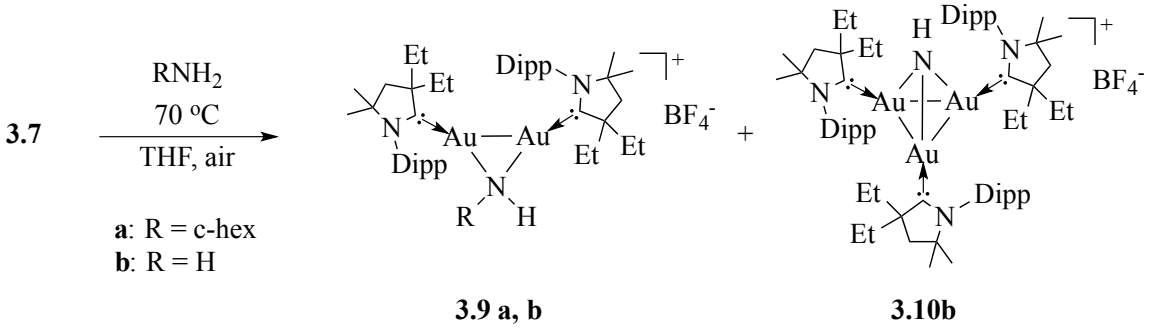

Scheme 3.7: Addition of cyclohexylamine and ammonia to **3.7**.

Under the same experimental conditions, but using ammonia, a mixture of the dinuclear species **3.9b** (56 %), and trinuclear complex **3.10b** (44%) was obtained. The structures of **3.9a/b** and **3.10b** were ascertained by X-ray diffraction (**Scheme 3.7**). In all of these complexes, the Au-Au bond distances (3.16 to 3.31 Å) are typical for gold(I)-gold(I) aurophilic interactions, and are similar to those observed in the μ^3-oxo complex **3.6**.

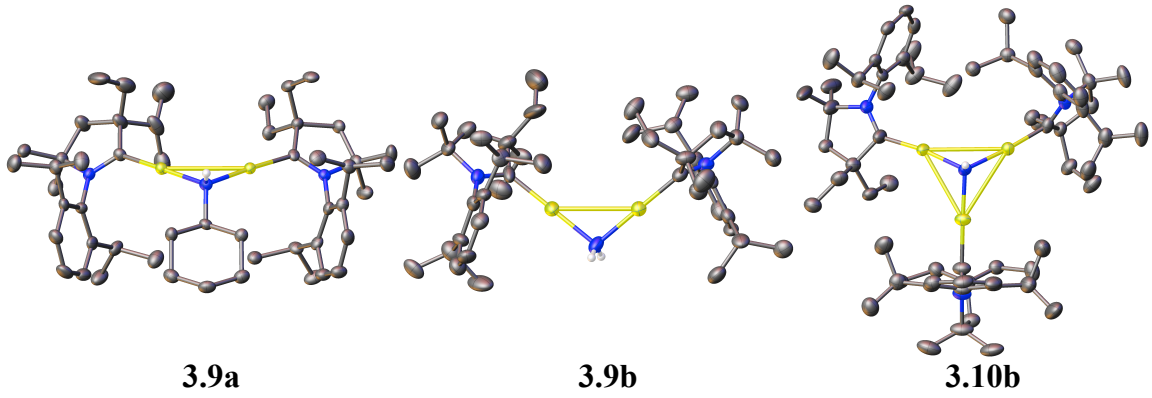

Figure 3.3: X-ray crystal structures of **3.9a**, **3.9b** and **3.10b**.

To further elucidate the mechanism, the next question was whether CO is able to displace the nitrogen fragment of complexes **3.9** and **3.10**. Indeed, when **3.9a**, **b** and **3.10b** were treated with carbon monoxide (30 psi) at 70 ^{o}C, the trinuclear cluster **3.7** was recovered. In the case of **3.9a**, we were also able to observe the formation of the cyclohexyl isocyanate.

During the first step of the catalytic process (**3.7** to **3.9** or **3.10**), two gold centers are oxidized. We hypothesize that oxygen is necessary to scavenge the hydrogen atoms, but the mechanism remains unclear. During the second step (**3.9** and **10** to **7**), two gold centers are reduced, and the carbon monoxide is oxidized by two electrons.

Conclusion

Even though the preparation of a neutral trinuclear gold species was not possible, the corresponding cationic trinuclear gold cluster was prepared. This allowed a catalytic study of amines and carbon monoxide, under relatively low pressures, to produce urea derivatives. The isolation of **3.7** allowed for the intermediate complexes, **3.9** and/or **3.10**, to also be accessed and a redox process mechanism proposed. The carbonylation of amines reported here is a very rare example of a gold catalyzed process involving a definite change of oxidation state of the metal from $Au_2(0)Au(I)$ to $Au_3(I)$. **3.7** is just the second trinuclear gold cluster to be isolated, and demonstrates a general preparation which paves the way to a variety of carbene-supported multinuclear gold clusters, using known well-defined mixed-valence phosphine-gold clusters

Chapter 3 has been adapted from material published in:L. Jin, D. S. Weinberger, M. Melaimi, C. E. Moore, A. L. Rheingold, G. Bertrand *Angew. Chem. Int. Ed.* **2014**, *submitted*. The dissertation author initiated the project and participated in the chemistry.

Appendix: Experimental Section

General: Solvents were dried by standard methods and distilled under argon. ^{1}H and ^{13}C NMR spectra were recorded on Bruker Avance 300 (300 MHz for ^{1}H, 75 MHz for ^{13}C) and Varian Inova 500 spectrometers (500 MHz for ^{1}H, 125 MHz for ^{13}C) at 25 °C. NMR multiplicities are abbreviated as follows: *s* = singlet, *d* = doublet, *t* = triplet, *q* = quartet, *sx* = sextet, *sept* = septet, *m* = multiplet, *br* = broad signal. Chemical shifts are given in ppm and are referenced to $SiMe_4$ (^{1}H, ^{13}C). Coupling constants *J* are given in Hz. Mass spectra were performed at the UC San Diego Mass Spectrometry Laboratory. Melting points were measured with a Büchi melting point apparatus. Single crystal X-ray diffraction data were collected on a Bruker Apex II-CCD detector using Mo-K_α radiation (λ = 0.71073 Å) or Cu-K_α radiation (λ = 1.54178 Å). Crystals were selected under oil, mounted on nylon loops, then immediately placed in a cold stream of N_2. Structures were solved and refined using Olex2 and SHELXTL. Et_2CAAC,[8] Cy-CAAC[7], Cy-CAACAuCl,[7] and $(PPh_3Au)_3O^+BF_4^-$[9] were prepared following literature procedures while all other starting materials were purchased from commercial sources.

3.3

A mixture of freshly prepared Ag_2O, Cy-CAACAuCl (200 mg, 0.36 mmol) and $NaBF_4$ (220 mg, 2.0 mmol) in acetone (20 mL) was stirred at room temperature for 1 h. Volatiles were removed under vacuum and complex **3.3** was extracted with dichloromethane (3 x 10 mL). After removal of the solvent under vacuum, the solid was washed with diethyl ether (3 x 10 mL). Complex **3.3** was obtained as an off-white solid [124 mg, 62 %, m.p. 208 °C (dec.)]. ^{1}H NMR ($CDCl_3$, 500MHz) d 7.29 (t, *J* = 7.6 Hz, 3 H), 7.14 (d, *J* = 7.6 Hz, 6 H), 2.61 (sept., *CH*CH_3, *J* = 6.4 Hz, 6 H), 2.20 (m, 6H), 2.11 (s, 6 H), 1.85-1.70 (m, 12 H), 1.49-1.34 (m, 12 H), 1.29 (s, 18 H), 1.25 (d, *J* = 6.4 Hz, 18 H), 1.19 (d, *J* = 6.4 Hz, 18 H); $^{13}C\{^{1}H\}$ NMR ($CDCl_3$, 125 MHz) d 230.4 (C_{carb}), 145.0 (C_{ortho}), 133.9 (C_{ipso}), 129.6 (C_{para}), 124.7 (C_{meta}), 79.9 (C_{quat}), 59.4 (C_{quat}), 45.1 (C_{H2}), 36.9 (C_{H2}), 29.7, 29.1, 27.8, 25.5, 23.0, 21.9.

3.4

A THF solution (10 mL) of **3.3** (80 mg, 0.048 mmol) was stirred under 30 psi of CO for 12 h. The solvent was removed under vacuum and **3.4** was obtained as a yellow solid [59 mg, 75 %, m.p. 240 °C (dec.)]. ^{1}H NMR ($CDCl_3$, 500MHz) d 7.35 (t, *J* = 7.7 Hz, 3 H), 7.16 (d, *J* = 7.7 Hz, 6 H), 2.61 (sept., *CH*CH_3, *J* = 6.7 Hz, 6 H), 2.04-1.90 (m, 12 H), 1.76 (m, 6 H), 1.62 (m 6 H), 1.40-1.17 (m, 48 H), 1.09 (d, *J* = 6.7 Hz, 18 H); $^{13}C\{^{1}H\}$ NMR ($CDCl_3$, 125 MHz) = 262.5 (C_{carb}), 145.0 (C_{ortho}), 133.9 (C_{ipso}), 129.4 (C_{para}), 124.5 (C_{meta}), 81.0 (C_{quat}), 60.1 (C_{quat}), 46.6 (C_{H2}), 36.5 (C_{H2}), 29.5 , 29.1, 28.1, 25.2, 22.8, 22.1; HRMS (ESI-TOFMS): m/z calculated for $C_{69}H_{105}Au_3N_3^+$ 1566.7305; found 1566.7299.

3.6

A THF solution (30 mL) of Et_2CAAC (1.1 g, 3.5 mmol) was added slowly to a THF solution (90 mL) of $(PPh_3Au)_3O^+BF_4^-$ (1.5 g, 1.0 mmol). After 20 minutes, volatiles were removed under vacuum and the residue was washed with diethyl ether (3 x 10 mL). After drying, complex 6 was obtained as an off-white solid [1.42 g, 86 % yield, m.p. 220 °C (dec.)]. ^{1}H NMR ($CDCl_3$, 500MHz) = 7.36 (t, J = 7.7 Hz, 3 H), 7.18 (d, J = 7.7 Hz, 6 H),

2.67 (sept, CHCH3, J = 7.0 Hz, 6 H), 2.00 (s, 6 H), 1.76-1.63 (m, 6 H), 1.61-1.49 (m, 6 H), 1.29-1.23 (m, 36 H), 1.23-1.17 (m, 18 H), 0.96 (t, J = 7.0 Hz, 18 H); $^{13}C\{^{1}H\}$ NMR (CDCl3, 125 MHz) = 231.0 (C_{carb}), 145.1 (C_{ortho}), 134.1 (C_{ipso}), 129.7 (C_{para}), 124.7 (C_{meta}), 80.6 (C_{quat}), 62.8 (C_{quat}), 40.3 (CH_2), 32.1 (CH_2), 29.3, 29.2, 27.7, 22.6, 9.71; HRMS (ESI-TOFMS): m/z calculated for $C_{66}H_{105}Au_3N_3O^+$ 1546.7254, found 1546.7226. Single crystals of **3.6** were obtained by vapor diffusion of diethyl ether into a saturated THF solution.

Crystal data and structure refinement for **3.6.**

Identification code	MM11
Empirical formula	$C_{74}H_{121}Au_3BF_4N_3O_3$
Formula weight	1778.44
Temperature/K	100 (2)
Crystal system	monoclinic
Space group	$P2_1/n$
a/Å	13.9536(8)
b/Å	20.3034(13)
c/Å	26.1176(15)
α/°	90
β/°	90.610(3)
γ/°	90
Volume/Å^3	7398.8(8)
Z	4
ρ_{calc}mg/mm^3	1.597
m/mm^{-1}	5.990
F(000)	3552.0
Crystal size/mm^3	0.117 × 0.083 × 0.055
Radiation	MoKα (λ = 0.71073)
2Θ range for data collection	5.082 to 52.814°
Index ranges	-17 ≤ h ≤ 17, -25 ≤ k ≤ 25, -32 ≤ l ≤ 32
Reflections collected	52678
Independent reflections	15069 [R_{int} = 0.0403, R_{sigma} = 0.0420]
Data/restraints/parameters	15069/0/727
Goodness-of-fit on F^2	1.041
Final R indexes [I>=2σ (I)]	R_1 = 0.0356, wR_2 = 0.0870
Final R indexes [all data]	R_1 = 0.0492, wR_2 = 0.0923
Largest diff. peak/hole / e Å^{-3}	3.93/-1.73

3.7

A THF solution (15 mL) of **3.6** (1.4 g, 0.87 mmol) was stirred under 30 psi of CO for 12 h. The solvent was removed under vacuum and **3.7** was obtained as a yellow solid [1.28 g, 91 % yield, m.p. 328 °C (dec.)]. ^1H NMR ($CDCl_3$, 500MHz) = 7.37 (t, J = 7.8 Hz, 3 H),

7.18 (d, J = 7.8 Hz, 6 H), 2.68 (sept., $CHCH_3$, J = 6.6 Hz, 6 H), 1.90 (s, 6 H), 1.64-1.53 (m, 6 H), 1.45-1.35 (m, 6 H), 1.28-1.19 (m, 36 H), 1.09 (d, J = 6.5 Hz, 18 H), 0.89 (t, J = 7.3 Hz, 18 H); $^{13}C\{^1H\}$ NMR ($CDCl_3$, 125 MHz) = 264.8 (C_{carb}), 145.0 (C_{ortho}), 134.0 (C_{ipso}), 129.5 (C_{para}), 124.5 (C_{meta}), 81.7 (C_{quat}), 63.6 (C_{quat}), 41.9 (CH_2), 31.5 (CH_2), 29.2 , 29.1, 28.0, 22.4, 9.80; HRMS (ESI-TOFMS): m/z calculated for $C_{66}H_{105}Au_3N_3^+$ 1530.7305, found 1530.7312. Single crystals of **3.7** were obtained by vapor diffusion of diethyl ether into a saturated THF solution.

Crystal data and structure refinement for **3.7**.

Identification code	MM40
Empirical formula	$C_{70}H_{113}Au_3BF_4N_3O$
Formula weight	1690.34
Temperature/K	100.0
Crystal system	triclinic
Space group	P-1
a/Å	19.0405(13)
b/Å	19.8807(14)
c/Å	38.750(3)
α/°	89.409(4)
β/°	79.696(4)
γ/°	89.662(4)
Volume/Å^3	14431.0(18)
Z	8
ρ_{calc}mg/mm^3	1.556
m/mm^{-1}	6.136
F(000)	6720.0
Crystal size/mm^3	0.117 × 0.052 × 0.041
Radiation	MoKα (λ = 0.71073)
2Θ range for data collection	2.048 to 52.91°
Index ranges	$-20 \le h \le 23$, $-19 \le k \le 24$, $-44 \le l \le 48$
Reflections collected	179323
Independent reflections	59126 [R_{int} = 0.0547, R_{sigma} = 0.0639]
Data/restraints/parameters	59126/374/3023
Goodness-of-fit on F^2	1.059
Final R indexes [I>=2σ (I)]	R_1 = 0.0797, wR_2 = 0.2000
Final R indexes [all data]	R_1 = 0.1077, wR_2 = 0.2163
Largest diff. peak/hole / e Å^{-3}	8.11/-2.21

Crystal data and structure refinement for **3.8.**

Identification code	MM26
Empirical formula	$C_{62}H_{85}Au_3BF_4N_2P$

Formula weight	1566.99
Temperature/K	100.0
Crystal system	monoclinic
Space group	$P2_1/c$
a/Å	15.1851(8)
b/Å	24.1624(15)
c/Å	17.1284(10)
α/°	90
β/°	108.536(2)
γ/°	90
Volume/Å^3	5958.5(6)
Z	4
ρ_{calc}mg/mm^3	1.747
m/mm^{-1}	7.447
F(000)	3056.0
Crystal size/mm^3	0.113 × 0.013 × 0.005
Radiation	MoKα (λ = 0.71073)
2Θ range for data collection	3.022 to 50.866°
Index ranges	$-18 \leq h \leq 18$, $-29 \leq k \leq 29$, $-20 \leq l \leq 20$
Reflections collected	69665
Independent reflections	10951 [R_{int} = 0.0769, R_{sigma} = 0.0622]
Data/restraints/parameters	10951/60/711
Goodness-of-fit on F^2	1.051
Final R indexes [I>=2σ (I)]	R_1 = 0.0374, wR_2 = 0.0554
Final R indexes [all data]	R_1 = 0.0777, wR_2 = 0.0665
Largest diff. peak/hole / e Å^{-3}	1.34/-1.54

3.9a

A THF solution (1 mL) of cluster **3.7** (100 mg, 0.06 mmol) and cyclohexylamine (120 mg, 1.2 mmol) was stirred at 70 °C for 48 h. Volatiles were removed under vacuum and the residue was washed with diethyl ether (3 x 5 mL). After drying, **3.9a** was obtained as an off-white solid [68 mg, 63 % yield, m.p. 208 °C (dec.)]. ^{1}H NMR ($CDCl_3$, 500MHz) = 7.38 (t, J = 7.8 Hz, 2 H), 7.23 (d, J = 7.8 Hz, 4 H), 2.76 (sept, $CHCH_3$, J = 6.6 Hz, 4 H), 2.28 (br, 1 H), 2.11 (s, 4 H), 1.91-1.78 (m, 4 H), 1.76-1.66 (m, 4 H), 1.58 (d, J = 3.6 Hz, 12 H), 1.35-1.23 (m, 24 H), 1.05 (t, J = 7.8 Hz, 12 H), 0.95-0.84 (m, 3 H), 0.80-0.57 (m, 4 H), 0.44-0.27 (m, 3 H); $^{13}C\{^1H\}$ NMR ($CDCl_3$, 125 MHz) = 240.3 (C_{carb}), 145.1 (C_{ortho}), 134.8 (C_{ipso}), 129.9 (C_{para}), 125.2 (C_{meta}), 125.0 (C_{meta}), 81.2 (Cq_{uat}), 62.3 (C_{quat}), 60.4 (CH), 41.4 (CH_2), 40.0 (CH_2), 31.7, 29.4, 29.2, 26.9, 26.8, 25.2, 25.1, 23.2, 23.1, 9.7, 9.6; HRMS (ESI-TOFMS): m/z calculated for $C_{50}H_{82}Au_2N_3^+$ 1118.5834, found 1118.5829. Single crystals of **3.9a** were obtained by vapor diffusion of diethyl ether into a saturated $CHCl_3$ solution.

Crystal data and structure refinement for **3.9a.**

Identification code	MM46
Empirical formula	$C_{51}H_{83}Au_2BCl_2F_4N_3$
Formula weight	1289.84
Temperature/K	100 (2)
Crystal system	triclinic
Space group	P-1
a/Å	11.8855(9)
b/Å	14.1926(11)
c/Å	18.4163(12)
α/°	71.650(2)
β/°	88.721(2)
γ/°	66.067(2)
Volume/Å^3	2675.1(3)
Z	2
ρ_{calc}mg/mm^3	1.601
m/mm^{-1}	5.627
F(000)	1286.0
Crystal size/mm^3	0.211 × 0.152 × 0.145
Radiation	MoKα (λ = 0.71073)
2Θ range for data collection	4.15 to 52.858°
Index ranges	-14 ≤ h ≤ 14, -17 ≤ k ≤ 17, -23 ≤ l ≤ 23
Reflections collected	55249
Independent reflections	10962 [R_{int} = 0.0773, R_{sigma} = 0.0579]
Data/restraints/parameters	10962/0/600
Goodness-of-fit on F^2	1.040
Final R indexes [I>=2σ (I)]	R_1 = 0.0307, wR_2 = 0.0559
Final R indexes [all data]	R_1 = 0.0480, wR_2 = 0.0613
Largest diff. peak/hole / e Å^{-3}	0.90/-0.58

3.9b & 3.10b

A THF solution (1 mL) of cluster **3.7** (45 mg, 0.028 mmol) and NH_3 (1 ml) was stirred at 70 °C for 60 h. Volatiles were removed under vacuum and the residue was washed with pentane (3 x 5 mL). A 1.3:1mixture of **3.9b** and **3.10b** was obtained as an off-white solid. Extraction of the solid with diethyl ether (3 x 5 mL) and evaporation of the solvent under vacuum allow for the isolation of pure **3.9b** [10 mg, m.p. 189 °C (dec.)]. Extraction of the remaining solid with a 1:1 diethyl ether/dichloromethane solution (10 mL) and evaporation of the solvents under vacuum led to the isolation of pure **10b** as a colorless solid [7 mg, m.p. 224 °C (dec.)].

9b: ^{1}H NMR ($CDCl_3$, 500MHz) = 7.44 (t, *J* = 7.4 Hz, 2 H), 7.25 (d, *J* = 7.8 Hz, 4 H), 2.74 (sept, *CH*CH_3, *J* = 6.7 Hz, 4 H), 2.08 (s, 4 H), 1.89-1.79 (m, 4 H), 1.77-1.66 (m, 4 H), 1.37 (s, 12 H), 1.30 (d, *J* = 6.7 Hz, 12 H), 1.27 (d, *J* = 6.7 Hz, 12 H), 1.05 (t, *J* = 7.0

Hz, 12 H), 0.66 (br, 2 H); $^{13}C\{^{1}H\}$ NMR ($CDCl_3$, 125 MHz) = 239.1 ($C_{carbene}$), 145.1 (C_{ortho}), 134.2 (C_{ipso}), 130.1 (C_{para}), 125.0 (C_{meta}), 81.3 (C_{quat}), 62.5 (C_{quat}), 41.2 (C_{H2}), 31.8, 29.3, 29.2, 27.1, 22.8, 9.6. HRMS (ESI-TOFMS): m/z calculated for $C_{44}H_{72}Au_2N_3^+$ 1036.5052, found 1036.5052. Single crystals of **3.9b** were obtained by vapor diffusion of diethyl ether into a saturated THF solution.
3.10b: ^{1}H NMR ($CDCl_3$, 500MHz) = 7.34 (t, J = 7.8 Hz, 3 H), 7.15 (d, J = 7.8 Hz, 6 H), 2.69 (sept, *CH*CH_3, J = 6.7 Hz, 6 H), 1.99 (s, 6 H), 1.91-1.78 (m, 6 H), 1.72-1.63 (m, 6 H), 1.37 (br, 1 H), 1.28 (s, 18 H), 1.25 (d, J = 6.7 Hz, 18 H), 1.15 (d, J = 6.7 Hz, 18 H), 1.02 (t, J = 7.4 Hz, 18 H); $^{13}C\{^{1}H\}$ NMR ($CDCl_3$, 125 MHz) = 242.1 ($C_{carbene}$), 145.2 (C_{ortho}), 134.4 (C_{ipso}), 129.4 (C_{para}), 125.0 (C_{meta}), 124.6 (C_{meta}), 80.2 (C_{quat}), 62.8 (C_{quat}), 41.3 (C_{H2}), 31.9, 29.3, 29.1, 27.5, 22.9, 9.6. HRMS (ESI-TOFMS): m/z calculated for $C_{66}H_{106}Au_3N_4^+$ 1545.7414; found 1545.7407. Single crystals of **10b** were obtained by vapor diffusion of diethyl ether into a saturated THF solution.

Crystal data and structure refinement for **3.9b.**

Identification code	MM47
Empirical formula	$C_{46}H_{76}Au_2BF_4N_3O_{0.5}$
Formula weight	1159.84
Temperature/K	100 (2)
Crystal system	monoclinic
Space group	C 1 C1
a/Å	18.618(4)
b/Å	19.464(4)
c/Å	15.459(3)
α/°	90
β/°	122.006(5)
γ/°	90
Volume/Å^3	4750.3(16)
Z	4
ρ_{calc}mg/mm^3	1.622
m/mm^{-1}	6.220
F(000)	2304.0
Crystal size/mm^3	0.124 × 0.053 × 0.047
Radiation	MoKα (λ = 0.71073)
2Θ range for data collection	3.322 to 52.824°
Index ranges	$-23 \le h \le 23$, $-24 \le k \le 24$, $-19 \le l \le 19$
Reflections collected	47755
Independent reflections	9622 [R_{int} = 0.0455, R_{sigma} = 0.0413]
Data/restraints/parameters	9622/60/506
Goodness-of-fit on F^2	1.048
Final R indexes [I>=2σ (I)]	R_1 = 0.0487, wR_2 = 0.1207
Final R indexes [all data]	R_1 = 0.0684, wR_2 = 0.1331

Largest diff. peak/hole / e $Å^{-3}$	4.68/-0.85
Flack parameter	0.412(6)

Crystal data and structure refinement for **3.10b.**

Identification code	MM49
Empirical formula	$C_{76}H_{126}Au_3BF_4N_4O_{2.5}$
Formula weight	1813.51
Temperature/K	100 (2)
Crystal system	monoclinic
Space group	$P2_1/n$
a/Å	14.0639(13)
b/Å	20.3365(19)
c/Å	26.107(2)
α/°	90
β/°	90.716(2)
γ/°	90
Volume/$Å^3$	7466.4(12)
Z	4
$\rho_{calc}mg/mm^3$	1.613
m/mm^{-1}	5.937
F(000)	3632.0
Crystal size/mm^3	0.145 × 0.098 × 0.055
Radiation	MoKα (λ = 0.71073)
2Θ range for data collection	3.306 to 52.874°
Index ranges	$-17 \leq h \leq 17$, $-25 \leq k \leq 25$, $-32 \leq l \leq 32$
Reflections collected	92301
Independent reflections	15356 [R_{int} = 0.0919, R_{sigma} = 0.0556]
Data/restraints/parameters	15356/155/795
Goodness-of-fit on F^2	1.033
Final R indexes [I>=2σ (I)]	R_1 = 0.0405, wR_2 = 0.0916
Final R indexes [all data]	R_1 = 0.0580, wR_2 = 0.0994
Largest diff. peak/hole / e $Å^{-3}$	1.88/-1.32

General procedure for the catalytic carbonylation of amines.

In a pressure flask, 60 mg of cyclohexanamine (0.6 mmol), **3.7** or **3.4** (0.015 mmol, 2.5 mol %), and THF (0.5 mL) were loaded. The flask was charged with 30 psi of CO and 10 psi of O_2 (if mentioned in **Table 3.1**). The reaction mixture was stirred at the temperature and for the time mentioned in **Tables 3.1 and 3.2**. In the series described in **Table 3.1**, yields of the 1,3-dicyclohexylurea were determined by GC using biphenyl as the internal standard. In the series described in **Table 3.2**, yields were determined by ^1H NMR using

triphenylmethane as the internal standard. Ureas produced were characterized by ^{1}H and ^{13}C NMR techniques and compared with reported data.

References

[1] a)Leyva-Pérez, A., Oliver-Meseguer, J., Cabrero-Antonino, J. R., Rubio-Marqués, P., Serna, P., Al-Resayes, S. I., Corma, A., *ACS Catalysis* **2013**, *3*, 1865-1873; b)Oliver-Meseguer, J., Cabrero-Antonino, J. R., Domínguez, I., Leyva-Pérez, A., Corma, A., *Science* **2012**, *338*, 1452-1455; c)Oliver-Meseguer, J., Leyva-Pérez, A., Corma, A., *ChemCatChem* **2013**, *5*, 3509-3515.

[2] Robilotto, T. J., Bacsa, J., Gray, T. G., Sadighi, J. P., *Angew. Chem., Int. Ed.* **2012**, *51*, 12077-12080.

[3] Ramamoorthy, V., Wu, Z., Yi, Y., Sharp, P. R., *J. Am. Chem. Soc.* **1992**, *114*, 1526-1527.

[4] Yang, Y., Sharp, P. R., *J. Am. Chem. Soc.* **1994**, *116*, 6983-6984.

[5] Zeller, E., Beruda, H., Schmidbaur, H., *Inorg. Chem.* **1993**, *32*, 3203-3204.

[6] Tsui, E. Y., Müller, P., Sadighi, J. P., *Angew. Chem., Int. Ed.* **2008**, *47*, 8937-8940.

[7] Frey, G. D., Dewhurst, R. D., Kousar, S., Donnadieu, B., Bertrand, G., *J. Organomet. Chem.* **2008**, *693*, 1674-1682.

[8] Mahoney, J. K., Martin, D., Moore, C. E., Rheingold, A. L., Bertrand, G., *J. Am. Chem. Soc.* **2013**, *135*, 18766-18769.

[9] Nesmeyanov, A. N., Perevalova, E. G., Struchkov, Y. T., Antipin, M. Y., Grandberg, K. I., Dyadhenko, V. P., *J. Organomet. Chem.* **1980**, *201*, 343-349.

[10] Yang, Y., Ramamoorthy, V., Sharp, P. R., *Inorg. Chem.* **1993**, *32*, 1946-1950.

[11] a)Pyykkö, P., *Angew. Chem., Int. Ed.* **2004**, *43*, 4412-4456; b)Pyykkö, P., *Inorg. Chim. Acta* **2005**, *358*, 4113-4130; c)Schmidbaur, H., Schier, A., *Chem. Soc. Rev.* **2012**, *41*, 370-412.

[12] a)Kinjo, R., Donnadieu, B., Bertrand, G., *Angew. Chem., Int. Ed.* **2011**, *50*, 5560-5563; b)Lavallo, V., Frey, G. D., Donnadieu, B., Soleilhavoup, M., Bertrand, G., *Angew. Chem., Int. Ed.* **2008**, *47*, 5224-5228; c)Lavallo, V., Frey, G. D., Kousar, S., Donnadieu, B., Bertrand, G., *Proc. Natl. Acad. Sci. U. S. A.* **2007**, *104*, 13569-13573; d)Zeng, X., Frey, G. D., Kinjo, R., Donnadieu, B., Bertrand, G., *J. Am. Chem. Soc.* **2009**, *131*, 8690-8696; e)Zeng, X., Kinjo, R., Donnadieu, B., Bertrand,

G., *Angew. Chem., Int. Ed.* **2010**, *49*, 942-945; f)Zeng, X., Soleilhavoup, M., Bertrand, G., *Org. Lett.* **2009**, *11*, 3166-3169.

[13] a)Díaz, D. J., Darko, A. K., McElwee-White, L., *Eur. J. Org. Chem.* **2007**, *2007*, 4453-4465; b)Ragaini, F., *Dalton Trans.* **2009**, 6251-6266.

[14] a)Mitsudome, T., Noujima, A., Mizugaki, T., Jitsukawa, K., Kaneda, K., *Chem. Commun. (Cambridge, U. K.)* **2012**, *48*, 11733-11735; b)Shelton, P. A., Zhang, Y., Nguyen, T. H. H., McElwee-White, L., *Chem. Commun.* **2009**, 947-949.

CHAPTER 4:

Isolation of a neutral $(CAAC)_2Cu(0)$ complex

Adapted from:

D. S. Weinberger, N. A. SK, K. C. Mondal, M. Melaimi, G. Bertrand, A. C. Stuckl, H. W. Roesky, B. Dittrich, S. Demeshko, B. Schwederski, W. Kaim, P. Jerabek, G. Frenking

J. Am. Chem. Soc. **2014**, *136*, 6235.

Introduction

Copper has been shown to be prevalent in redox-active metalloproteins with its most common oxidation states being +I and +II.[1] Therefore, this has motivated research in the study of copper complexes that show reduction possibilities. The closest copper complexes to be isolated in the zero oxidation state are thin layers and small clusters of copper deposited on a metal oxide surface. These have been shown to be active catalysts for the water-gas shift reaction and the hydrogenation of CO_2 to methanol;[2] however, it has been established, both experimentally and computationally, that the overall charge on the copper is between 0 and 1.[3]

Excluding elemental copper, mononuclear ligated copper (0) complexes have been reported as intermediates in copper-catalyzed arylation of nitrogen and oxygen and have only been detected by cyclic voltammetry (CV) at fast scan rates.[4] Addition of an aryl halide to the CV cell shows higher concentration of the proposed copper (0) species due to the suggested outer-sphere one-electron reduction of the aryl halide.[5] Furthermore, even the addition of phenanthroline as a π-acceptor, copper(0) was still precipitated and absorbed at the electrode surface. On the other hand, the electrogenerated $[Cu(phen)_2]$ neutral species have been clearly identified by EPR spectroscopy as Cu(I) complexes with partially reduced non-innocent phenanthroline ligands.[6]

There is some evidence presented by Bowmaker for the existence of $[Cu(PH_3)_n]^0$.[7] These complexes were claimed to be prepared by co-deposition of copper vapor with neat phosphine at 60 K. Subsequent calculations show the HOMO for $[Cu(PH_3)_2]^0$, $[Cu(PH_3)_3]^0$, and $[Cu(PH_3)_4]^0$ to be bonding orbitals with a combination of the Cu 4p and the ligand orbitals of π-symmetry.[8] While the calculations show the opportunity to isolate

such complexes, they have only been characterized at low temperatures by infrared (IR) spectroscopy.

Additionally, Atkins and Timms reported that when P≡N was condensed with copper at low temperatures in a krypton matrix, the IR spectrum produced was different from that of the starting material.[9] It was postulated that the resulting complex, which decomposed upon warming, was N≡P→Cu←P≡N. Despite all of the interest in forming stable copper zero complexes, no complexes have been fully characterized in which the formal charge on the copper atom is zero.

We reasoned, that in order to stabilize an electron-rich copper (0) and prevent it from precipitating as metal, a ligand that forms very strong bonds to copper and is capable of accepting electron density would be required. As discussed in Chapter 1, CAACs were electrophilic enough to allow for the isolation and full characterization of a Au(0) species. Consequently, we hypothesized that the analogous Cu(0) could be prepared.

Synthesis and Characterization of Cu(0) complexes.

To start, complex $(Et_2\text{-CAAC})_2Cu^+I^-$ **4.1** was synthesized by reacting 2 equivalents of free carbene and copper(I) iodide with a yield of 75 %. (**Scheme 4.1**).

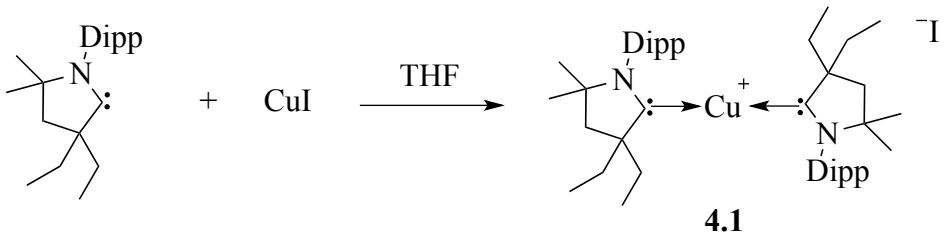

Scheme 4.1: Synthesis of $(CAAC)_2CuI$.

Interestingly, **4.1** crystallized with two different orientations. The first orientation (**Figure 4.1 A**) correlates to the geometry with the 2,6-diisopropylphenyl groups 180° apart. The second orientation (**Figure 4.1 B**) differs by 112.89° rotation around the Cu-C bond. Consequently, the two sterically large groups force the C-Cu-C angle to change from 180.0°, which is expected for divalent Cu(I), to 168.4°.

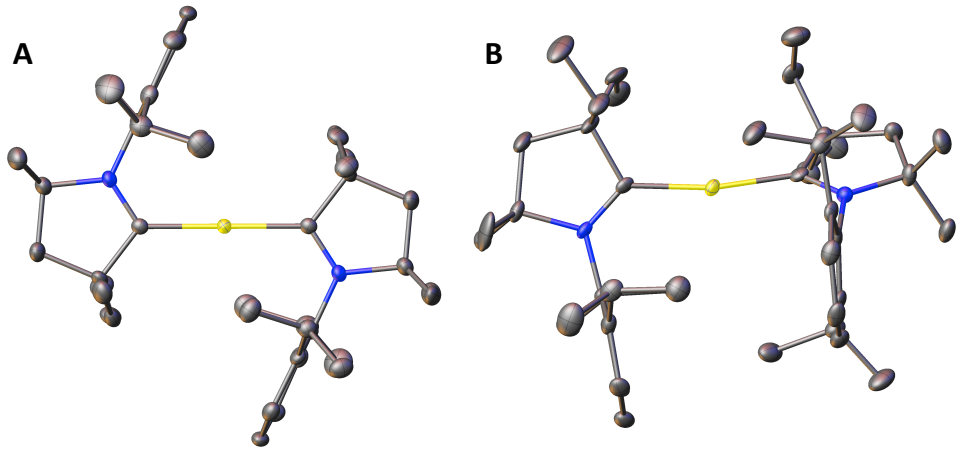

Figure 4.1: Crystal structure of **4.1** showing both conformers. Thermal ellipsoids are at 50 % probability and hydrogens are omitted for clarity.

The cyclic voltammogram of **4.1** in THF, containing 0.1M nBu$_4$NPF$_6$ as electrolyte, showed a quasi-reversible one-electron reduction at $E_{1/2}$ = -1.36 V versus Cp*$_2$Fe$^+$/ Cp*$_2$Fe (Cp*$_2$Fe = decamethylferrocene).

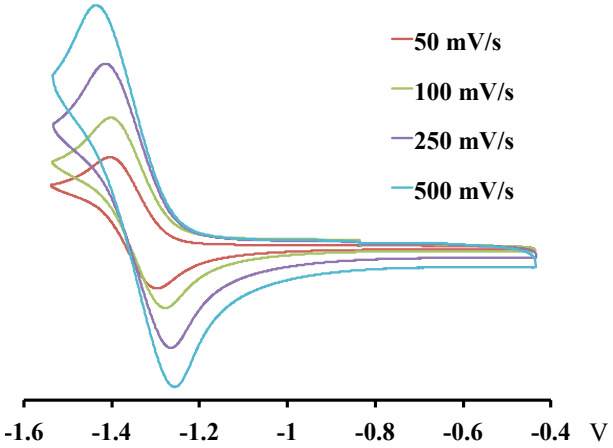

Figure 4.2: Cyclic voltammogram of complex **4.1** (nBu$_4$NPF$_6$ as electrolyte, potential versus Cp*$_2$Fe$^+$/Cp*$_2$Fe).

Therefore, we attempted the reduction of complex **1** with sodium metal (**Scheme 4.2**).

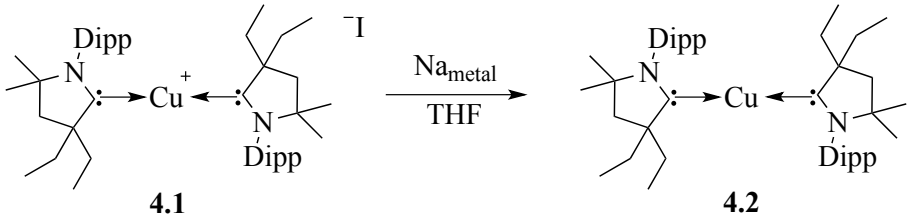

4.1 **4.2**

Scheme 4.2: Synthesis of (Et$_2$-CAAC)$_2$Cu(0) by the one electron reduction of **4.1**.

4.2 was prepared from the one electron reduction of **4.1** with sodium metal in THF. The neutral complex was isolated as a highly water- and air-sensitive solid (35 % yield). Crystals of **4.2** were obtained from a concentrated solution of hexanes at -30 °C.

In collaboration with the group of Herbert Roesky at Georg-August-Universitat in Gottingen Germany, a similar copper structure was obtained through a different route using the Me$_2$-CAAC instead of the Et$_2$-CAAC. A one-pot reaction of Me$_2$-CAAC, CuCl$_2$, and KC$_8$ in a molar ration of 2:1:2 in toluene produced a green solution from which dark

plates of the desired complex $(Me_2\text{-CAAC})_2Cu$ **4.3** were isolated in 7% yield (**Scheme 4.3**).

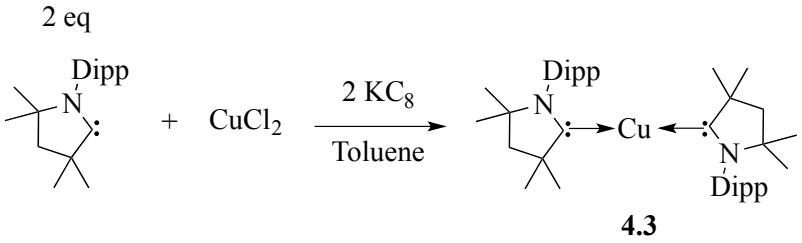

4.3

Scheme 4.3: Synthesis of $(Me_2\text{-CAAC})_2Cu(0)$ by one pot synthesis.

Single crystals were obtained from a toluene solution at -32 °C. **4.3** is stable under an inert atmosphere and decomposes above 142 °C where as **4.2** decomposes above 131°C. The C-Cu bond distances are experimentally found to be 1.8636(15) and 1.8674(10) Å for **4.2** and **4.3**, respectively. The C-N bond distances are 1.3492(19) and 1.3510(13) Å, respectively, which are considerably longer compared to an average C-N bond distance of 1.300 Å in **4.1**. The C-Cu-C bond angles in **4.2** and **4.3** are 180°, which is very close to the angle in one of the geometries of **4.1**.

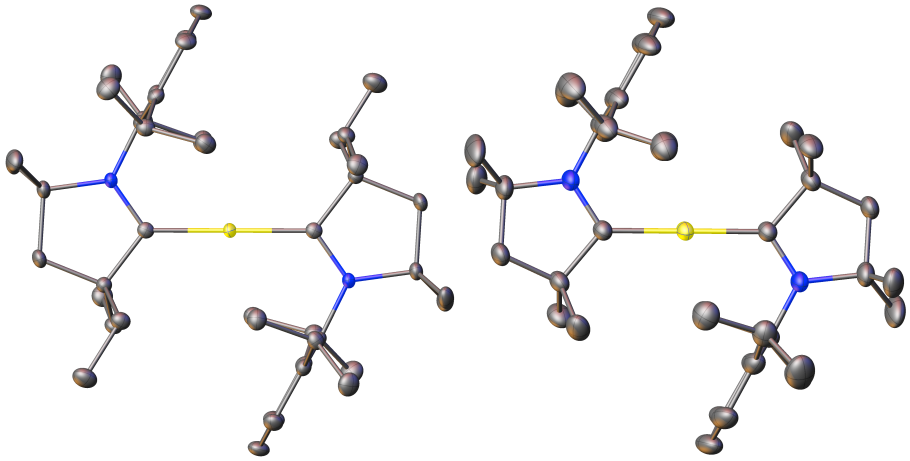

4.2 **4.3**

Figure 4.3: Crystal Structures of **4.2** and **4.3**. Thermal ellipsoids are at 50 % probability and hydrogens are omitted for clarity.

4.3 is not stable in benzene and *n*-hexane, in which it decomposes to produce a light yellow solution. Interestingly, **4.2** is completely stable for at least several days in both hexane and benzene. The crystals of both **4.2** and **4.3** can be stored in a glove box for at least a month at room temperature, whereas on exposure to air they lose their color to produce a light yellow solid after a few minutes. In solution, the color changes almost immediately upon exposure to air. The UV-vis-near-IR spectrum of the toluene solution of **4.3** showed absorption bands at 330, 435, 595, 655, 755, and 1214 nm (**Figure 4.4**).

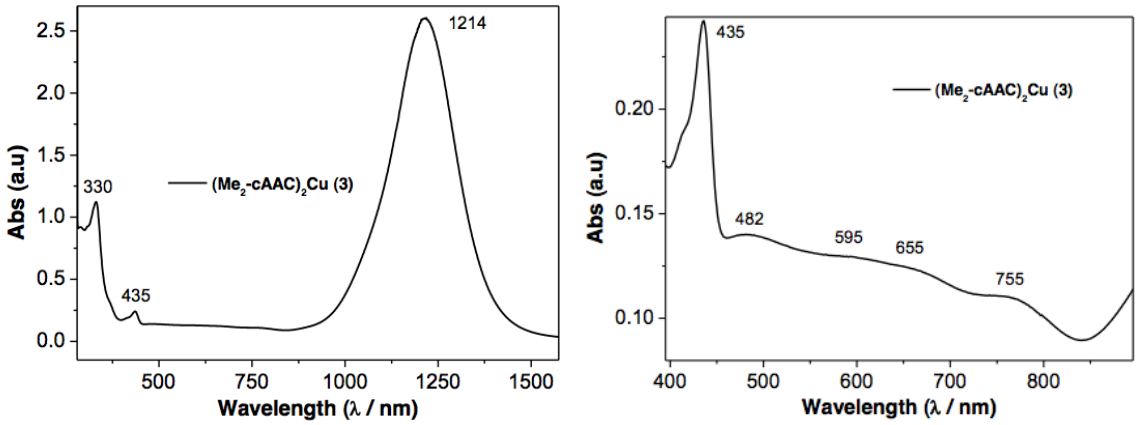

Figure 4.4: UV-vis-near-IR spectrum in toluene of **4.3**.

Quantum chemical calculations using DFT at the M06/def2-SVP level gives insight into the bonding situation. The calculated structure of **4.3** (**Figure 4.5)** is in excellent agreement with the experimental results.

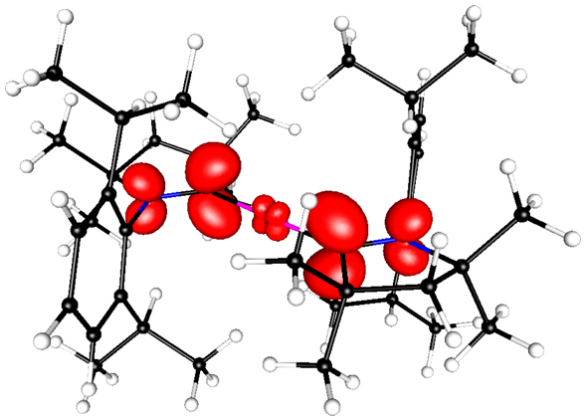

Figure 4.5: Calculated HOMO of **4.3**.

The calculated spin density of the unpaired electron in **4.2** shows that it is delocalized over the p(π) orbitals of the N1-C1-Cu-C1'-N1' moiety, with much larger coefficients at C1/C1'(0.34 than at N1/N1' (0.09) (**Figure 4.5)**.

Similar to the $(CAAC)_2Au(0)$ described in detail in Chapter 1, the calculated ligand-metal bonding scenario in **4.3** is very comparable. As shown in **Figure 4.6**, the strongest interaction is the π-backbonding from the Au p-orbital to the carbon and nitrogen p-orbitals (**Figure 4.6**, **A**). Next is the σ-donation from the lone pair molecular orbital into the vacant Au s-orbital (**Figure 4.6**, **B**). Subsequent bonding is from the π-backdonation of the Au d-orbital into the carbene p-orbital (**Figure 4.6**, **C**) and the carbon's lone-pair molecular orbital into the p(σ) atomic orbital of gold (**Figure 4.6**, **D**).

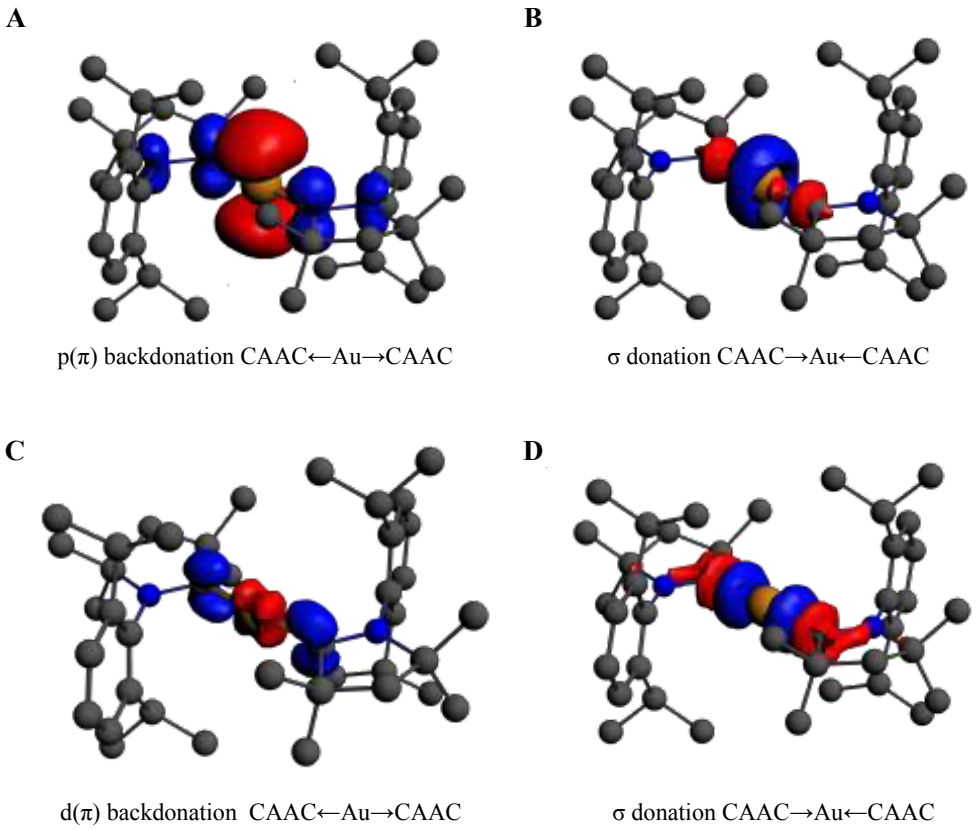

Figure 4.6: EDA-NOCV calculations for **4.3**. Electron flow is from red to blue.

Complexes **4.2** and. **4.3** are EPR active and NMR silent. The room temperature EPR spectrum of **4.2** shows a signal at g = 1.997, with partially resolved hyperfine coupling of about 7 G, involving the copper isotopes ^{63}Cu (69.2%, I = 3/2) and ^{65}Cu (30.8%, I = 3/2) (**Figure 4.7 A**).

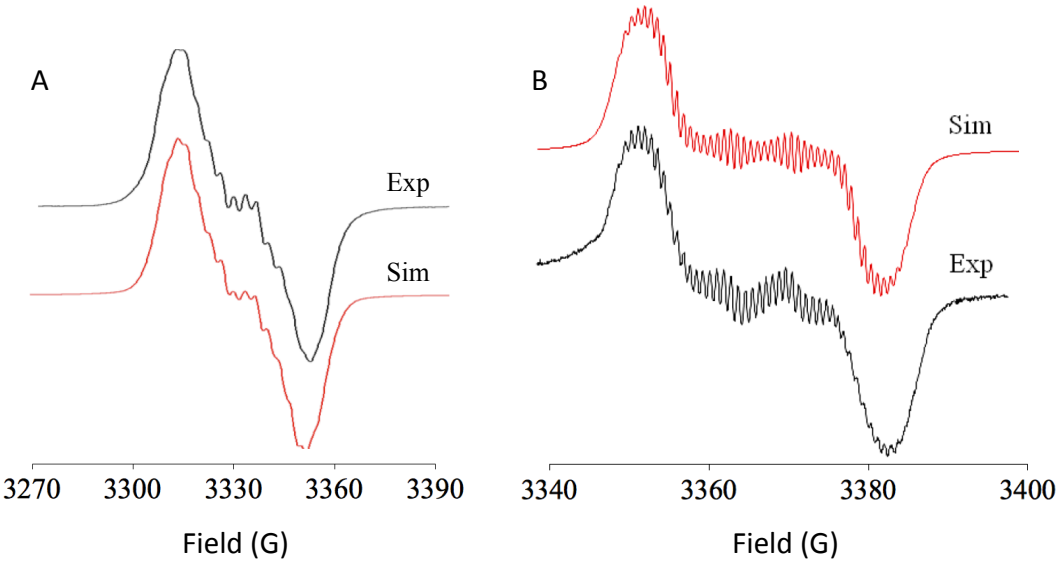

Figure 4.7: Solution state EPR spectra for **4.2** (A) and **4.3** (B).

A similar, well-resolved spectrum was obtained for **4.3** in toluene at room temperature (g=1.9996; **Figure 4.7 B**). It could be simulated with $a(^{63}Cu)$ = 7.95 G, $a(^{65}Cu)$ = 8.51 G, $a(^{14}N)$ = 2.5 G (2N), and $a(^{1}H)$ = 0.9 G (12 H). The latter coupling can be tentatively attributed to the four-methyl groups (CMe_2) of the ligand in the position β to the carbene carbon, whose hyperfine coupling could not be determined due to the low natural abundance of ^{13}C. An alternative for the ^{1}H coupling would be the four inside-oriented methyl groups of the N-aryl substituents, as suggested by the spin density plot (**Figure 4.5**). However, since this coupling is not seen in the EPR of **4.2**, it is most likely from the two-methyl substituents. In agreement with the calculated spin density distribution, the nitrogen hyperfine coupling is relatively small, as is the metal hyperfine coupling in comparison to that of paramagnetic compounds of Cu(I) or Cu(II),[10] signifying little copper participation at the singly occupied molecular orbital (SOMO). Furthermore, the isotropic *g* factors close to the free electron value of 2.0023 confirm

marginal contributions from the transition element to the SOMO, suggesting a three-center carbene/copper/carbene description with predominantly carbene radical character.

The magnetic properties of **4.3** were further investigated by temperature-dependent susceptibility measurements. The experimental magnetic moment of **4.3** is 1.74 μ_B at 155 K (**Figure 4.8**), which is very close to the spin-only value of 1.73 μ_B for one unpaired electron. Magnetic moment remains nearly constant down to 7 K. Some decrease below this temperature can be attributed to the weak intermolecular antiferromagnetic interaction.

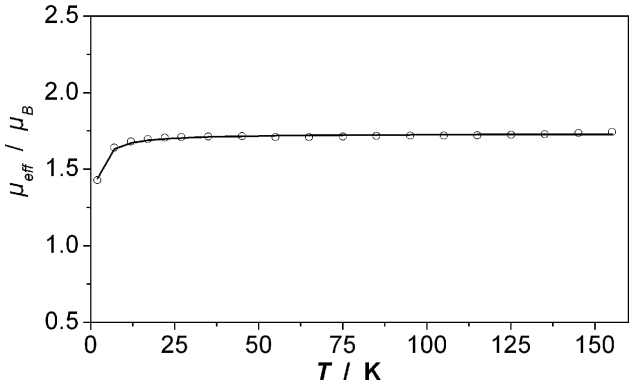

Figure 4.8: Magnetic moment vs. temperature for **4.3**.

Conclusion

We have shown that by utilizing CAACs, which are both excellent σ-donor and π-acceptor ligands, the first neutral two-coordinate Cu complexes could be prepared, isolated, and fully characterized by X-ray crystallography and EPR. Accessing what previously had only been a hypothesized intermediate in copper catalysis will now allow for reactivity and further mechanistic studies.

Chapter 4 has been adapted from materials published in D. S. Weinberger, N. A. SK, K. C. Mondal, M. Melaimi, G. Bertrand, A. C. Stuckl, H. W. Roesky, B. Dittrich, S.

Demeshko, B. Schwederski, W. Kaim, P. Jerabek, G. Frenking *J. Am. Chem. Soc.* **2014**, *136*, 6235. The dissertation author was the primary investigator of this paper.

Appendix: Experimental section

4.1

(Et_2-CAAC)$_2$CuI: In the glove box, a schlenk flask was loaded with CAAC (1.53 g, 4.88 mmol) and CuI (0.45 eq, 0.418 g, 2.19 mmol). At -78 °C, 60 mL of THF was added, and the mixture was warmed to room temperature over 14 h. The THF solution was evaporated to dryness and subsequently washed with 20 mL of *n*-hexane three times. **4.2** was extracted with 3 x 10 mL of CH_2Cl_2, and after evaporation of the solvent under vacuum, **4.2** was obtained as a white powder and dried to produce a white powder. Crystals suitable for X-ray analysis were grown from layering a saturated CH_2Cl_2 solution with *n*-hexane. (1.35g; 75% yield) Mp: 203 °C (dec); ^{1}HNMR(CD_2Cl_2, 400 MHz): δ=7.35(t, J=7.2Hz, 1H), 7.14 (d, J = 7.2 Hz, 2H), 2.62 (br, 2 H), 1.95 (s, 2 H), 1.71 (br, 2 H), 1.56 (br, 2 H), 1.26 (br, 6 H), 1.20 (br, 6 H), 1.18 (d, J = 6 Hz, 6 H) 0.94 (br, 6 H), 0.7 (br, 6H). ^{13}C NMR (CD_2Cl_2, 75 MHz): δ = 249.33 (C), 144.3 (C), 134.1 (C), 129.9 (CH), 124.1 (CH), 83.0 (C), 64.0 (C), 39.9 (CH_2), 31.5 (CH_2), 29.1 (CH_3), 28.8 (CH_3), 27.2 (CH), 21.8 (CH_3), 9.6 (CH_3) ppm; HRMS (ESI-TOFMS) *m/z* calculated for $[C_{44}H_{70}CuN_2]^+$ 689.4835, found 689.4843.

Crystal data and structure refinement for **4.1**

Identification code	ja502521b_si_002
Empirical formula	$C_{142}H_{220}Cl_{30}Cu_3I_3N_6$
Formula weight	3646.05
Temperature/K	100.0
Crystal system	triclinic
Space group	P-1
a/Å	15.9571(12)
b/Å	16.2774(13)
c/Å	18.1897(14)
α/°	72.796(3)
β/°	72.890(2)
γ/°	77.158(2)
Volume/Å^3	4265.9(6)
Z	1
ρ_{calc}mg/mm^3	1.419
m/mm^{-1}	1.429
F(000)	1870.0
Crystal size/mm^3	0.13 × 0.13 × 0.11
2Θ range for data collection	2.418 to 52.744°

Index ranges	$-19 \leq h \leq 19, -20 \leq k \leq 20, -22 \leq l \leq 22$
Reflections collected	49762
Independent reflections	17217[R(int) = 0.0676]
Data/restraints/parameters	17217/223/865
Goodness-of-fit on F^2	1.021
Final R indexes [I>=2σ (I)]	$R_1 = 0.0552$, $wR_2 = 0.1126$
Final R indexes [all data]	$R_1 = 0.0923$, $wR_2 = 0.1342$
Largest diff. peak/hole / e $Å^{-3}$	2.12/-1.60

4.2

$(Et_2\text{-CAAC})_2Cu$: To a solution of **4.1** (125 mg, 0.153 mmol) in 20 mL of THF was added a clean piece of Na metal (200 mg). After 15 min at room temperature, the solution turned to a red/brown color. The solution was allowed to stir for an additional hour and subsequently filtered. The filtrate was evaporated under vacuum. The solid was then extracted with 4 × 20 mL of *n*-hexanes, and the solvent was evaporated under vacuum to yield **4.2** as a reddish-brown solid. Crystals suitable for X-ray analysis were grown at −30 °C from a concentrated solution of n-hexanes (37 mg; 35% yield); **4.2** decomposes above 131 °C.

Crystal data and structure refinement for **4.2**

Identification code	ja502521b_si_003
Empirical formula	$C_{44}H_{70}CuN_2$
Formula weight	690.56
Temperature/K	100 (2)
Crystal system	triclinic
Space group	P-1
a/Å	9.5174(3)
b/Å	12.0455(3)
c/Å	17.6337(5)
α/°	86.172(2)
β/°	84.756(2)
γ/°	76.646(2)
Volume/$Å^3$	1956.49(10)
Z	2
$\rho_{calc}mg/mm^3$	1.172
m/mm^{-1}	0.590
F(000)	754.0
Crystal size/mm^3	0.1 × 0.1 × 0.1
2Θ range for data collection	2.32 to 53°
Index ranges	$-11 \leq h \leq 11, -15 \leq k \leq 14, -22 \leq l \leq 22$
Reflections collected	40843
Independent reflections	7958[R(int) = 0.0365]

Data/restraints/parameters	7958/0/443
Goodness-of-fit on F^2	1.065
Final R indexes [I>=2σ (I)]	$R_1 = 0.0314$, $wR_2 = 0.0795$
Final R indexes [all data]	$R_1 = 0.0379$, $wR_2 = 0.0830$
Largest diff. peak/hole / e $Å^{-3}$	0.36/-0.63

4.3

$(Me_2\text{-CAAC})_2Cu$: A 1:2:2 molar mixture of $CuCl_2$ (76 mg, 0.562 mmol), Me_2-CAAC (322 mg, 1.13 mmol), and KC_8 (152 mg, 1.12 mmol) and toluene (70 mL) were separately cooled to −78 °C, and then the toluene was added to the mixture through a cannula. The reaction solution was then slowly warmed to room temperature and stirred for 12 h. During this period the color of the solution changed to dark green, and it was subsequently filtered. The filtrate was stored at room temperature for 6 h. Then the solution was filtered again to remove colorless byproducts and stored at −32 °C in a freezer overnight. Dark plates of **4.3** were formed (23 mg, 7% yield) which were separated by filtration. C, H, and N analysis (%) found (calculated) for $C_{40}H_{62}N_2Cu$; C, 75.70 (75.72); H, 9.65 (9.84); N, 4.45 (4.41). **4.3** decomposes above 142 °C and turns to a black liquid. UV−visible bands are observed at 330, 435, 482, 595, 655, 755, and 1214 nm.

Crystal data and structure refinement for 4**.3**

Identification code	ja502521b_si_004
Empirical formula	$C_{27}H_{39}Cu_{0.5}N$
Formula weight	409.36
Temperature/K	100 (2)
Crystal system	triclinic
Space group	P-1
a/Å	10.567(2)
b/Å	10.594(2)
c/Å	11.848(2)
α/°	70.38(3)
β/°	74.26(3)
γ/°	75.68(3)
Volume/$Å^3$	1184.5(5)
Z	2
$\rho_{calc}mg/mm^3$	1.148
m/mm^{-1}	0.348
F(000)	445.0
Crystal size/mm^3	0.1 × 0.1 × 0.1
2Θ range for data collection	3.252 to 57.272°
Index ranges	$-14 \le h \le 15$, $-16 \le k \le 16$, $-18 \le l \le 18$
Reflections collected	24014

Independent reflections	8201[R(int) = 0.0175]
Data/restraints/parameters	8201/90/329
Goodness-of-fit on F^2	1.081
Final R indexes [I>=2σ (I)]	$R_1 = 0.0329$, $wR_2 = 0.0941$
Final R indexes [all data]	$R_1 = 0.0357$, $wR_2 = 0.0965$
Largest diff. peak/hole / e $Å^{-3}$	0.51/-0.45

References

[1] a)Barondeau, D. P., Getzoff, E. D., *Curr. Opin. Struct. Biol.* **2004**, *14*, 765-774; b)Lu, Y., Berry, S. M., Pfister, T. D., *Chem. Rev.* **2001**, *101*, 3047-3080; c)Malkin, R., Malmstro.Bg, *Adv. Enzymol. Relat.* **1970**, *33*, 177; d)Rorabacher, D. B., *Chem. Rev.* **2004**, *104*, 651-698; e)Valentine, J. S., Doucette, P. A., Potter, S. Z., in *Annu. Rev. Biochem.,* **2005**, 563-593; f)Jernigan, G. G., Somorjai, G. A., *J. Catal.* **1994**, *147*, 567-577.

[2] a)Gokhale, A. A., Dumesic, J. A., Mavrikakis, M., *J. Am. Chem. Soc.* **2008**, *130*, 1402-1414; b)Ratnasamy, C., Wagner, J. P., *Catal. Rev.* **2009**, *51*, 325-440.

[3] Zuo, Z.-J., Han, P.-D., Li, Z., Hu, J.-S., Huang, W., *Appl. Surf. Sci.* **2012**, *261*, 640-646.

[4] Lefèvre, G., Franc, G., Tlili, A., Adamo, C., Taillefer, M., Ciofini, I., Jutand, A., *Organometallics* **2012**, *31*, 7694-7707.

[5] Mansour, M., Giacovazzi, R., Ouali, A., Taillefer, M., Jutand, A., *Chem. Comm.* **2008**, 6051-6053.

[6] Stange, A. F., Waldhor, E., M., M., Kaim, W., *Z. Naturforsch* **1995**, *50b*, 115-122.

[7] Bowmaker, G., *Aust. J. Chem.* **1978**, *31*, 2549-2553.

[8] Bowmaker, G. A., Pabst, M., Roesch, N., Schmidbaur, H., *Inorg. Chem.* **1993**, *32*, 880-887.

[9] Atkins, R. M., Timms, P. L., *Inorg. Nuc. Chem. Lett.* **1978**, *14*, 113-115.

[10] Rall, J., Kaim, W., *J. Chem. Soc., Faraday Trans.* **1994**, *178*, 42-55.

CHAPTER 5:

Isolation and reactivity of a Cu-Cu Dimer

Introduction

As discussed in the general introduction, the synthesis of gold clusters is of interest due to the varying reactivity that gold clusters acquire depending on the size of the cluster. For example, in chapter 3, the trinuclear gold species showed the carbonylation of amines at relatively low pressures of carbon monoxide. Similarly, copper clusters have attracted significant interest due to size-dependence on chemical, physical, and structural properties as the size goes from small molecules to bulk material.[1] Furthermore, the high ionic and electric conductivity in the solid state leads to properties between those of semiconducting and metallic phases to be investigated for copper clusters.[2]

One major area of study in the synthesis of clusters ranging in size between 4 and 146 copper atoms has been the synthesis of copper/chalcogen complexes with the addition of ancillary phosphine ligands to stabilize the complexes.[3] The general synthesis (**Scheme 5.1**) involves the addition of a phosphine to a copper halogen species followed by the addition of a chalcogen-silane.

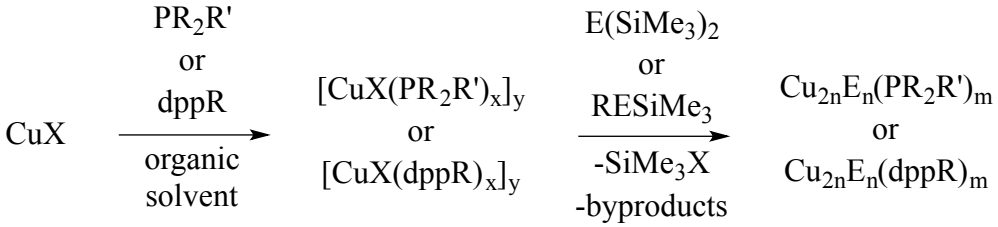

X = Cl, OAc
R, R' = organic group
dppR = bis(diphenylphosphanyl)-alkane, -alkene, or arene
E = S, Se, Te

Scheme 5.1: General synthesis of copper/chalcogen clusters.

By varying the sterics of the phosphine, the final size and shape of the cluster can be modulated; however, there is no linear relationship between the Tolman's cone angle of the phosphine and the resulting size of the cluster.[3] Given that the charges on the chalcogens are -2, the majority of the complexes formed are with copper in the +1 oxidation state.[4] However, the exceptions are mixed-valence Cu(II)/Cu(I) complexes such as $Cu_{20}Se_{13}(PEt_3)_{12}$.[5] Unlike gold clusters which are most often mixed Au(I)/Au(0), or Au(III)/Au(I) no copper clusters exist with the copper having an oxidation state of zero.

Numerous examples of Cu^I-Cu^I dimers exist with bond lengths typically in the range of 2.60 to 3.50 Å.[6] Very similar to aurophilic bonding, these cuprophilic interactions are between the mixed 4s and 4p orbitals of the copper and the 3d orbitals.[7] These interactions also tend to be approximately one third as strong as gold/gold aurophilic interactions.

The shortest Cu^I-Cu^I bond to date, with neutral ligands, utilizes two pyridazine annelated bis(NHC) ligands (**Figure 5.**1) which are twisted 70° to force the coppers to be in close proximity, resulting in a Cu-Cu bond of 2.4923Å.[8] The authors propose that due to the strongly donating character of the NHCs, the coulombic repulsion between the two copper centers is decreased.

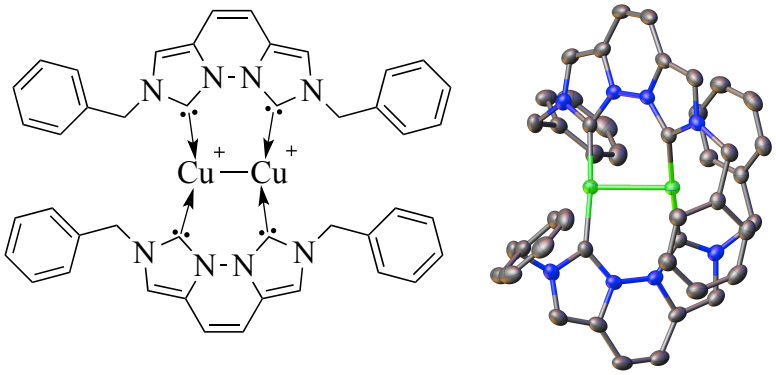

Figure 5.1: Structure of the pyridazine annelated bis(NHC). Hydrogen atoms are omitted for clarity; thermal ellipsoids are drawn at 50% probability.

Given that the only examples of Cu-Cu bonds, where the copper is in the reduced zero oxidation state, are those described in elemental copper, the next question is whether it is possible to isolate L-Cu-Cu-L similar to the L-Au-Au-L in Chapter 2.

Synthesis of (CAAC)Cu-Cu(CAAC)

Starting with the (CAAC)CuCl **5.1**, which was previously published,[9] we postulated that a one-electron reduction would result in the corresponding Cu-Cu dimer. Addition of lithium powder or 4,4'-di-tert-butylbiphenyl reduced with lithium did not proceed cleanly as was the case for the Au-Au dimer. Therefore, lithium/anthracene was prepared by the addition of 2 eq of lithium powder to anthracene in THF. After filtration of excess lithium, the dark blue solution was added drop-wise to a stirring solution of **5.1** to yield a green solution **5.2**. Crystals suitable for an X-ray diffraction study were grown by slow evaporation of a saturated THF solution to yield green needles **5.2**. Crystals were highly air and water sensitive and only lasted in the oil at room temperature for less than 5 minutes. This reaction is the formal addition of two equivalents of (CAAC)CuCl to a doubly reduced anthracene. While 9,10-dilithioanthracene is known,[10] from the lithium-

halide exchange with 9,10-dibromoanthracene, the double reduction of anthracene with lithium and addition of coinage metals has not been shown.

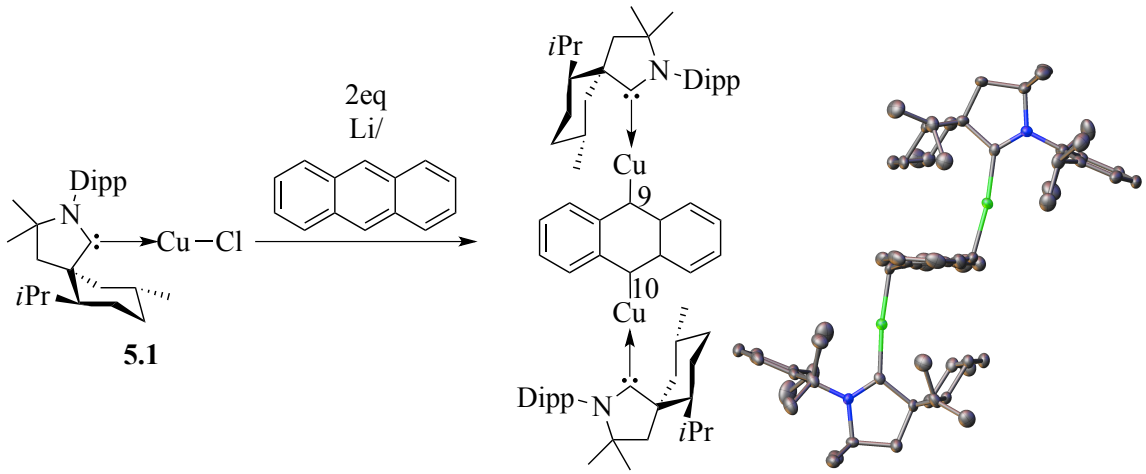

5.1 **5.2**

Scheme 5.2: 9,10 $[(CAAC)Cu]_2$ substituted anthracene synthesis and crystallization. Hydrogen atoms are omitted for clarity; thermal ellipsoids are drawn at 50 % probability.

Carbons 9 and 10 exhibit a distorted sp^3 hybridization with C-C-Cu bond angles of 101.39°, 98.43°, 99.88° and 107.83°. While the addition of an aryl- or alkyl- lithium reagent to CuX is not new, this reaction is the only example of a 9,10 Cu and proton substituted anthracene.

As lithium did not cleanly reduce **5.1** on its own, the one-electron reduction of **5.1** with stoichiometric addition of KC_8 to a stirring solution of **5.1** in THF yielded the desired Cu-Cu dimer **5.3**. The neutral complex is completely soluble in non-polar solvents, and crystals for X-ray diffraction study were grown from a concentrated solution of **5.3** in *n*-hexane at -30°C.

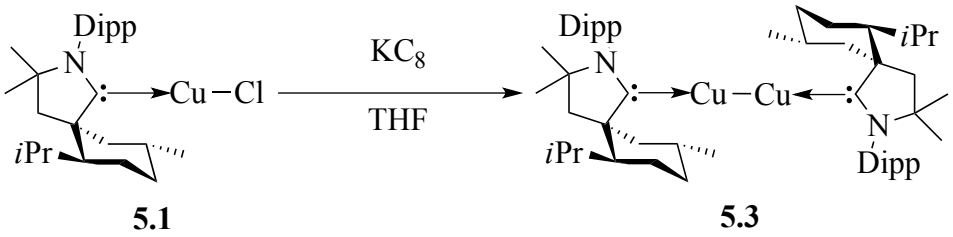

5.1 **5.3**

Scheme 5.3: Addition of KC_8 to (CAAC)CuCl yields (CAAC)Cu-Cu(CAAC) dimer.

The Cu-Cu bond is very short at 2.306Å with a C-Cu-Cu' bond angle of 176.62° and a Cu-Cu'-C' bond angle of 177.54°. The short Cu-Cu bond length is the shortest of any reported Cu-Cu bond. As expected, the complex is nearly linear similar to the (CAAC)Au-Au(CAAC). Calculations for this complex are currently being performed to elucidate the bonding scenario.

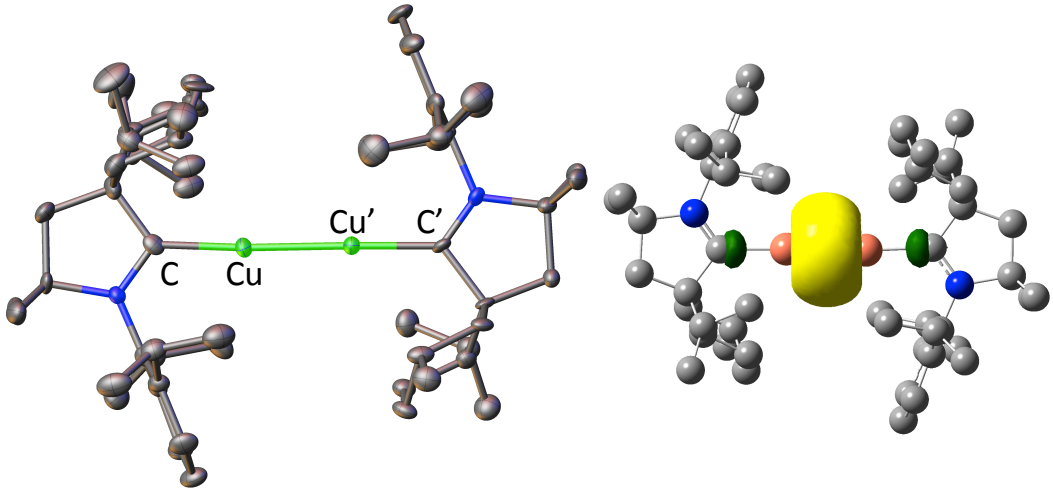

Figure 5.2: X-ray crystal structure (left) and calculation of the HOMO (right) for (CAAC)Cu-Cu(CAAC) **5.3**. Hydrogen atoms are omitted for clarity; thermal ellipsoids are drawn at 50% probability.

The HOMO is calculated (UM052X/Def2SV) to be the Cu-Cu bond (**Figure 5.2**, right), which is very similar to (CAAC)Au-Au(CAAC). As shown with (CAAC)Au-Au(CAAC), **5.3** should also be a reactive complex and we should be able to do chemistry between the two copper atoms. Unfortunately, the ^{13}C NMR for the carbene carbon **5.3**

only shifts 1.1 ppm from 251.4 ppm for cationic complex **5.1** to 250.3 ppm for the neutral complex **5.3**. Therefore, NMR doesn't give a good handle on the oxidation state of the copper.

As we know from our previous study with the gold dimer, the sterically bulky menthyl groups on the CAACs prevent reactivity with large substituents; therefore, an attempt to make the copper dimer with the Et_2CAAC was undertaken. As shown in chapter 3, the addition of Et_2CAAC to CuI results in the bis-substituted copper complex: $(Et_2CAAC)_2Cu^I$. However, addition of Et_2CAAC to CuCl affords (Et_2CAAC)CuCl in excellent yields.

Reduction of **5.4** with a stoichiometric amount of KC_8 gave a mixture of starting material and an unidentified complex only detectable by EPR. The addition of 3 eq of KC_8 cleanly produced the same unidentified paramagnetic complex. Unfortunately, after leaving a solution of the paramagnetic complex in the freezer for a week at -30°C, the crystals obtained were the decomposition product **5.5**.

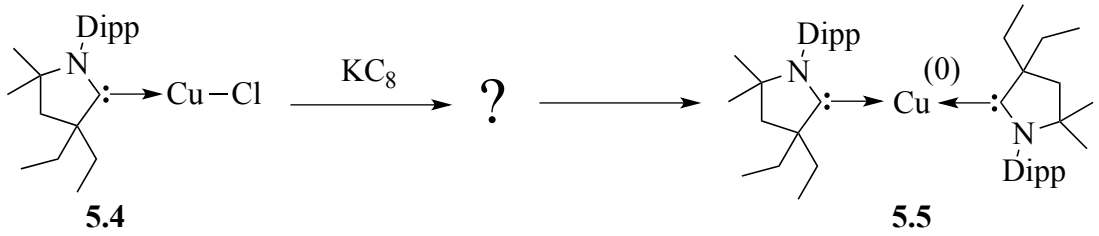

5.4 **5.5**

Scheme 5.4: Reduction of (Et_2CAAC)CuCl with 3 eq of KC_8 to give a paramagnetic species that decomposes into $(Et_2CAAC)_2Cu(0)$.

As shown in **Figure 5.3**, the spectrum for the intermediate product formed is very different than $(Et_2CAAC)_2Cu(0)$, which was described in Chapter 4. Attempts to simulate the spectrum by varying the number of copper atoms and nitrogens failed. Each attempt

to crystallize this species was unsuccessful and **5.5** was systematically crystallized. EPR of the solution after one week only showed **5.5**.

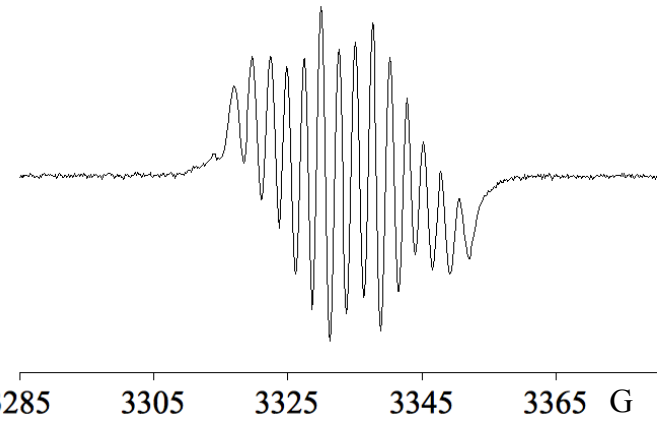

Figure 5.3: EPR spectrum of the unknown intermediate from the reduction of $(Et_2CAAC)CuCl$ with KC_8.

Reactivity of (CAAC)Cu-Cu(CAAC)

The reactivity of the copper dimer **5.3** with electron deficient alkynes was the first area under investigation. Addition of **5.3** to dimethyl acetylenedicarboxylate resulted in a mixture of products, with two carbene ^{13}C NMR signals at δ = 254.3 and 253.1 ppm. Since there are nearly two identical shifts for each carbon, we assume the products to be the cis and trans additions **5.6**. Unfortunately, due to the exact same solubility in polar and non-polar solvents alike, the two complexes could not be separated. We postulate that the reaction undergoes side on addition to the alkyne to form the cis conformer, and then due to the large steric bulk of the menthyl groups, the cis conformer undergoes conversion to the trans isomer. The mechanism for the interconversion could go through copper dissociation followed by association; however, this is only speculation.

Unlike the reactivity of (CAAC)Au-Au(CAAC), **5.3** reacted instantaneously in benzene with diphenylacetylene **5.7**. The color of the solution changed from green to

orange; and after evaporation, the solid was washed with *n*-hexane to yield a yellow solid. The ^{13}C NMR shows a significant shift of the carbene carbon to 257.9 ppm and the alkene carbon at 119.2 ppm. In addition, only one product is detected. Unfortunately, single crystals suitable for X-ray crystallography could not be grown, so the exact structure is still unknown.

Since **5.3** reacted with diphenylacetylene, it was of some interest whether **5.3** could react with acetylene. Therefore, dried acetylene was bubbled through a solution of **5.3** in hexane and a brown solid precipitated from the hexane solution. The ^{13}C NMR shows two carbene shifts at 257.4 and 254.8 ppm corresponding to the two different isomers. Interestingly, there is only one carbon signal corresponding to an alkene at 114.1 ppm.

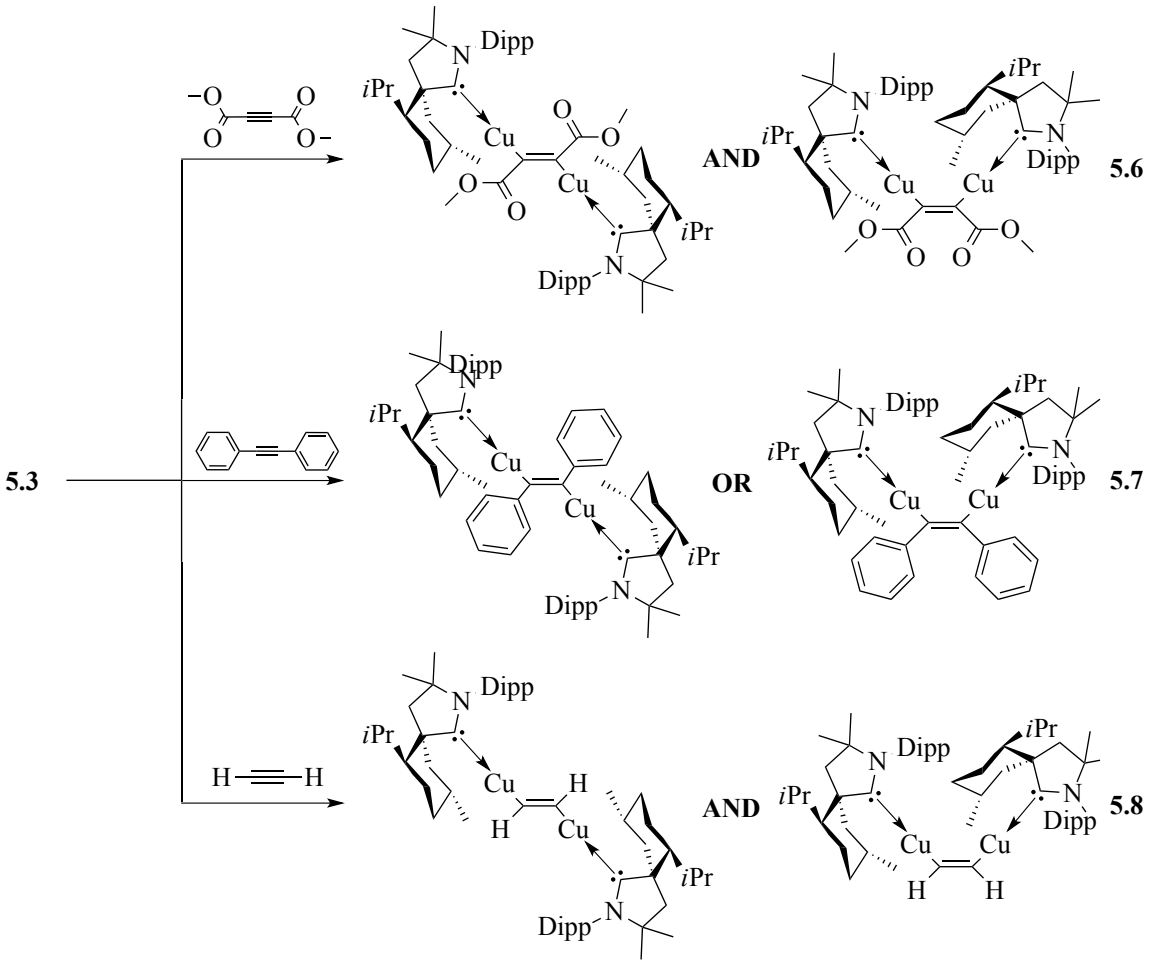

Scheme 5.5: Addition of alkynes to **5.3**.

Due to the large and growing concentration of CO_2 in the atmosphere, there is an ever-increasing interest in the copper catalyzed reduction of CO_2 to chemical feedstocks.[11] Upon bubbling CO_2 through a solution of **5.3** in hexane, the green solution instantaneously turned yellow and a white precipitate formed. After subsequent hexane washes, colorless single crystals of **5.9** were grown from a concentrated ether solution at -30°C.

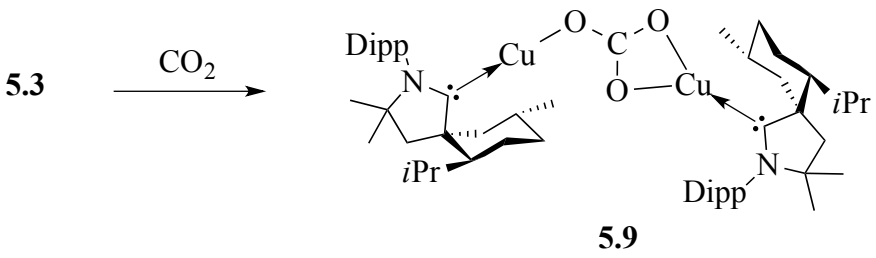

5.9

Scheme 5.6: Synthesis of a bridging CO_3^{2-} between two Cu(I) complexes.

5.9 is a rare example of an isolated crystal structure of two Cu^{I} atoms bound to a reduced CO_2 molecule (**Figure 5.4**). The carbene and CO_3 chemical shifts in the ^{13}C NMR are at 252.3 and 172.1 ppm, respectively. In the literature Bouwman *et al.* have shown addition of two CO_2 molecules to two Cu(I) centers which are subsequently reductively coupled. After the addition of HCl, oxalic acid is formed.[12] This system then becomes catalytic after applying a potential. Electrocatalytic systems also developed by Kubiak *et al.* have shown the possibility of using copper catalysts for the catalytic reduction of CO_2.[13] Therefore, further catalytic studies with **5.9** need to be investigated.

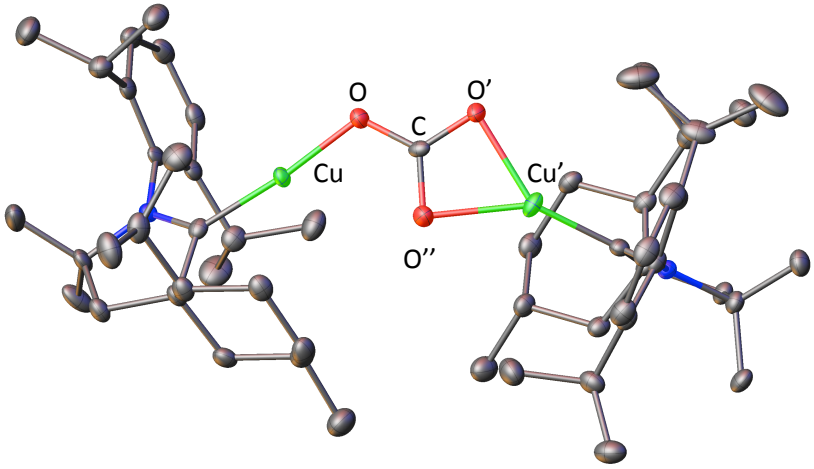

Figure 5.4: X-ray crystal structure of $[(CAAC)Cu]_2^{2+}$ CO_3^{2-} **5.9**. Hydrogen atoms are omitted for clarity, thermal ellipsoids are drawn at 50% probability.

Since **5.3** is able to reduce CO_2, we decided to investigate the possibility to use complex **5.3** to reduce carbon monoxide. After keeping a solution of **5.3** in a high-pressure Schlenk tube with approximately 7 atmospheres of CO pressure for one week, a ^{13}C NMR spectra of **5.10** was quickly recorded. The carbene carbon shift and carbonyl signals at 251.73 and 200.38 ppm , respectively, were observed. Unfortunately, **5.10** decomposed before it could be further investigated. The intensity of the CO peak in the ^{13}C NMR and the diamagnetic nature of **5.10** leads the structure to be predicted as shown in **Scheme 5.7**.

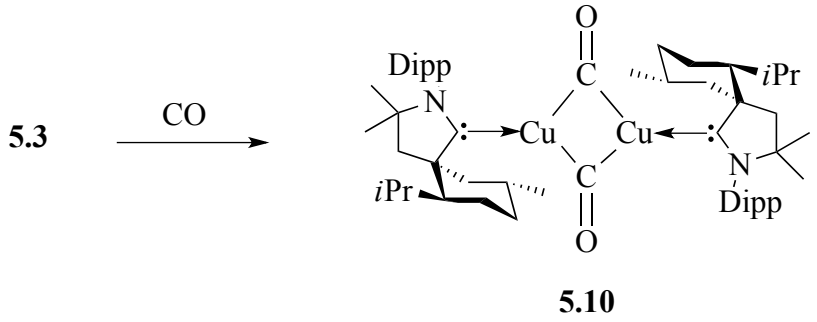

5.10

Scheme 5.7: Addition of carbon monoxide to **5.3**.

Since the experiments with carbon monoxide proved challenging to isolate due to the lack of stability, a similar reaction was attempted with the isolabile tert-butyl isocyanide. Upon addition of tert-butyl isocyanide to a stirring solution of **5.3** in hexane a white precipitate was formed. After washing with *n*-hexanes, single crystals suitable for X-ray crystallography were grown from slow evaporation of **5.11** in benzene.

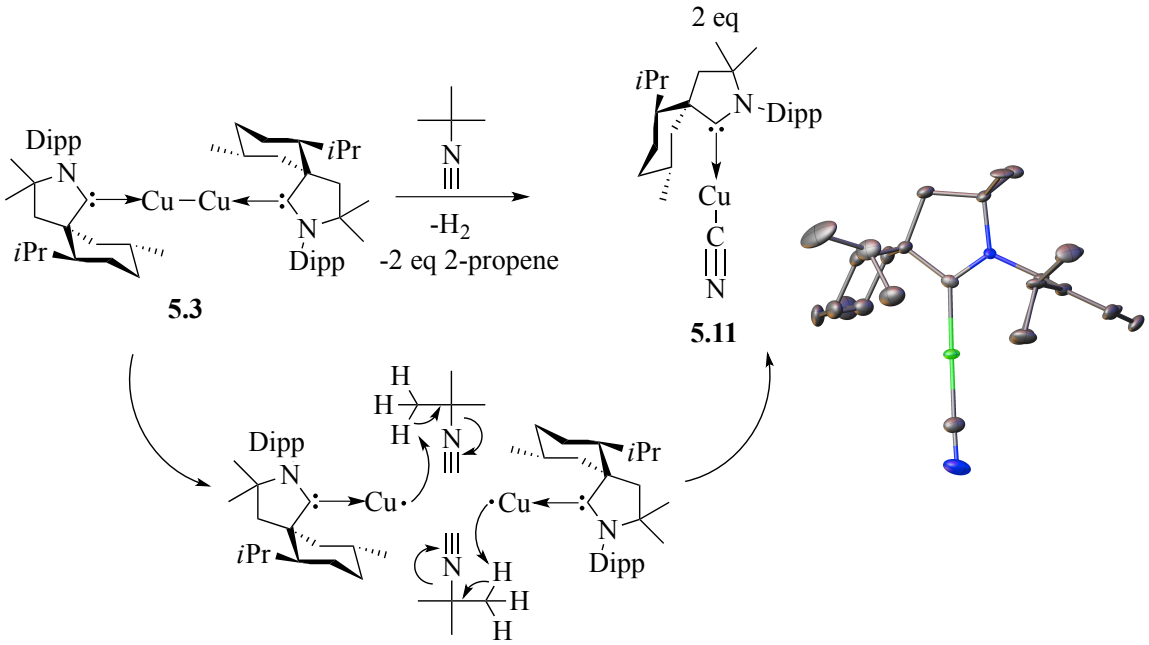

Scheme 5.8: Addition of tert-butyl isocyanide to **5.3.** Crystal structure of **5.11,** hydrogen atoms are omitted for clarity, thermal ellipsoids are drawn at 50% probability.

This reactivity can be explained by the radical abstraction of a methyl proton followed by the elimination of 2-propene and the addition of the cyanide to the copper. We assume the hydrogen is eliminated as H_2 with two equivalents of **5.11** being formed. In order to prevent the elimination of the isocyanide substituent, 2,6-dimethylphenyl isocyanide was utilized. Indeed, **5.12** was isolated with the C=N peak in the ^{13}C NMR at δ = 235.02 ppm and the carbene carbon at δ = 258.52. Unfortunately, **5.12** could not be crystallized; therefore, **5.12** is believed to be the actual structure due to is diamagnetic nature, and the intensity of the C=N peak to the carbene peak in the ^{13}C NMR and the proton integration in the ^{1}H NMR.

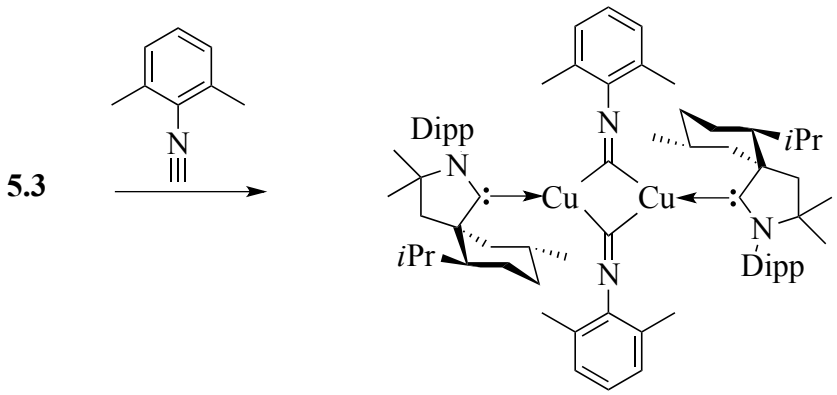

5.12

Scheme 5.9: Addition of 2,6-dimethylphenyl isocyanide to **5.3** to yield the bridging isocyanides.

Similar to the reaction of (CAAC)Au-Au(CAAC) with iron pentacarbonyl in Chapter 2, **5.3** was reacted with an excess of $Fe(CO)_5$ to reduce the iron and give quantitative conversion to **5.13** with the ^{13}C NMR for the carbene and CO at 249.6 ppm and 216.9 ppm, respectively.

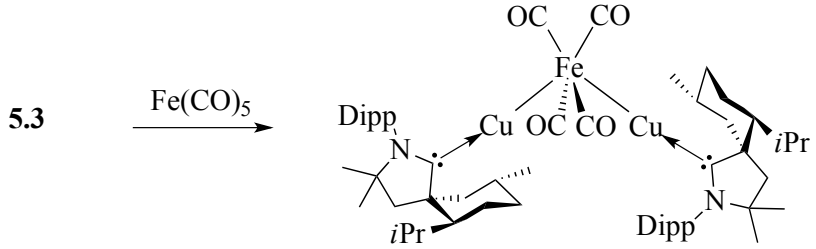

5.13

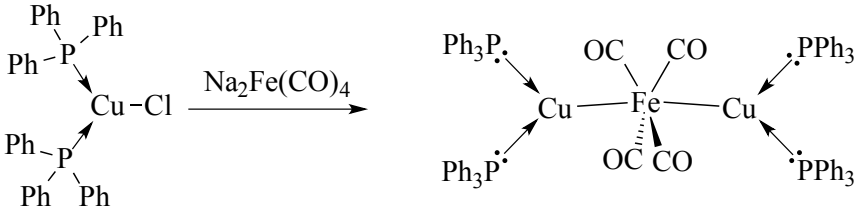

5.14

Scheme 5.10: Two electron reduction of $Fe(CO)_5$ with **5.3** to yield (CAAC)-Cu-$Fe(CO)_5$-Cu(CAAC) **5.13** and addition of $Na_2Fe(CO)_4$ to $(Ph_3P)_2CuCl$ to yield to $(Ph_3P)_2Cu$-$Fe(CO)_4$-$Cu(Ph_3P)_2$.

A similar phosphine complex, $(Ph_3P)_2Cu\text{-}Fe(CO)_4\text{-}Cu(PPh_3)_2$ **5.14** had been previously prepared by Eriksen *et al*. by reacting the diphosphine copper chloride with 0.67 equivalent of $Na_2Fe(CO)_8$ (**Scheme 5.10)**.[14] In contrast to the bond angle in **5.13**, Cu-Fe-Cu = 118.7°, the Cu-Fe-Cu bond angle for **5.14** is nearly linear with an angle of 168.7° (**Figure 5.5 B**). The Cu-Fe bond lengths in **5.13** are 2.390 Å and 2.404 Å, which are approximately 0.1 Å shorter than in **5.14 (Figure 5.5 B**), 2.499 Å and 2.522 Å. This shortening is most likely due to the increased π- accepting properties of the CAAC compared to the phosphines. This is also apparent by comparing the carbonyl stretching frequencies. For both complexes, one weak stretch and three more intense stretches of equal intensity are observed. The CO stretches for complex **5.13** are at 1954, 1873, 1859 and 1835 cm^{-1}. Except for the weak stretch, the stretches are approximately 50-60 wave numbers higher than complex **5.14** (1965, 1820, 1799, 1780 cm^{-1}), indicative of better back-donation to the CAAC than the phosphines. Calculations are currently being performed to fully decipher the electronic structure of **5.13**, and give an insight on the drastic change for the Cu-Fe-Cu bond angle.

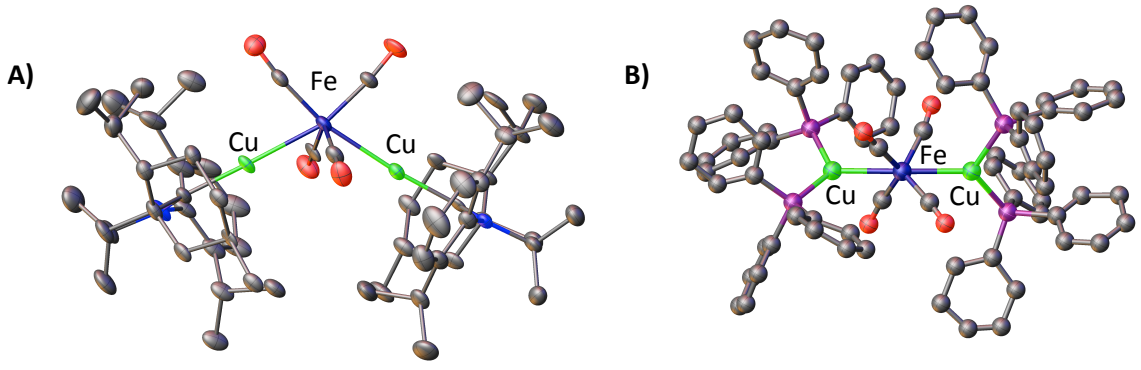

Figure 5.5: A) X-ray crystal structure of **5.13**. B) $(Ph_3P)_2Cu\text{-}Fe(CO)_4\text{-}Cu(PPh_3)_2$ 5.14. Hydrogen atoms are omitted for clarity; thermal ellipsoids are drawn at 50% probability.

Conclusion

Similar to the work described in Chapter 2, the analogous (CAAC)Cu-Cu(CAAC) dimer **5.3** was synthesized by a one-electron reduction of the (CAAC)CuCl precursor. The HOMO was calculated to be the Cu-Cu bond; therefore, reactivity with alkynes and small molecules were investigated. Unlike the Au-Au dimer, **5.3** reacted with both electron poor and unsubstituted alkynes. Addition of CO and RNC gave interesting results. However, due to their intrinsic instability, the resulting species have not been fully characterized. Nonetheless, NMR experiments are in favor of the bridged species. **5.3** also reacted with CO_2 to yield a CO_3 dianion bridging between the two (CAAC)Cu fragments. These bridging species could give rise to the potential of further small molecule activation and catalysis with complex **5.3**.

Chapter 5 has been composed from results that have not been published. These results will be published in the future as D. S. Weinberger, M. Melaimi, C. E. Moore, A. L. Rheingold, G. Frenking, P. Jerabek, G. Bertrand. "Reactivity of Dinuclear Gold And Copper Complexes With a Variety of Substrates and Metals." The dissertation author was the primary investigator.

Appendix: Experimental Section

General

All manipulations were performed under an inert atmosphere of dry Nitrogen, using standard Schlenk techniques. Dry, oxygen-free solvents were employed. EPR spectra were recorded on Bruker EMX. ^{1}H, ^{13}C, spectra were recorded on Bruker Avance 300 (300.13 MHz for 1H, 75.48 MHz for ^{13}C) and Varian Inova 500 spectrometers (500.1 MHz for ^{1}H, 125.8 MHz for ^{13}C). All spectra were obtained in the solvent indicated at 25 °C. Chemical shifts are given in ppm and are referenced residual protonated solvent. Melting points were measured with a Büchi melting point apparatus system.

5.2

Lithium powder (~10 mg) and Anthracene (23 mg, 1.290 x 10^{-4} mol) were stirred in 5 mL of THF for 2 h. The excess lithium was filtered off and added to a stirring solution of **5.1** (65 mg, 1.352 x 10^{-4} mol, 0.95 eq) in 5 mL of THF. After stirring for 2 h, the solution was evaporated to dryness and washed with 5 x 3 mL of *n*-hexane. Crystals suitable for X-ray diffraction study were grown from a concentrated solution of **5.2** in THF at -30 °C.

Crystal data and structure refinement for **5.2**

Identification code	GB_DSW_027_0m_b
Empirical formula	$C_{68}Cu_2N_2$
Formula weight	1068.55
Temperature/K	100(2)
Crystal system	monoclinic
Space group	$P2_1$
a/Å	12.6079(7)
b/Å	15.3661(7)
c/Å	15.4623(8)
α/°	90.00
β/°	94.347(3)
γ/°	90.00
Volume/Å^3	2987.0(3)
Z	2
ρ_{calc}mg/mm^3	1.188
m/mm^{-1}	0.753
F(000)	1152.0
Crystal size/mm^3	0.1× 0.1 × 0.1
Radiation	MoKα (λ = 0.71073)
2Θ range for data collection	2.64 to 52.74°
Index ranges	$-15 \leq h \leq 15$, $-19 \leq k \leq 19$, $-19 \leq l \leq 18$
Reflections collected	24487
Independent reflections	11922 [R_{int} = 0.0422, R_{sigma} = 0.0833]
Data/restraints/parameters	11922/207/649
Goodness-of-fit on F^2	1.999
Final R indexes [I>=2σ (I)]	R_1 = 0.0691, wR_2 = 0.1717
Final R indexes [all data]	R_1 = 0.0954, wR_2 = 0.1764
Largest diff. peak/hole / e Å^{-3}	0.66/-0.48

5.3

5.1 (130 mg, 2.705 x 10^{-4} mol) was dissolved in 10 mL of THF. To the stirring solution, a slurry of KC_8 (30 mg, 2.066 x 10^{-4} mol , 0.77 eq) in 2 mL of THF was added drop wise. The solution turned green and was allowed to stir for 15 minutes. The THF was subsequently evaporated under vacuum. The complex was extracted with 3 x 4 mL of *n*-

hexanes and then evaporated to yield a green solid, 73 mg (29 % yield). ^{1}H NMR (C_6D_6, 500MHz) = 7.15 (t, $^{3}J_{HH}$=7.45 Hz, 3H, $H_{p, ar}$), 7.07 (d, $^{3}J_{HH}$=7.45 Hz, 4H, $H_{p, ar}$), 3.62-3.67 (m, 4H), 3.53 (br, 2H), 2.88 (sept, $^{3}J_{HH}$ = 6.53 Hz, 4H, C*H*$(CH_3)_2$), 2.18(m, 2H), 1.93 (d, $^{3}J_{HH}$ = 14.45 Hz, 2H), 1.79 (m, 2H), 1.70 (m, 4H), 1.54 (d, $^{3}J_{HH}$ = 6.05 Hz, 6H), 1.50 (d, $^{3}J_{HH}$ = 7.12, 4H), 1.33 (d, $^{3}J_{HH}$ = 13.44 Hz, 6H), 1.25 (d, $^{3}J_{HH}$ = 6.55 Hz, 6H) 1.22 (d, $^{3}J_{HH}$ = 6.63 Hz, 6H), 1.19 (d, $^{3}J_{HH}$ = 6.89 Hz, 6H), 1.11 (m, 6H), 1.01 (br, 12H), 0.99 (d, $^{3}J_{HH}$ = 6.49 Hz, 6H), 0.87 (d, $^{3}J_{HH}$ = 6.41, 2H). $^{13}C\{^{1}H\}$ NMR (C_6D_6, 500 MHz) = 250.34 ($C_{carbene}$), 146.4 (C_{ortho}), 146.96 (C_{ortho}), 136.5 (C_{ipso}), 127.8 (C_{para}), 123.9 (C_{meta}), 123.8 (C_{meta}), 75.9 (C_{quat}), 66.2 (C_{quat}), 53.4 (C_{H2}), 52.0 (C_{H}), 48.2 (C_{H2}), 37.3 (C_{H2}), 29.6, 29.4, 29.2, 28.8, 28.5, 28.3, 27.2, 25.4, 25.1, 23.5, 23.1, 23.0, 20.2. Mp: 168 °C(dec.)

Crystal data and structure refinement for **5.3.**

Identification code	CuDimer
Empirical formula	$C_{50}H_{50}Cu_2N_2$
Formula weight	806.00
Temperature/K	100 (2)
Crystal system	triclinic
Space group	P1
a/Å	9.8296(9)
b/Å	11.0801(9)
c/Å	13.2859(11)
α/°	107.466(3)
β/°	103.359(3)
γ/°	105.152(3)
Volume/Å^3	1254.78(19)
Z	1
ρ_{calc}mg/mm^3	1.067
m/mm^{-1}	0.877
F(000)	422.0
Crystal size/mm^3	.2 × .1 × .1
Radiation	Mo (λ = 0.71073)
2Θ range for data collection	3.412 to 52.732°
Index ranges	-12 ≤ h ≤ 12, -13 ≤ k ≤ 13, -16 ≤ l ≤ 16
Reflections collected	33888
Independent reflections	9947 [R_{int} = 0.0690, R_{sigma} = 0.0622]
Data/restraints/parameters	9947/193/626
Goodness-of-fit on F^2	1.042
Final R indexes [I>=2σ (I)]	R_1 = 0.0366, wR_2 = 0.0892
Final R indexes [all data]	R_1 = 0.0450, wR_2 = 0.0936
Largest diff. peak/hole / e Å^{-3}	0.30/-0.26
Flack parameter	0.164(12)

5.5

To a solution of **5.4** (130 mg, 3.151 x 10^{-4} mol) in 10 mL THF, a slurry of KC_8 (128 mg, 9.454 x 10^{-4} mol, 3 eq) in 4 mL of THF was added. The solution turned green/brown after addition, and the solution was allowed to stir for 1 h. After filtration, the solution was set to crystallize and EPR was taken. Crystals grew from a THF solution at -30 °C.

5.6

To a stirring solution of **5.3** (65 mg, 7.300 x 10^{-5} mol) in 5 mL of benzene, dimethyl acetylenedicarboxylate (10 mg, 7.021 x 10^{-4} mol) was added. The solution immediately turned orange, and was stirred for an additional 2 h. Upon evaporation of the solvent, a brown/orange solid oil was collected. Products decomposed after heating oli to 50 °C under vacuum in attempts to evaporate the excess dimethyl acetylenedicarboxylate. $^{13}C\{^1H\}$ NMR (C_6D_6, 500 MHz) = 254.30 ($C_{carbene}$), 253.14 ($C_{carbene}$), 165.21 (C_{quat}), 156.86 (C_{quat}), 154.44 (C_{quat}), 145.79 (C_{ortho}), 145.75 (C_{ortho}), 145.21 (C_{ortho}), 135.31 (C_{ipso}), 134.40 (C_{ipso}), 130.00 (C_{para}), 125.05 (C_{meta}), 124.85 (C_{meta}), 98.16 (C_{quat}), 92.89 (C_{quat}), 77.93 (C_{quat}), 77.49 (C_{quat}), 66.11 (C_{quat}), 65.81 (C_{quat}), 55.73 (C_{H2}), 54.79 (C_{H2}), 53.55 (C_{H3}), 52.17 (C_{H3}), 51.02 (C_{H3}), 47.84 (C_{H3}), 36.26, 35.88, 31.46, 31.19, 29.43 29.14, 27.83, 27.64, 27.38, 26.71, 26.53, 25.51, 25.17, 24.88, 24.12, 22.90, 22.39, 22.25, 20.01, 19.99.

5.7

A vial of **5.3** (65 mg, 7.300 x 10^{-5} mol) and diphenylacetylene (250 mg, 1.404 x 10^{-4} mol, 20 eq) was charged with 8 mL of benzene and allowed to stir for 1 h. The resulting light red solution was pumped down to yield a yellow solid. The solid was washed with 3 x 5 mL *n*-hexane and dried to give 52 mg (67 % yield). ^1H NMR (C_6D_6, 500 MHz) = 7.22 (t, $^3J_{HH}$ = 7.56 Hz, 2H, H_p), 7.05 (d, $^3J_{HH}$ = 7.56 Hz, 4H, H_m), 6.99 (dd, $^3J_{HH}$ = 6.45 Hz, 2H, H_o), 6.95 (t, $^3J_{HH}$ = 7.45 Hz, 2H, $H_{p, ar}$), 6.72 (dd, $^3J_{HH}$ = 7.56Hz, 4H$_m$), 2.74 (m, 2H), 2.67 (m, 4H, C*H*$(CH_3)_2$), 2.21(m, 4H), 2.08 (s, 2H), 1.85 (m, 2H), 1.75 (d, $^3J_{HH}$ = 13.61 Hz, 2H), 1.58 (m, 4H), 1.52 (s, 2H), 1.26 (d, $^3J_{HH}$=6.75 Hz, 6H), 1.12 (d, $^3J_{HH}$=6.88, 6H), 1.11 (d, $^3J_{HH}$ = 6.88, 6H), 1.05 (d, $^3J_{HH}$ = 6.44, 6H), 0.94 (d, $^3J_{HH}$ = 6.88, 6H), 0.89 (d, $^3J_{HH}$ = 7.07Hz, 6H), 0.85 (d, $^3J_{HH}$ = 8.52, 16H), 0.80 (d, $^3J_{HH}$ = 6.31, 6H). $^{13}C\{^1H\}$ NMR (C_6D_6, 500 MHz) = 257.87 ($C_{carbene}$), 182.36, 163.52, 145.47 (C_{ortho}), 145.03 (C_{ortho}), 136.20 (C_{ipso}), 127.59, 127.04 (C_{para}), 125.15 (C_{meta}), 124.83 (C_{meta}), 119.24 (C_{meta}), 76.38 (C_{quat}), 67.80 (C_{quat}), 65.97 (C_{quat}), 53.43 (C_{H2}), 52.35 (C_H), 48.90 (C_{H2}), 36.58 (C_{H2}), 30.16, 29.41, 29.20, 29.08, 28.01, 27.25, 25.77, 24.57, 24.36, 23.53, 23.00, 22.76, 20.35.

5.8

In the glove box, a vial was charged with **5.3** (65 mg, 7.300 x 10^{-5} mol) and 8 mL of *n*-hexane. Acetylene gas (dried through tubing at -78 °C and passed through a column of $CaCl_2$ and molecular sieves) was then bubbled through the solution of **5.3** for 3 min to yield a brown precipitate. The vial was taken back into the glove box, and the liquid decanted. The solid was subsequently washed with 3 x 3 ml of *n*-hexane to yield 37 mg (55 % yield) as a brown solid. $^{13}C\{^1H\}$ NMR (C_6D_6, 500 MHz) = 257.44 ($C_{carbene}$), 254.88 ($C_{carbene}$), 157.78, 154.31, 145.91 (C_{ortho}), 145.71 (C_{ortho}), 145.46 (C_{ortho}), 145.29 (C_{ortho}), 135.79 (C_{ipso}), 135.38 (C_{ipso}), 129.80 (C_{para}), 129.36 (C_{para}), 124.89 (C_{meta}), 124.78

(C_{meta}), 114.00 (C_{quat}), 92.90 (C_{quat}), 77.22 (C_{quat}), 76.43 (C_{quat}), 65.86 (C_{quat}), 65.74 (C_{quat}), 53.28 (C_{H2}), 52.92 (C_{H2}), 51.83 (C_{H}), 51.51 (C_{H}), 48.49 (C_{H2}), 48.09 (C_{H2}), 36.37 (C_{H2}), 36.00 (C_{H2}), 31.03, 30.61, 29.47, 29.15, 28.86, 28.80, 27.92, 26.96, 26.48, 25.38, 25.26, 24.54, 24.40, 23.14, 22.70, 22.60, 20.25, 20.14

5.9

To a stirring solution of complex **5.3** (65 mg, 7.300 x 10^{-5} mol) in 6 mL of benzene, CO_2 was bubbled through the solution for 3 min to yield a light green solution. The benzene was evaporated under vacuum. The resulting solid is then washed with 3 x 4 ml of hexane to produce a white solid. Crystals suitable for X-ray diffraction were grown from a concentrated solution in THF layered with hexane. (45 mg, 65 % yield) ^{1}H NMR (C_6D_6, 500 MHz) = 7.04 (t, $^{3}J_{HH}$ = 7.74 Hz, 2H, $H_{p, ar}$), 6.98 (dd, $^{3}J_{HH}$ = 7.74 Hz, $^{3}J_{HH}$ = 6.71 Hz, 4H, $H_{m, ar}$), 3.25 (m, 2H), 3.10 (br, 2H), 2.83 (m, 4H), 2.10 (d, $^{3}J_{HH}$ = 8.05 Hz, 2H), 1.93 (d, $^{3}J_{HH}$ = 13.19 Hz, 2H), 1.80 (m, 4H), 1.72 (br, 4H), 1.37 (d, $^{3}J_{HH}$ = 6.88 Hz, 6H), 1.35 (d, $^{3}J_{HH}$ = 6.88 Hz, 6H), 1.27 (br, 2H), 1.24 (br, 2H), 1.20 (d, $^{3}J_{HH}$ = 7.01 Hz, 6H), 1.15 (d, $^{3}J_{HH}$ = 6.76, 6H), 1.10 (d, $^{3}J_{HH}$ = 6.84, 6H), 0.99 (d, $^{3}J_{HH}$ = 7.01, 6H) 0.91 (br, 18H). ^{13}C{^{1}H} NMR (C_6D_6, 500 MHz) = 252.3 ($C_{carbene}$), 172.1 (C_{CO3}), 146.0 (C_{ortho}), 145.5 (C_{ortho}), 136.1 (C_{ipso}), 129.3 (C_{para}), 124.6 (C_{meta}), 75.9 (C_{quat}), 65.2 (C_{quat}), 53.2 (C_{H2}), 52.0 (C_{H}), 49.0 (C_{H2}), 36.3 (C_{H2}), 30.2, 29.5, 29.2, 28.3, 27.8, 26.9, 25.0, 24.9, 23.6, 22.8, 20.2.

Crystal data and structure refinement for **5.9.**

Identification code	gb_dsw_040_0m
Empirical formula	$C_{75}H_{75}Cu_2N_2O_5$
Formula weight	1211.45
Temperature/K	100 (2)
Crystal system	orthorhombic
Space group	$P2_12_12_1$
a/Å	15.5372(8)
b/Å	16.2590(9)
c/Å	24.3684(13)
α/°	90
β/°	90
γ/°	90
Volume/Å^3	6155.9(6)
Z	4
ρ_{calc}mg/mm^3	1.307
m/mm^{-1}	0.745
F(000)	2548.0
Crystal size/mm^3	0.1 × 0.1 × 0.1
Radiation	MoKα (λ = 0.71073)
2Θ range for data collection	3.342 to 52.742°
Index ranges	-19 ≤ h ≤ 19, -20 ≤ k ≤ 20, -30 ≤ l ≤ 30

Reflections collected	72294
Independent reflections	12593 [R_{int} = 0.0568, R_{sigma} = 0.0440]
Data/restraints/parameters	12593/190/671
Goodness-of-fit on F^2	1.027
Final R indexes [I>=2σ (I)]	R_1 = 0.0298, wR_2 = 0.0679
Final R indexes [all data]	R_1 = 0.0360, wR_2 = 0.0706
Largest diff. peak/hole / e $Å^{-3}$	0.39/-0.28
Flack parameter	0.014(4)

5.10

In the glove box, a thick walled Teflon schlenk tube was loaded with **5.3** (65 mg, 7.300 x 10^{-5} mol) in 5 ml of benzene. The benzene was frozen in liquid nitrogen, and a vacuum was pulled. The tube was then charged with 20 psi of carbon monoxide while still immersed in liquid nitrogen. The solution was warmed up to room temperature, and stirred for 7 days. Subsequently, the benzene was evaporated and the dark green solid was washed twice with 2 mL of *n*-hexane. ^{1}H NMR (C_6D_6, 500 MHz) = 7.08 (t, $^3J_{HH}$ = 7.98 Hz, 2H, $H_{p, ar}$), 6.93 (dd, $^3J_{HH}$ = 7.98 Hz, 4H, $H_{p, ar}$), 3.22-3.28 (m, 2H), 2.94 (m, 2H), 2.75 (sept., $^3J_{HH}$ = 7.04 Hz, 4H, C*H*$(CH_3)_2$), 2.11 (m, 2H), 2.17 (d, $^3J_{HH}$ = 9.90 Hz, 2H), 1.87 (d, $^3J_{HH}$ = 13.41 Hz, 2H), 1.81 (d, $^3J_{HH}$ = 12.75 Hz, 2H), 1.73 (m, 2H), 1.63 (d, $^3J_{HH}$ = 12.09 Hz, 2H), 1.23 (d, $^3J_{HH}$ = 76.37 Hz, 6H), 1.19 (d, $^3J_{HH}$ = 5.52 Hz, 6H), 1.10 (m-br, 12H), 1.06 (d, $^3J_{HH}$ = 3.15 Hz, 6H), 1.03 (d, $^3J_{HH}$ = 6.23 Hz, 6H), 0.97 (d, $^3J_{HH}$ = 6.00 Hz, 6H), 0.88 (br, 20H). ^{13}C{^{1}H} NMR (C_6D_6, 500 MHz) = 251.73 ($C_{carbene}$), 200.38 (C≡O), 145.96 (C_{ortho}), 145.24 (C_{ortho}), 135.57 (C_{ipso}), 129.71 (C_{para}), 124.90 (C_{meta}), 124.82 (C_{meta}), 77.02 (C_{quat}), 65.38 (C_{quat}), 53.23 (C_{H2}), 51.86 (C_H), 48.49 (C_{H2}), 36.06 (C_{H2}), 30.70, 29.43, 29.15, 28.09, 27.83, 27.06, 25.15, 24.46, 23.51, 22.50, 20.30.

5.11

To a stirring solution of **5.3** (65 mg, 7.300 x 10^{-5} mol) in 6 mL of benzene, 6 drops of tert-butyl isocyanide was added. The solution turned nearly colorless over 20 min. of stirring. The benzene was evaporated to dryness to give an off-white solid. The solid was washed with 3 x 3 mL of *n*-hexanes and extracted with benzene. Crystals suitable for X-ray diffraction were grown from a solution of THF at -30 °C. (48 mg, 72 %). ^{1}H NMR (C_6D_6, 500 MHz) = 7.13 (t, $^3J_{HH}$= 7.57Hz, 2H, $H_{p, ar}$), 7.00 (dd, $^3J_{HH}$= 7.57 Hz, 4H, $H_{m, ar}$), 2.70 (m, 2H), 2.58 (m, 2H), 1.94 (d, $^3J_{HH}$=11.79 Hz, 2H), 1.81 (d, $^3J_{HH}$=13.71 Hz, 2H), 1.67 (br, 6H), 1.32 (d, $^3J_{HH}$=6.87 Hz, 6H), 1.29 (d, $^3J_{HH}$=6.20 Hz, 6H), 1.23 (br, 2H), 1.18 (br, 2H), 1.16 (br, 2H), 1.11 (d, $^3J_{HH}$=6.74, 6H), 1.07 (d, $^3J_{HH}$=6.97, 6H), 0.87 (br, 10H) 0.85 (br, 6H), 0.80 (d, $^3J_{HH}$=6.19, 6H). ^{13}C{^{1}H} NMR (C_6D_6, 500MHz) = 253.03 ($C_{carbene}$), 145.59 (C_{ortho}), 145.12 (C_{ortho}), 139.74 (C_{ipso}), 135.07 (C_{CN}), 130.15 (C_{para}), 125.12 (C_{meta}), 124.92 (C_{meta}), 77.91 (C_{quat}), 65.66 (C_{quat}), 52.68 (C_{H2}), 51.22 (C_H), 47.64 (C_{H2}), 35.76 (C_{H2}), 31.60, 29.38, 29.08, 28.69, 27.74, 26.79, 25.78, 24.10, 23.00, 22.43, 22.29, 22.24, 19.86.

Crystal data and structure refinement for **5.11**.

Identification code	DSW42
Empirical formula	$C_{36}H_{59}CuN_2O_2$
Formula weight	615.39
Temperature/K	100.0
Crystal system	monoclinic
Space group	$P2_1$
a/Å	12.3081(15)
b/Å	12.0893(15)
c/Å	21.979(3)
α/°	90
β/°	99.416(3)
γ/°	90
Volume/Å^3	3226.3(7)
Z	4
ρ_{calc}mg/mm^3	1.267
m/mm^{-1}	0.711
F(000)	1336.0
Crystal size/mm^3	0.257 × 0.223 × 0.211
Radiation	MoKα (λ = 0.71073)
2Θ range for data collection	3.566 to 52.928°
Index ranges	$-15 \leq h \leq 15$, $-15 \leq k \leq 15$, $-16 \leq l \leq 27$
Reflections collected	46934
Independent reflections	13212 [R_{int} = 0.0689, R_{sigma} = 0.0772]
Data/restraints/parameters	13212/1/577
Goodness-of-fit on F^2	1.031
Final R indexes [I>=2σ (I)]	R_1 = 0.0568, wR_2 = 0.1312
Final R indexes [all data]	R_1 = 0.0814, wR_2 = 0.1423
Largest diff. peak/hole / e Å^{-3}	0.38/-0.67
Flack parameter	0.080(10)

5.12

To a stirring solution of **5.3** (65 mg, 7.021 x 10^{-5} mol) in 6 mL of benzene, 2,6-dimethyl phenylisocyanide (20 mg, 1.474 x 10^{-4} mol, 2.1 eq) was added and the solution turned brown. After stirring for 14 h, the solution was evaporated and the orange solid was washed with 3 x 3 mL of cold *n*-hexane. ^{1}H NMR (C_6D_6, 500 MHz) = 7.20 (t, $^3J_{HH}$= 7.36Hz, 2H, $H_{p, ar}$), 7.04 (d, $^3J_{HH}$ = 7.36 Hz, 2H), 7.01 (d, $^3J_{HH}$ = 7.75 Hz, 2H, $H_{m, ar}$), 6.96 (d, $^3J_{HH}$ = 7.36 Hz, 2H, $H_{m, ar}$), 6.95 (d, $^3J_{HH}$ = 8.03 Hz, 2H, $H_{m, ar}$), 6.95 (t, $^3J_{HH}$ = 7.36 Hz, 2H, $H_{p, ar}$), 3.25 (dd, $^3J_{HH}$ = 7.20 Hz, 2H), 3.03 (br, 4H), 2.77 (m, 2H), 2.58 (m, 2H), 2.15 (s, 6H), 1.78 (s, 6H), 1.36 (d, $^3J_{HH}$ = 6.50 Hz, 6H), 1.17 (br, 2H), 1.10 (d, $^3J_{HH}$ = 6.74 Hz, 6H), 1.09 (d, $^3J_{HH}$ = 6.93 Hz, 6H), 1.07 (d, $^3J_{HH}$ = 6.97, 6H), 1.05 (d, $^3J_{HH}$ = 6.64, 14H), 0.90 (br, 6H) 0.85 (br, 14H), 0.77 (d, $^3J_{HH}$ = 6.74, 6H), 0.69 (d, $^3J_{HH}$ = 6.34, 6H).

$^{13}C\{^{1}H\}$ NMR (C_6D_6, 500 MHz) = 258.52 ($C_{carbene}$), 235.02 (C_{CN}), 157.24, 145.11, 136.14, 129.12, 127.54, 127.23, 125.28, 124.77, 124.63, 119.31, 76.79, 66.25, 52.97, 52.11, 49.14, 36.52, 29.59, 29.04, 28.98, 28.03, 26.69, 25.92, 24.70, 23.21, 23.14, 22.95, 20.60, 19.65, 19.29.

5.13

To a stirring solution of **5.13** (65 mg, 7.021 x 10^{-5} mol) in 6 mL of benzene, 6 drops of iron pentacarbonyl (excess) was added. The solution turned red over the course of 15 min. After an additional 12 h of stirring, the solution was yellow. The benzene and excess iron pentacarbonyl were evaporated under vacuum. The solid was extracted with 2 x 8 mL of n-hexanes and evaporated to dryness. Crystals for x-ray diffraction were grown from a concentrated solution in *n*-hexane at -30 °C. (67 mg, 89 % yield) ^{1}H NMR (C_6D_6, 500 MHz) = 7.16 (t, $^{3}J_{HH}$ = 7.52 Hz, 2H, $H_{p, ar}$), 7.08 (d, $^{3}J_{HH}$ = 7.52 Hz, 4H, $H_{m, ar}$), 3.35 (br, 2H), 3.15 (m, 2H), 2.89 (sept, $^{3}J_{HH}$ = 6.7 Hz, 4H, C*H*$(CH_3)_2$), 2.46 (d, $^{3}J_{HH}$ = 9.88 Hz, 2H), 1.91-2.01 (m, 8H), 1.56 (d, $^{3}J_{HH}$ = 7.00 Hz, 6H), 1.51 (d, $^{3}J_{HH}$ = 6.59 Hz, 6H), 1.34 (d, $^{3}J_{HH}$ = 7.00 Hz, 6H), 1.31 (d, $^{3}J_{HH}$ = 13.45 Hz, 6H), 1.16 (d, $^{3}J_{HH}$ = 6.50 Hz, 6H), 1.13 (d, $^{3}J_{HH}$ = 6.54 Hz, 6H), 1.10 (d, $^{3}J_{HH}$ = 6.40, 6H), 1.07 (d, $^{3}J_{HH}$ = 6.69, 6H), 0.98 (br, 12H), 0.89 (br, 2H). $^{13}C\{^{1}H\}$ NMR (C_6D_6, 500 MHz) = 249.64 ($C_{carbene}$), 216.86 (C≡O), 145.56 (C_{ortho}), 145.15 (C_{ortho}), 135.73 (C_{ipso}), 129.74 (C_{para}), 125.22 (C_{meta}), 76.98 (C_{quat}), 65.70 (C_{quat}), 53.63 (C_{H2}), 52.58 (C_{H}), 48.54 (C_{H2}), 36.59 (C_{H2}), 30.4, 29.89, 29.55, 29.34, 28.13, 27.58, 26.66, 25.53, 24.27, 23.35, 23.21, 23.09, 20.75.

Crystal data and structure refinement for **5.13.**

Identification code	gb_dsw_046_0m_a_a
Empirical formula	$C_{29}CuFe_{0.5}NO_2$
Formula weight	529.11
Temperature/K	100
Crystal system	triclinic
Space group	P1
a/Å	10.3651(9)
b/Å	17.0831(16)
c/Å	18.7940(17)
α/°	77.584(4)
β/°	89.759(3)
γ/°	83.053(3)
Volume/Å^3	3225.3(5)
Z	4
ρ_{calc}mg/mm^3	1.090
m/mm^{-1}	0.914
F(000)	1128.0
Crystal size/mm^3	0.1 × 0.1 × 0.1
Radiation	MoKα (λ = 0.71073)
2Θ range for data collection	2.936 to 52.754°

Index ranges	$-12 \leq h \leq 12$, $-12 \leq k \leq 21$, $-17 \leq l \leq 21$
Reflections collected	12481
Independent reflections	11692 [$R_{int} = 0.0225$, $R_{sigma} = 0.0960$]
Data/restraints/parameters	11692/1179/1243
Goodness-of-fit on F^2	1.016
Final R indexes [I>=2σ (I)]	$R_1 = 0.0643$, $wR_2 = 0.1788$
Final R indexes [all data]	$R_1 = 0.0851$, $wR_2 = 0.1908$
Largest diff. peak/hole / e Å^{-3}	1.11/-0.69
Flack parameter	0.039(13)

References

[1] a)Kappes, M. M., *Chem. Rev.* **1988**, *88*, 369-389; b)Koutecky, J., Fantucci, P., *Chem. Rev.* **1986**, *86*, 539-587.

[2] a)Okubo, T., Anma, H., Nakahashi, Y., Maekawa, M., Kuroda-Sowa, T., *Polyhedron* **2014**, *69*, 103-109; b)Ryzhkov, M. V., Finkelshtein, L. D., Kurmaev, É. Z., Gubanov, V. A., *J. Struct. Chem.* **1995**, *36*, 578-583.

[3] Dehnen, S., Eichhöfer, A., Fenske, D., *Eur. J. Inorg. Chem.* **2002**, *2002*, 279-317.

[4] a)Dehnen, S., Fenske, D., *Angew. Chem., Int. Ed. Engl.* **1994**, *33*, 2287-2289; b)Dehnen, S., Schäfer, A., Fenske, D., Ahlrichs, R., *Angew. Chem., Int. Ed. Engl.* **1994**, *33*, 746-749.

[5] Fenske, D., Krautscheid, H., *Angew. Chem., Int. Ed. Engl.* **1990**, *29*, 1452-1454.

[6] a)Yang, L., Powell, D. R., Klein, E. L., Grohmann, A., Houser, R. P., *Inorg. Chem.* **2007**, *46*, 6831-6833; b)Beck, J., Strähle, J., *Angew. Chem., Int. Ed. Engl.* **1985**, *24*, 409-410; c)Churchill, M. R., Kalra, K. L., *J. Am. Chem. Soc.* **1973**, *95*, 5772-5773.

[7] Hermann, H. L., Boche, G., Schwerdtfeger, P., *Chem. – Eur. J.* **2001**, *7*, 5333-5342.

[8] Gierz, V., Seyboldt, A., Maichle-Mössmer, C., Törnroos, K. W., Speidel, M. T., Speiser, B., Eichele, K., Kunz, D., *Organometallics* **2012**, *31*, 7893-7901.

[9] Frey, G. D., Donnadieu, B., Soleilhavoup, M., Bertrand, G., *Chem. – Asian J.* **2011**, *6*, 402-405.

[10] Schröck, R., Angermaier, K., Sladek, A., Schmidbaur, H., *J. Organomet. Chem.* **1996**, *509*, 85-88.

[11] a)Company, A., Jee, J.-E., Ribas, X., Lopez-Valbuena, J. M., Gómez, L., Corbella, M., Llobet, A., Mahía, J., Benet-Buchholz, J., Costas, M., van Eldik, R., *Inorg. Chem.* **2007**, *46*, 9098-9110; b)Verdejo, B., Aguilar, J., García-España, E., Gaviña, P., Latorre, J., Soriano, C., Llinares, J. M., Doménech, A., *Inorg. Chem.* **2006**, *45*, 3803-3815; c)Verdejo, B., Blasco, S., González, J., García-España, E., Gaviña, P., Tatay, S., Doménech, A., Doménech-Carbó, M. T., Jiménez, H. R., Soriano, C., *Eur. J. Inorg. Chem.* **2008**, *2008*, 84-97.

[12] Angamuthu, R., Byers, P., Lutz, M., Spek, A. L., Bouwman, E., *Science* **2010**, *327*, 313-315.

[13] a)Haines, R. J., Wittrig, R. E., Kubiak, C. P., *Inorg. Chem.* **1994**, *33*, 4723-4728; b)Lilio, A. M., Grice, K. A., Kubiak, C. P., *Eur. J. Inorg. Chem.* **2013**, *2013*, 4016-4023.

[14] Doyle, G., Eriksen, K. A., Van Engen, D., *J. Am. Chem. Soc.* **1985**, *107*, 7914-7920.

Conclusion

We have illustrated that by using cyclic (alkyl) (amino) carbenes (CAACs), which are both highly nucleophilic and electrophilic, one-electron reduction of the corresponding $(CAAC)_2M^+$ complexes yielded the neutral species.

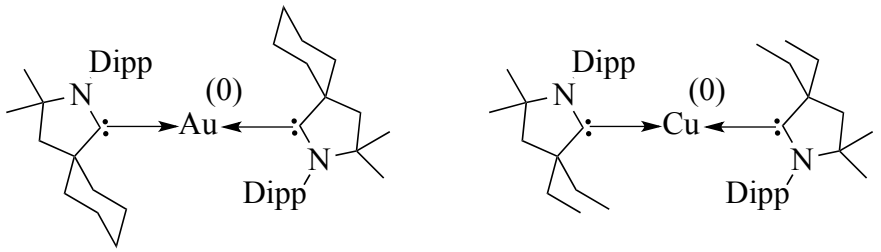

Figure C.1: $(CAAC)_2Au^0$ and $(CAAC)_2Cu^0$.

From both EPR and X-ray crystallography, we found that in $(CAAC)_2Au$ and $(CAAC)_2Cu$ (**Figure C.1**) the electron density of the radical resides on both the metal center and the ligands. Previous research in this area resulted in complexes that were stable only at low temperatures or as transient species. Therefore, these two highly air and water sensitive complexes represent the only gold and copper complexes to be isolated and fully characterized with an oxidation state of zero. Furthermore, this research has paved the way for CAAC ligands to be considered and used as non-innocent ligands.

By expanding this chemistry, neutral (CAAC)M-M(CAAC) (**Figure C.2**) complexes were isolated for both gold and copper by reducing the corresponding $(CAAC)M^+Cl^-$. These complexes are nearly linear with short metal-metal bond lengths. Calculations on the bonding show that the bond is the result of the combination of partially filled s-orbitals. Consequently, the HOMOs for both the gold and copper complexes were calculated to be the metal-metal bond. Therefore, experiments showed that when electrophilic alkynes and alkenes were added to the Au_2 dimer, addition across the triple and double bonds occurred.

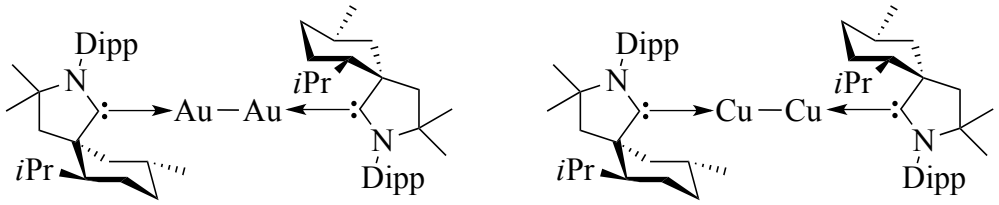

Figure C.2: (CAAC)Au-Au(CAAC) and (CAAC)Cu-Cu(CAAC).

In the case of the Cu_2 dimer, the copper added to alkyl and aryl alkynes, including acetylene, without the need of electron withdrawing substituents. Reactivity was also shown with CO_2, P_4, and isocyanides. Mixed metal complexes were readily obtained by addition of $Fe(CO)_5$ to the coinage metal dimers.

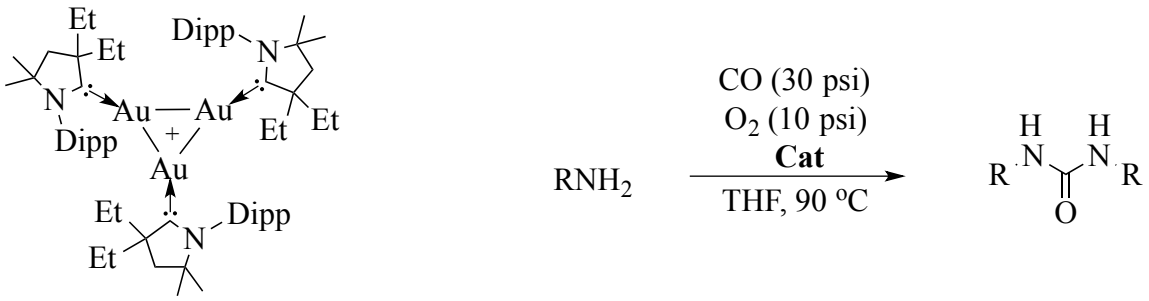

Figure C.3: $[(CAAC)Au]_3^+$ used for the carbonylation of amines with carbon monoxide.

Attempts to prepare a neutral trinuclear gold species were unsuccessful; however, the mixed valence $Au(0)_2$/Au(I) trimer prepared with CAAC ligands proved to be active for the carbonylation of amines (**Figure C.3**).

The method of substituting phosphines by CAACs on a previously prepared gold cluster support leads to the possibility of making even larger well defined clusters bearing the CAAC ligand.